Thesis Biobased Chemistry and Technology

Modelling of an integrated plant-fish system

Thomas Slinkert

October 8, 2015

WAGENINGEN UNIVERSITY
AGROTECHNOLOGY AND
FOOD SCIENCES

INAPRO

WAGENINGEN UR

Modelling of an integrated plant-fish system

Integrated modelling of the INAPRO-aquaponic system to minimise water and nitrogen usage

Name course	:	Thesis project Biobased Chemistry and Technology
Number	:	YEI-80324
Study load	:	24 ects
Date	:	October 8, 2015

Student	:	Thomas Slinkert
Registration number	:	890417-767-070
Study programme	:	BAT (Biosystems Engineering)
Report number	:	008BCT

Supervisor(s)	:	dr. ir. K.J. Keesman
Examiners	:	ir. H.J. Cappon, D. Reyes Lastiri MSc, dr. ir. K.J. Keesman
Group	:	Biobased Chemistry and Technology
Address	:	Bornse Weilanden 9 6708 WG Wageningen the Netherlands Tel: +31 (317) 48 21 24 Fax: +31 (317) 48 49 57

WAGENINGEN UNIVERSITY
AGROTECHNOLOGY AND
FOOD SCIENCES

Contents

Abstract

The research of this thesis is part of a larger project under the name “Innovative model & demonstration-based water management for resource efficiency in integrated multitrophic aquaculture and horticulture systems” (INAPRO). This project is based on a novel type of aquaponics system, combining fish production (aquaculture) and soilless plant production (hydroponics). The aim of the project is to minimise total water and nutrient losses in the combined plant and fish systems.

The integrated model presented in this thesis combines a recirculating aquaculture system (RAS) sub-model with a greenhouse sub-model containing nutrient film technique (NFT) plant production. These sub-models describe the nitrogen dynamics and water and (to a lesser extent) energy balances in the different INAPRO system components. The sub-models are based on simple modelling principles using zero- and first-order dynamics, and use the Euler Forward method for numerically solving differential equations.

The model presented gives qualitative insight into the relations between the flows and nitrogen processes in the RAS and NFT systems. This is used to facilitate optimisation of the design and component sizing of the INAPRO system. For a full quantitative analysis, however, the model needs further calibration and validation.

It was found that both the fish and plant production systems show a cyclic behaviour, but their cycles are not in phase. This means that it is difficult to couple the two systems, because production and demand of water and nitrogen in the two systems do not always match. Some of the fluctuations can be absorbed by using buffer tanks, however, it was found that the buffer tank that buffers RAS water must be very large (250 m^3) if zero waste water discharge is to be achieved.

It was found that the optimisation goals for minimising water and nitrogen use and waste water discharge are mutually exclusive. Nitrogen fertiliser usage is at a minimum of about 35% when the NFT production area is 1000 m^2 or smaller, and increases when the NFT area is increased. RAS water discharge, however, is lowest at the largest NFT production area modelled (3000 m^2) and increases when the NFT production area is decreased. Clean water usage has a minimum at an NFT area of about 2500 m^2. Using arbitrary cost factors, an overall optimal solution was found at an NFT production area of 2100 m^2.

1. Introduction

1.1 Background

Maximising reuse of water and nutrients will be needed to meet future regulatory discharge demands and minimise spillage. Moreover, water and nutrient recycling contributes to food security of the XXI century.

In an aquaponics system, two food production systems are coupled; aquaculture (aquatic animal farming) and hydroponics (soilless plant farming) (Love et al. 2015). The nutrients excreted by the fish are used by the plants, which in turn clean the water that is recycled to the fish. In fact, this is a small scale example of a (closed) natural ecosystem with water and nutrient exchange.

In this thesis, a novel type of aquaponics system is discussed. This system is developed under the project name “Innovative model & demonstration-based water management for resource efficiency in integrated multitrophic aquaculture and horticulture systems” (INAPRO). INAPRO is a collaborative project that has received funding from the European Union’s Seventh Framework Programme (FP7)(Staaks 2015).

1.2 The INAPRO aquaponics system

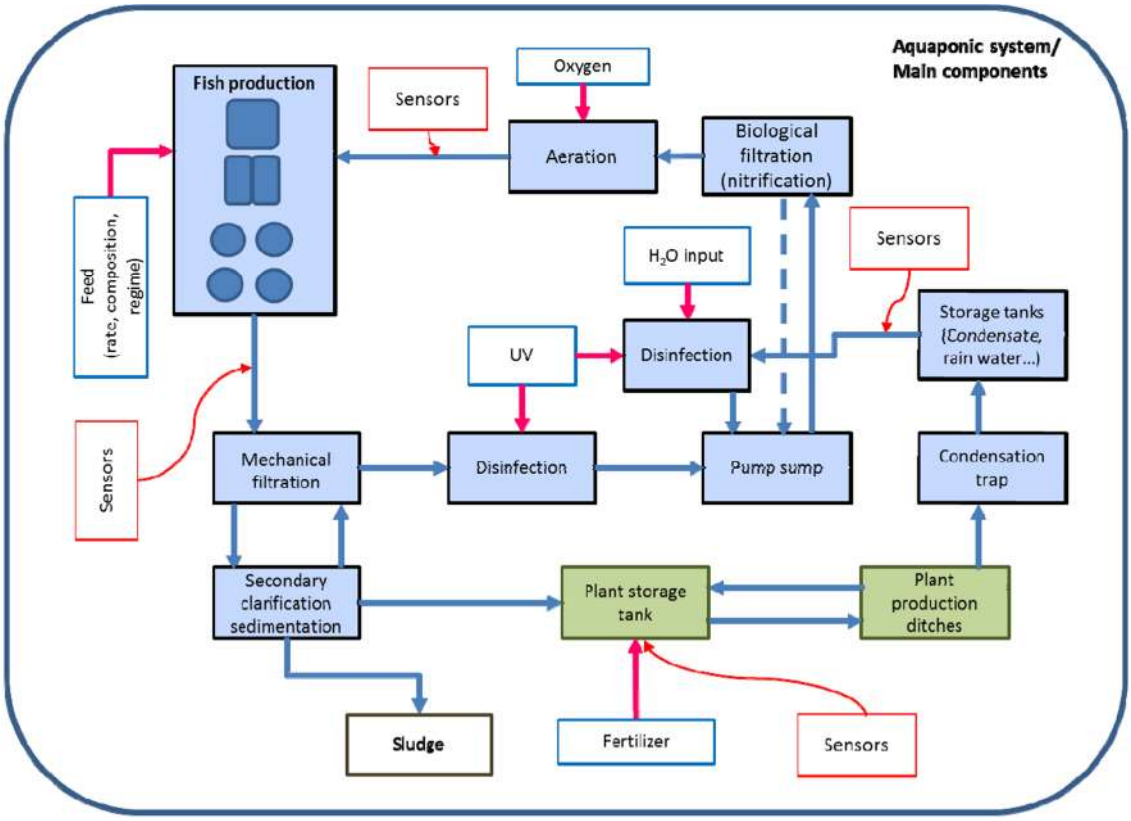

Figure 1 The INAPRO aquaponic system: water is exchanged between fish and crops

The aquaponic system developed in the INAPRO project combines breeding of Tilapia fish in a recirculating aquaculture system (RAS) and growing tomato plants in a separate nutrient film technique (NFT) system. The two systems are combined by way of water exchange at two exchange locations; from the RAS sedimentation tank to the NFT storage tank and from the NFT clean water storage tank to the RAS pump sump (Figure 1).

The novelty of the INAPRO aquaponic system and a possible advantage over other types of aquaponic systems lies in the decoupling of the two separate systems. Instead of directly recirculating water from the NFT gutters back to the RAS system, only the condensated, nutrient-free water from the greenhouse is used as a return flow. This allows for more freedom with respect to optimisation. For instance, fertiliser can be added to the NFT system without the need to consider its toxicity to fish.

The RAS consists of a loop that includes water treatment operations like filtration and nitrification. During the nitrification process, ammonium is converted to nitrate, which is less toxic to the fish than ammonium. Both ammonium and nitrate can be used by the tomato plants in the NFT system as nutrients for growth. The NFT system can also be described as a recirculating loop; the tomato plants are constantly fed by fertilised water from the storage tank, with a return flow containing the excess water.

The first coupling flow between RAS and greenhouse is established by periodic feeding of water from the RAS settling tank into the NFT buffer tank. The return coupling flow contains the evaporated water from the greenhouse, which is collected in a storage tank and fed back into the RAS pumping sump when needed.

1.3 Research questions

The goal of this thesis is to give insight into the processes and interactions of the RAS and NFT systems, so that the design of the INAPRO aquaponics system can be optimised. Experimental optimisation would be time consuming and expensive, because of the high interaction of processes and parameters in the two systems.

The main goal for the INAPRO project is to minimise RAS water discharge and total water usage. Furthermore, limiting the amount of plant fertiliser is investigated. Other goals include reduction of energy usage and CO_2 emissions, but these are not discussed in this thesis.

The following research questions will be treated in this thesis:

1. What are the relationships between flows and nitrogen processes in the RAS and NFT parts of the INAPRO system?
2. How can the design and component sizing of the INAPRO system be optimised to minimise:
    - RAS water discharge;
    - Clean water usage;
    - Nitrogen fertiliser usage?

1.4 Approach

No models integrating RAS and NFT systems were found in literature; therefore, a novel model was developed. This model is split up into two parts; a RAS sub-model including fish growth, flows and nitrogen processes; and an NFT sub-model including plant growth, greenhouse climate, flows and nitrogen processes. Only nitrogen is modelled; other nutrients required for plant growth are assumed to be either abundantly available in fish faeces (i.e. phosphorus) or available in such low amounts that it has to be added in the form of fertiliser (i.e. potassium).

The model is based on simple modelling principles using zero- and first-order dynamics. Processes and flows are modelled using ordinary differential equations (ODEs). These differential equations are solved numerically using the Euler forward method. The time step used is one hour, except for the fish and plant growth parts which use a time step of one day.

The model is built within a Microsoft Excel®-environment. Excel® was used, because it facilitates direct visualisation of simulation results and quick updating of input parameters.

Table 1 Main component sizes of the INAPRO aquaponic system

	Fish tanks	**Drum filter**	**Settling tank**	**Biological filter**	**NFT buffer tank**	**H_2O buffer tank**	**NFT production area**
Size	40 m^3	0.5 m^3 1 m^2	10 m^3	0.5 m^3 800 m^2	10 m^3 / 2-250 m^3‡	10 m^3	1000 m^2 / 100-3000 m^2‡

‡ these value ranges are used for design optimisation, discussed in Chapter 4.4

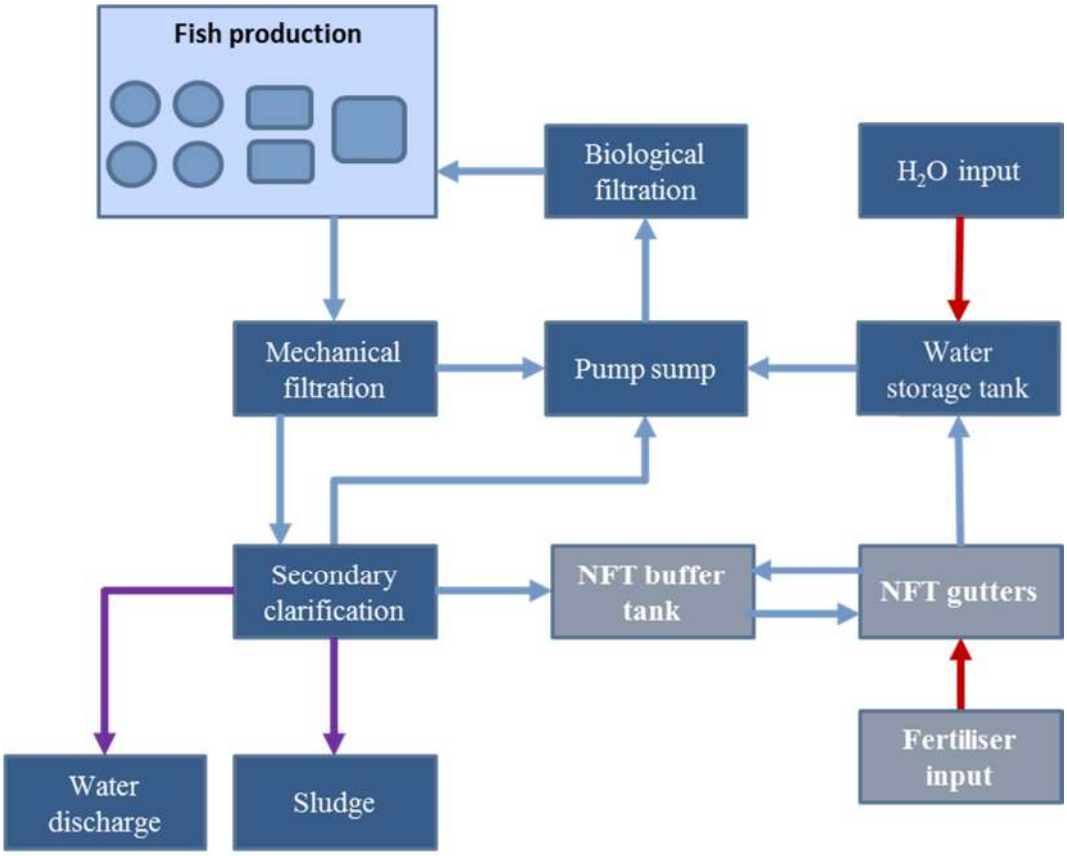

Figure 2 Essential elements of the INAPRO system model

Some components of the complete INAPRO system depicted in Figure 1; most notably disinfection and aeration; are not explicitly modelled. When modelling fish and plant growth and nitrification, oxygen is assumed to be always available in non-limiting amounts. An overview of the components modelled is depicted in Figure 2 and the sizing of the main components is shown in Table 1.

The input to the combined system is fish feed, water, fertiliser and a year-round climate scenario. The output includes fully grown fish and tomatoes, as well as discharged water and sludge.

For the greenhouse climate part of the NFT sub-model, a closed greenhouse is assumed with Dutch climate conditions. It is also assumed that a climate control system is included with temperature and humidity set points that are reached at all times. The potential presence of harmful (micro)organisms is not considered. Fish growth is assumed optimal at all times. Plant growth is assumed limited only by available photosynthetically active radiation (PAR); water and nutrients are assumed to be always available in amounts that are non-limiting to plant growth.

1.5 Outline of this thesis

The RAS model is developed in Chapter 2. Each tank component is discussed separately. The fish production sub-model is based on experimental data (IGB 2014). Sub-models for the drum filter and settling tank are designed specifically for this research. An overview of relevant nitrogen processes as well as a list of parameters is included in 2.8 Appendix.

In Chapter 3, the NFT model is developed. Again, each component is discussed separately. The plant growth model is based on a constant light use efficiency (LUE)(Heuvelink 1999), from which nitrogen uptake is calculated using a simulate uptake formula (Gallardo et al. 2009). Plant evaporation is based on research by C. Stanghellini (Stanghellini 1987; Prenger et al. 2002; Bontsema et al. 2011). A closed greenhouse climate model, based in part on research by R. van Ooteghem (Van Ooteghem 2007) is developed. An overview of relevant energy processes as well as a list of parameters is included in 3.8 Appendix.

Results are presented in Chapter 4. Individual results of the RAS and NFT systems are discussed, as well as the effect of coupling the two systems. Finally, results of design optimisation to minimise water discharge and water and fertiliser usage are also discussed.

2. RAS model

2.1 Introduction

The main goal for the RAS model is to calculate the amount and concentration of nutrients that need to be pumped to the NFT system or otherwise removed from the RAS system. To do this, fish growth, waste production and various nitrogen processes are modelled in different tank modules, and the water and nitrogen flows between the tanks are calculated.

The recirculating aquaculture system is modelled as consisting of tank modules, with one-way flows between tanks and with various processes inside the tanks.

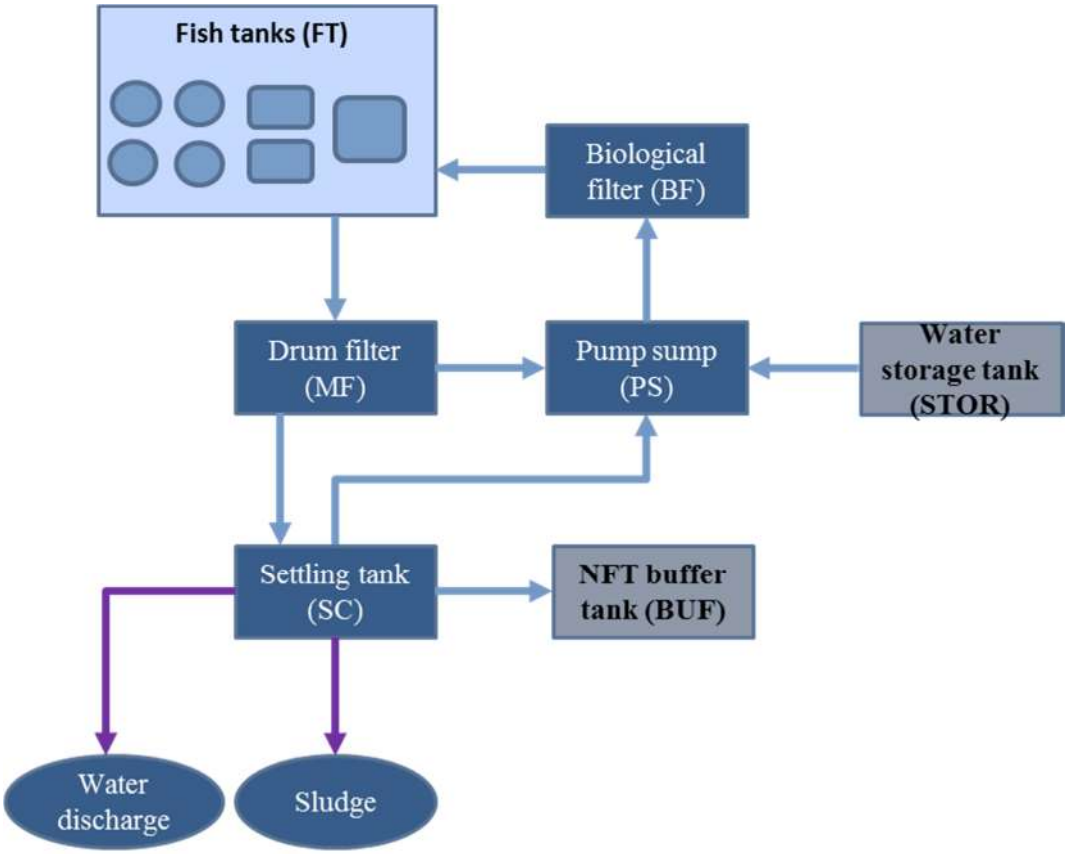

Figure 3 Overview of RAS system

The different tanks modelled in the RAS model are depicted as blue rectangles in Figure 3. There is a constant main recirculating flow between the fish tanks, the drum filter, the pump sump and the biological filter, flowing back to the fish tanks. A second recirculating flow contains the backwash from the drum filter which is fed to the settling tank, and the overflow returns to the main recirculating flow via the pump sump. Furthermore, discharge of water and sludge from the settling tank is modelled.

The coupling flows between the RAS and NFT systems are modelled by a flow of nutrient-rich water from the settling tank to the NFT buffer tank, and a return flow of clean water from the water storage tank to the pump sump in the RAS system.

Notation convention and abbreviations

In this chapter, all fluxes and compounds are given in the final units used. The unit used is included with every equation. Additionally, the following convention is used for notation:

- $\phi'_{x,y-z}$: a flow of component *x* from tank unit *y* to tank unit *z;*
- V_x: volume of water in tank *x;*
- $DV_x = \frac{dV_x}{dt}$: change in water volume in one time step in tank *x;*
- $C_{x,y}$: concentration of nitrogen component x in tank y;
- $m_{x,y}$: total mass of nitrogen component x in tank y;
- $Dm_{x,y} = \frac{dm_{x,y}}{dt}$: change in mass of nitrogen component x in tank y in one time step.

The following nitrogen compound abbreviations are used:

- TAN: total ammonia nitrogen (separated in ammonia and ammonium);
- NO_3: nitrate-N;
- sN_{org}: organic N in suspended solids;
- sTAN: TAN in suspended solids;
- sNO_3: nitrate-N in suspended solids;
- $setN_{org}$: organic N in settled solids;
- setTAN: TAN in settled solids;
- $setNO_3$: nitrate-N in settled solids.

The following tank unit abbreviations are used:

- BF: biological filter;
- FT: fish tanks;
- MF: mechanical filter (drum filter);
- SC: secondary clarifier (settling tank);
- BUF: NFT buffer tank;
- PS: pump sump;
- STOR: water storage tank.

The following abbreviations are used for production and consumption processes:

- ammon: ammonification of organic nitrogen;
- cond: condensation;
- disch: RAS water discharge;
- diss: dissolving of solids;
- evap: evaporation;
- fert: fertiliser addition;
- nit: nitrification of ammonia;
- resusp: resuspension of solids;
- set: settling of solids;
- sludge: sludge removal
- volat: volatilisation of ammonia.

Model description

In the model, fish growth and feed use is based on experimental data (IGB 2014). Feed evacuation is modelled as a constant percentage of feed use and a constant partitioning between solid excretion and gill excretion.

The RAS model is based on mass balances of water and selected nitrogen compounds. Interaction between the tanks takes places in the form of mass flows, modelled in most tanks as the product of the tank concentration of a specific nitrogen compound multiplied by the outflow of the tank. The mass balances for the tanks in Figure 3 are described in terms of inflow, outflow, production and accumulation, leading to a set of differential equations. In the model, these differential equations are solved numerically using the Euler Forward method. In this way, dynamic tank volumes and nitrogen compound masses inside the tanks can be calculated:

$$V_y(t) = V_y(t-1) + DV_y(t-1) \cdot \Delta t \qquad [l] \qquad (2.1)$$

$$m_{x,y}(t) = m_{x,y}(t-1) + Dm_{x,y}(t-1) \cdot \Delta t \qquad [mg_N] \qquad (2.2)$$

Where x denotes nitrogen compounds and y denotes the tank modelled. All masses, concentrations and buffer tank volumes are assumed zero at t=0.

Given the relatively large discrete time step used (one hour), transportation times between tanks or basins may be considered to be negligible. Therefore, the model does not incorporate volumes of water inside pipelines or gutters. All tanks are assumed to be perfectly mixed at all times, except for the settling tank which is modelled as a layer of perfectly mixed water and a separate layer of perfectly mixed sludge.

In the following sub-chapters, balances and fluxes are described in detail for every tank unit.

2.2 Fish

2.2.1 Fish growth

The fish growth model is made using fitted curves based on experimental data (IGB 2014). These curves describe the change of daily feeding weight per fish weight, feed conversion ratio and mortality rate of a single batch of tilapia during a 241 day long growth cycle. From this, the total fish stock, fish growth and feed input are calculated using a time step of 1 day.

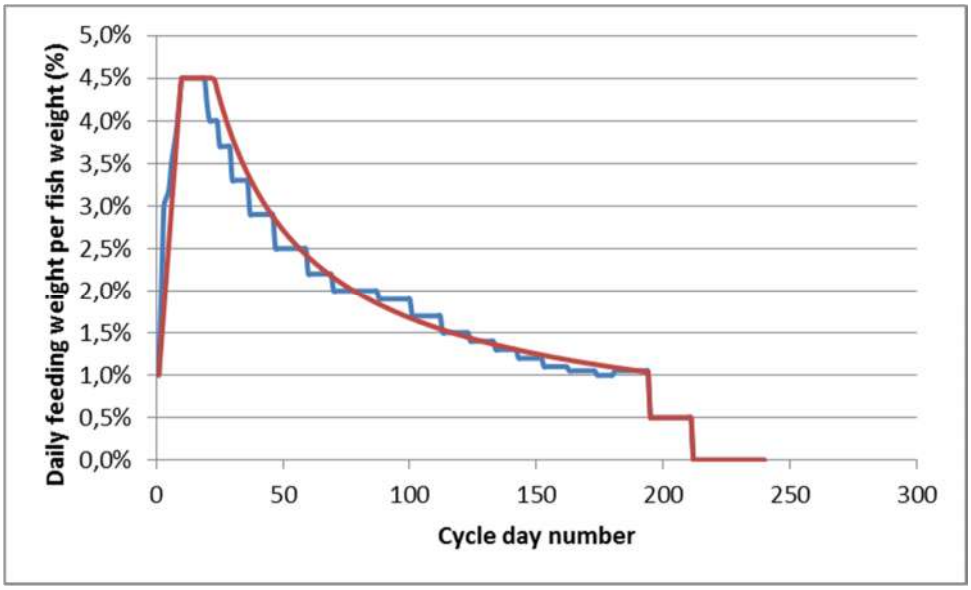

Figure 4 Feeding rate; data and fit curve

The change in feeding rate C_{feed}, depicted in Figure 4, is described by the following fit curve equations:

$$C_{feed} = \begin{cases} 0.00397 \cdot d_{cycle} + 0.996 \; if \; d_{cycle} < 10 \\ 0.045 \; if \; 10 \leq d_{cycle} < 24 \\ 0.5711 \cdot \left(d_{cycle} + 5.925\right)^{-0.7567} \; if \; 24 \leq d_{cycle} < 195 \\ 0.005 \; if \; 195 \leq d_{cycle} < 211 \\ 0 \; if \; d_{cycle} \geq 211 \end{cases} \quad [\%] \qquad (2.3)$$

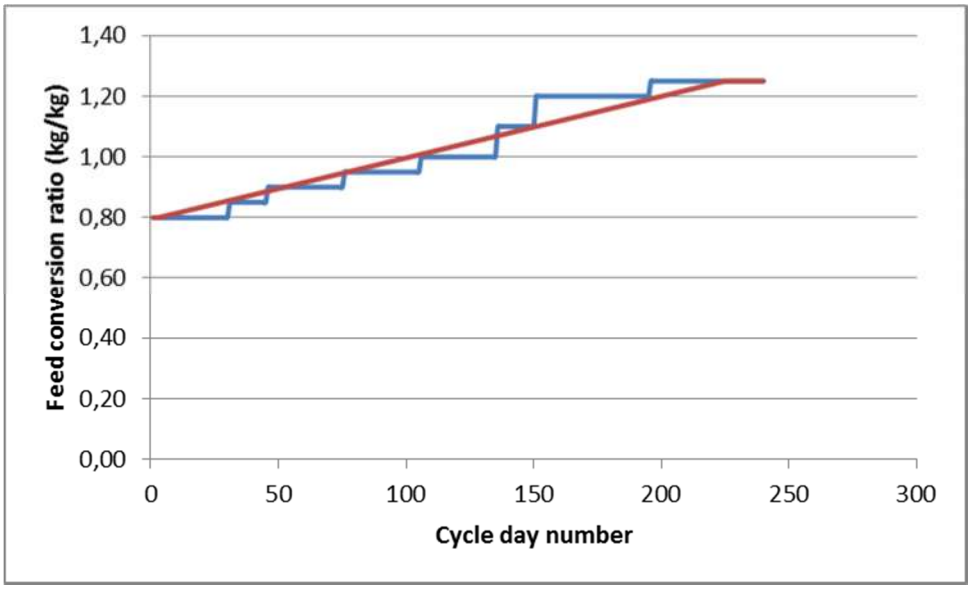

Figure 5 Feed conversion ratio (FCR); data and fit curve

The fish feed conversion ratio (FCR), expressed in required kg feed per kg fish growth, is expressed by the following fit curve equation:

$$FCR = \max\left(1.3, \quad 0.0021 \cdot d_{cycle} + 0.8\right) \qquad [kg\ kg^{-1}] \qquad (2.4)$$

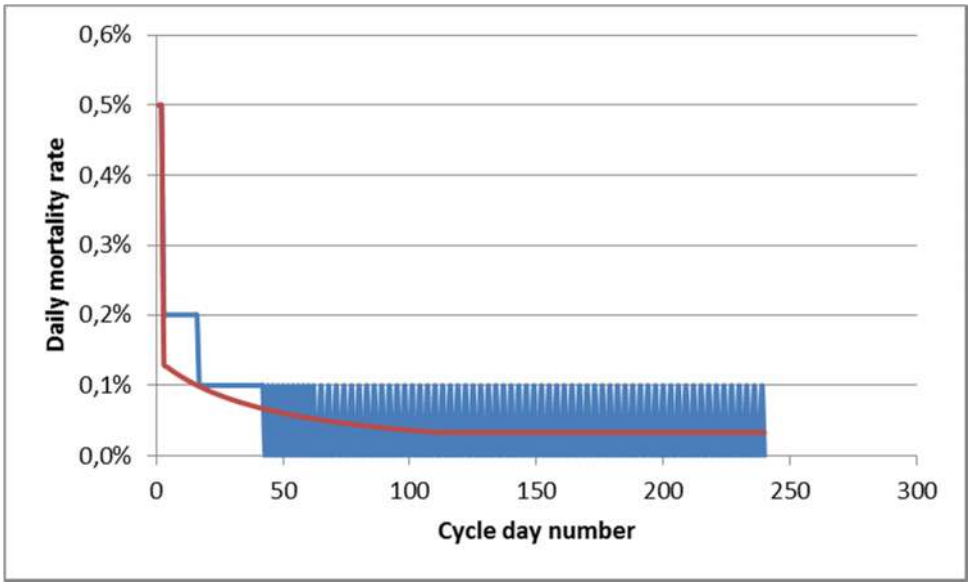

Figure 6 Daily mortality rate; data and fit curve

The daily fish mortality rate (DMR), expressed as percentage of total stock per day, is described by the following fit curve equations:

$$DMR = \begin{cases} 0.5\ if\ d_{cycle} < 3 \\ 0.3066 \cdot \left(d_{cycle} + 58.32\right)^{-1.328}\ if\ 3 \le d_{cycle} < 113 \\ 0.03038\ if\ d_{cycle} \ge 113 \end{cases} \qquad [\%\ day^{-1}] \qquad (2.5)$$

For every fish growth tank x, the total amount of feed fed daily $\phi''_{feed,x}$ is calculated by multiplying the modelled fish stock weight of that tank $m_{fish,x}$ with the cycle-dependent feeding rate $C_{feed,x}$:

$$\phi''_{feed,x} = C_{feed,x} \cdot m_{fish,x} \qquad [kg\ day^{-1}] \qquad (2.6)$$

The change in total fish stock (in kilograms) is calculated as the product of the feed input $\phi''_{feed,x}$ and the cycle dependent feed conversion ratio FCR, minus mortality expressed as the product of the daily mortality rate DMR multiplied by the stock and the amount of fish harvested:

$$Dm_{fish,x} = \phi''_{feed,x} \cdot FCR_x - m_{fish,x} \cdot DMR_x - harvest_x \qquad [kg\ day^{-1}] \qquad (2.7)$$

The fish stock $m_{fish,x}$ for every growth tank x, expressed in kilograms, is then calculated by adding the change in stock of the previous time step to the fish stock of the previous time step:

$$m_{fish,x}(t) = m_{fish,x}(t-1) + Dm_{fish,x}(t-1) \qquad [kg] \qquad (2.8)$$

2.2.2 Staggered fish production

The fish growth cycles are staggered over different fish production tanks. Each batch of fish starts in the fingerling tank. After two months, the batch is divided into two raising tanks. After seven months, the two batches are transported to a store tank where the growth cycle is completed after eight months. Each fish batch is harvested in four harvests of equal total weight, halfway and at the end of month seven and eight.

In the model, the amount of time between cycles in the raising tanks can be set to either alternating between two and three months or to a constant two and a half months.

The total amount of daily feed is the sum of the feed amount of all current fish batches in all tanks combined:

$$\phi''_{feed} = \sum \phi''_{feed,x} \qquad [kg\ day^{-1}] \qquad (2.9)$$

2.2.3 Fish nitrogen production

In order to go from the one day time step used in the fish growth model to the one hour time step used in the rest of the RAS model, the hourly influx of nitrogen from fish feed is calculated. This is done by taking the daily feeding rate ϕ''_{feed} calculated in *Chapter 2.2.1 Fish growth*, and using a constant protein N content of 16%, and a set feeding regime (feeding 25% of daily feed input at 00:00, 08:00, 12:00, and 16:00).

$$\phi'_{N,feed} = \begin{cases} \phi''_{feed} \cdot C_{feed,protein} \cdot 0.16 \cdot \frac{10^6}{4} \; if \; feeding \; time \\ 0 \; otherwise \end{cases} \qquad [mg_N \; h^{-1}] \qquad (2.10)$$

The feed input from the fish growth model is distributed over different parts with distribution percentages that are assumed to remain constant during the fish production cycles. Nitrogen is converted into fish growth with a fish nitrogen accumulation efficiency of 32%. The remaining part of the feed is either excreted through the fish gills in liquid form, ending up as ammonia in the fish tanks ($\phi'_{TAN,FT,fish}$, 40% of total), or excreted as faeces in solid form ($\phi'_{sN_{org},FT,fish}$, 28% of total)(Rafiee & Saad 2005). It is assumed that fish excretion remains constant throughout the day. Therefore, the average nitrogen feeding value is used for calculating excretion instead of the actual value based on the feeding time regime:

$$\phi'_{N,feed,avg} = \phi''_{feed} \cdot C_{feed,protein} \cdot 0.16 \cdot \frac{10^6}{24} \qquad [mg_N \; h^{-1}] \qquad (2.11)$$

$$\phi'_{TAN,FT,fish} = 0.40 \cdot \phi'_{N,feed,avg} \qquad [mg_N \; h^{-1}] \qquad (2.12)$$

$$\phi'_{sN_{org},FT,fish} = 0.28 \cdot \phi'_{N,feed,avg} \qquad [mg_N \; h^{-1}] \qquad (2.13)$$

Modelling of feed that is left uneaten is described in *Chapter 2.3 Fish tanks*.

2.3 Fish tanks

For the purpose of calculating the water and nitrogen balances, all the separate fish tanks, including the fingerling, raising and store tanks combined are modelled as a single well-stirred tank.

Water balance

The total volume is considered constant; water accumulation is zero. Outflow to the mechanical filter is then equal to the inflow from the biological filter minus evaporation:

$$DV_{FT} = \phi'_{H_2O,BF-FT} - \phi'_{H_2O,FT-MF} - \phi'_{H_2O,FT,evap} = 0 \qquad [l \; h^{-1}] \qquad (2.14)$$

Water fluxes

Equations for the water fluxes in *eq. (2.14)* are given in *Appendices 2.8.1 Water flows* and *2.8.2 Evaporation from tanks*.

Nitrogen balances

In the fish tanks, nitrogen is added in the form of uneaten fish feed, solids excreted by fish and fish gill excretion. Furthermore, dissolving of solids, volatilisation of ammonia, ammonification and nitrification in solids are modelled:

$$Dm_{NO_3,FT} = \phi'_{NO_3,BF-FT} - \phi'_{NO_3,FT-MF} + \phi'_{sNO_3,FT,diss} \quad [mg_N\ h^{-1}] \quad (2.15)$$

$$Dm_{TAN,FT} = \phi'_{TAN,BF-FT} - \phi'_{TAN,FT-MF} + \phi'_{TAN,FT,fish} + \phi'_{sTAN,FT,diss} - \phi'_{TAN,FT,volat} \quad [mg_N\ h^{-1}] \quad (2.16)$$

$$Dm_{sN_{org},FT} = \phi'_{sN_{org},BF-FT} - \phi'_{sN_{org},FT-MF} + \phi'_{sN_{org},FT,fish} + \phi'_{sN_{org},FT,uneat} - \phi'_{sN_{org},FT,ammon} \quad [mg_N\ h^{-1}] \quad (2.17)$$

$$Dm_{sTAN,FT} = \phi'_{sTAN,BF-FT} - \phi'_{sTAN,FT-MF} + \phi'_{sN_{org},FT,ammon} - \phi'_{sTAN,FT,nit} - \phi'_{sTAN,FT,diss} \quad [mg_N\ h^{-1}] \quad (2.18)$$

$$Dm_{sNO_3,FT} = \phi'_{sNO_3,BF-FT} - \phi'_{sNO_3,FT-MF} + \phi'_{sTAN,FT,nit} - \phi'_{sNO_3,FT,diss} \quad [mg_N\ h^{-1}] \quad (2.19)$$

Nitrogen fluxes

Feed left uneaten is only modelled to take into account nitrogen in organic form. The total amount of feed fed to the fish is calculated by modifying the feed uptake with a feeding efficiency $\eta_{feed} = 95\%$. This same constant is then used to calculate the amount of feed left uneaten:

$$\phi'_{sN_{org},FT,uneat} = \left(1 - \eta_{feed}\right) \cdot \frac{\phi'_{N,feed}}{\eta_{feed}} \quad [mg_N\ h^{-1}] \quad (2.20)$$

Fish faeces production and TAN production from fish gills are described in *Chapter 2.2.3 Fish nitrogen production*. Other nitrogen fluxes are described in *Appendices 2.8.3 Nitrogen flows*, *2.8.4 Volatilisation of ammonia*, *2.8.5 Ammonification*, *2.8.6 Nitrification* and *2.8.7 Dissolving of solids.*

2.4 Drum filter

The mechanical filter is modelled as a drum filter that is assumed to have a constant solids removal efficiency of 70%. This means that 70% of the total solids inflow is accumulated on the drum screen and leaves the filter as backwash flow to the secondary clarifier, and that 30% of the solids pass the filter unaffected and continue to the pump sump. All solids are assumed to be equal in particle size; the effect of different particle sizes is not modelled.

Water balance

The volume of water in the drum filter is considered constant; water accumulation is zero. The amount of water flowing to the pump sump $\phi'_{H_2O,MF-PS}$ is then calculated as the inflow from the fish tanks $\phi'_{H_2O,FT-MF}$ minus the backwash flow $\phi'_{H_2O,MF-SC}$:

$$DV_{MF} = \phi'_{H_2O,FT-MF} - \phi'_{H_2O,MF-SC} + \phi'_{H_2O,MF-PS} = 0 \qquad [l\ h^{-1}] \qquad (2.21)$$

Water fluxes

Of the total water flow through the drum filter, $\eta_{backw} = 1\%$ is used for backwashing to remove solids from the filter screen. This water with solids flows to the settling tank:

$$\phi'_{H_2O,MF-SC} = \eta_{backw} \cdot \phi'_{H_2O,FT-MF} \qquad [l\ h^{-1}] \qquad (2.22)$$

Other water fluxes are described in *Appendix 2.8.1 Water flows*.

Nitrogen balances

It is assumed that on the drum filter screen, a small amount of TAN nitrification takes place. Furthermore, volatilisation of ammonia, ammonification, and nitrification in solids are modelled:

$$Dm_{NO_3,MF} = \phi'_{NO_3,FT-MF} - \phi'_{NO_3,MF-SC} - \phi'_{NO_3,MF-PS} + \phi'_{TAN,MF,nit} \qquad [mg_N\ h^{-1}] \qquad (2.23)$$

$$Dm_{TAN,MF} = \phi'_{TAN,FT-MF} - \phi'_{TAN,MF-SC} - \phi'_{sTAN,MF-PS} - \phi'_{TAN,MF,nit} - \phi'_{TAN,MF,volat} \qquad [mg_N\ h^{-1}] \qquad (2.24)$$

$$Dm_{sN_{org},MF} = \phi'_{sN_{org},FT-MF} - \phi'_{sN_{org},MF-SC} - \phi'_{sN_{org},MF-PS} - \phi'_{sN_{org},MF,ammon} \qquad [mg_N\ h^{-1}] \qquad (2.25)$$

$$Dm_{sTAN,MF} = \phi'_{sTAN,FT-MF} - \phi'_{sTAN,MF-SC} - \phi'_{sTAN,MF-PS} + \phi'_{sN_{org},MF,ammon} - \phi'_{sTAN,MF,nitr} \qquad [mg_N\ h^{-1}] \qquad (2.26)$$

$$Dm_{sNO_3,MF} = \phi'_{sNO_3,FT-MF} - \phi'_{sNO_3,MF-SC} - \phi'_{sNO_3,MF-PS} + \phi'_{sTAN,MF,nitr} \qquad [mg_N\ h^{-1}] \qquad (2.27)$$

Nitrogen fluxes

A constant solids removal efficiency of $\eta_{MF} = 70\%$ is assumed. This means that only 30% of the inflowing solids continues to the pump sump, and the rest is backwashed from the drum screen to the settling tank:

$$\phi'_{sN_{org},MF-PS} = (1-\eta_{MF}) \cdot \left(\phi'_{sN_{org},FT-MF} - \phi'_{sN_{org},MF,ammon}\right) \quad [mg_N\ h^{-1}] \quad (2.28)$$

$$\phi'_{sTAN,MF-PS} = (1-\eta_{MF}) \cdot \left(\phi'_{sTAN,FT-MF} + \phi'_{sN_{org},MF,ammon} - \phi'_{sTAN,MF,nitr}\right) \quad [mg_N\ h^{-1}] \quad (2.29)$$

$$\phi'_{sNO_3,MF-PS} = (1-\eta_{MF}) \cdot \left(\phi'_{sNO_3,FT-MF} + \phi'_{sTAN,MF,nitr}\right) \quad [mg_N\ h^{-1}] \quad (2.30)$$

$$\phi'_{sN_{org},MF-SC} = \eta_{MF} \cdot \left(\phi'_{sN_{org},FT-MF} - \phi'_{sN_{org},MF,ammon}\right) \quad [mg_N\ h^{-1}] \quad (2.31)$$

$$\phi'_{sTAN,MF-SC} = \eta_{MF} \cdot \left(\phi'_{sTAN,FT-MF} + \phi'_{sN_{org},MF,ammon} - \phi'_{sTAN,MF,nitr}\right) \quad [mg_N\ h^{-1}] \quad (2.32)$$

$$\phi'_{sNO_3,MF-SC} = \eta_{MF} \cdot \left(\phi'_{sNO_3,FT-MF} + \phi'_{sTAN,MF,nitr}\right) \quad [mg_N\ h^{-1}] \quad (2.33)$$

Other relevant nitrogen fluxes are described in *Appendices 2.8.3 Nitrogen flows*, *2.8.4 Volatilisation of ammonia*, *2.8.5 Ammonification* and *2.8.6 Nitrification*.

2.5 Settling tank

The settling tank (secondary clarifier) is modelled as a two layered system, consisting of a layer containing suspended solids and a layer containing settled solids. Both layers are assumed to be perfectly mixed. The clarifier is assumed to have a settling efficiency of 60%, meaning that 60% of the total nitrogen inflow (from the mechanical filter into the suspended solids layer) is settled into the settled solids layer. Additionally, 5% of the settled solids is assumed to re-suspend into the suspended solids layer every hour by any turbulence occurring. The overflow of the clarifier is returned to the RAS or fed to the NFT tank when needed, as calculated in the volumes and flows sub-model. (Figure 7). An additional screen filter is modelled for the flow to the NFT buffer tank; it is assumed to have a solids removal efficiency of 60%. The settling and resuspension of solids in the NFT buffer tank is modelled the same way as in the settling tank.

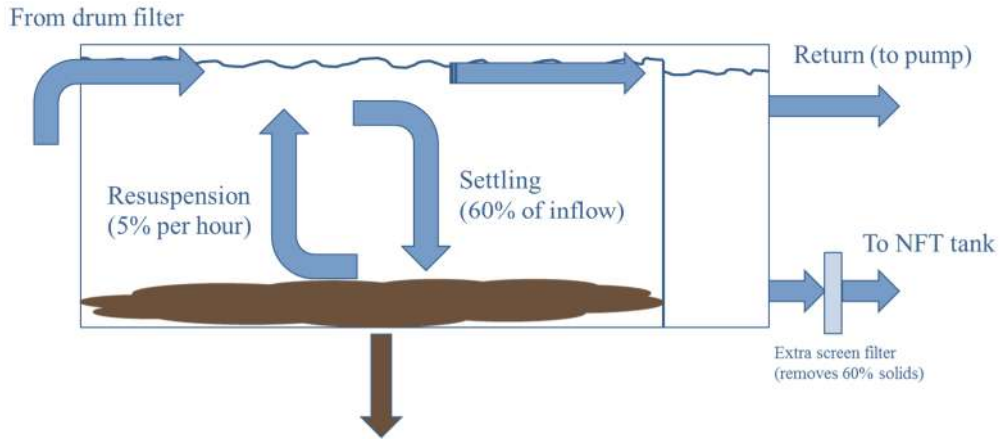

Figure 7 Settling and resuspension of solids in secondary clarifier

The settled solids layer builds up till it is in equilibrium with the suspended solids layer in the case of the NFT buffer tank, and is removed completely every day in the case of the settling tank in the RAS system.

Water balance

$$DV_{SC} = \phi'_{H_2O,MF-SC} - \phi'_{H_2O,SC-PS} - \phi'_{H_2O,SC-BUF} - \phi'_{H_2O,SC,sludge} - \phi'_{H_2O,SC,disch} - \phi'_{H_2O,SC,evap} \quad [l\,h^{-1}] \quad (2.34)$$

Water fluxes

$$\phi'_{H_2O,SC-BUF,const} = u_{F,SC,BUF} \quad [l\,h^{-1}] \quad (2.35)$$

$$\phi'_{H_2O,SC-BUF,fb} = u_{F,SC,BUF} \cdot \frac{\phi'_{N,feed}}{\phi'_{N,feed,avgy}} \quad [l\,h^{-1}] \quad (2.36)$$

where $\phi'_{N,feed,avgy}$ is the hourly rate of nitrogen in feed, averaged over one year.

$$\phi'_{H_2O,SC-BUF,reg} = C_{coupl,const} \cdot \phi'_{H_2O,SC-BUF,const} + (1 - C_{coupl,const}) \cdot \phi'_{H_2O,SC-BUF,fb} \quad [l\,h^{-1}] \quad (2.37)$$

The regular coupling flow between RAS and NFT (eq. (2.37)) is described by two cases:

1. Coupling flow is constant; $\phi'_{H_2O,SC-BUF,const}$ is used
2. Coupling flow is linearly dependent on the amount of fish feed fed into the RAS system; $\phi'_{H_2O,SC-BUF,fb}$ is used.

Excel® solver is used to find the minimum RAS-NFT coupling flow $u_{F,SC,BUF}$ required to keep the fish tank NO_3 concentration below an arbitrary value of 100 mg N/l.

Furthermore, if the NFT buffer tank volume is low, coupling flow is increased to keep the NFT buffer level at a minimum of 10% nominal volume:

$$\phi'_{H_2O,SC-BUF,x} = max\big(0.1p_{V,BUF} - V_{BUF} + \phi'_{H_2O,NFT-plants},\ \phi'_{H_2O,SC-BUF,reg}\big) \quad [l\ h^{-1}] \quad (2.38)$$

Coupling flow is stopped completely when it would cause an overflow of the NFT buffer tank. In case coupling flow is stopped, water from the RAS system is discharged to the sewage system instead:

$$\phi'_{H_2O,SC-BUF} = \big(1 - C_{SC,disch}\big) \cdot \phi'_{H_2O,SC-BUF,x} \quad [l\ h^{-1}] \quad (2.39)$$

$$\phi'_{H_2O,SC,disch} = C_{SC,disch} \cdot \phi'_{H_2O,SC-BUF,x} \quad [l\ h^{-1}] \quad (2.40)$$

$$C_{SC,disch} = \begin{cases} 1\ if\ V_{BUF} + \phi'_{H_2O,SC-BUF,x} - \phi'_{H_2O,NFT-plants} > p_{V,BUF} \\ 0\quad otherwise \end{cases} \quad [-] \quad (2.41)$$

If the settling tank is full, any excess inflowing water will overflow to the pump sump:

$$\phi'_{H_2O,SC-PS} = C_{SC,full} \cdot (\phi'_{H_2O,MF-SC} - \phi'_{H_2O,SC-BUF} - \phi'_{H_2O,SC,sludge} - \phi'_{H_2O,SC,disch} - \phi'_{H_2O,SC,evap}) \quad [l\ h^{-1}] \quad (2.42)$$

$$C_{SC,full} = \begin{cases} 1\ if\ V_{SC} > 10000 \\ 0\quad otherwise \end{cases} \quad [-] \quad (2.43)$$

Other water fluxes are described in *Appendices 2.8.1 Water flows, 2.8.2 Evaporation from tanks* and *2.8.10 Sludge removal*.

Nitrogen balances

The daily build-up of sludge is taken into account by modelling settling and resuspension. The build-up of sludge is assumed to be removed completely when drainage takes place. Furthermore, dissolving of solids, volatilisation of ammonia, ammonification, and nitrification in solids are modelled:

$$Dm_{NO_3,SC} = \phi'_{NO_3,MF-SC} - \phi'_{NO_3,SC-PS} - \phi'_{NO_3,SC-BUF} - \phi'_{NO_3,SC,sludge} - \phi'_{NO_3,SC,disch} + \phi'_{sNO_3,SC,diss} + \phi'_{setNO_3,SC,diss} \quad [mg_N\ h^{-1}] \quad (2.44)$$

$$Dm_{TAN,SC} = \phi'_{TAN,MF-SC} - \phi'_{TAN,SC-PS} - \phi'_{TAN,SC-BUF} - \phi'_{TAN,SC,sludge} - \phi'_{TAN,SC,disch} + \phi'_{sTAN,SC,diss} + \phi'_{setTAN,SC,diss} - \phi'_{TAN,SC,volat} \quad [mg_N\ h^{-1}] \quad (2.45)$$

$$Dm_{sN_{org},SC} = \phi'_{sN_{org},MF-SC} - \phi'_{sN_{org},SC-PS} - \phi'_{sN_{org},SC-BUF} - \phi'_{sN_{org},SC,sludge} - \phi'_{sN_{org},SC,disch} - \phi'_{sN_{org},SC,set} + \phi'_{setN_{org},SC,resusp} - \phi'_{sN_{org},SC,ammon} \quad [mg_N\ h^{-1}] \quad (2.46)$$

$$Dm_{sTAN,SC} = \phi'_{sTAN,MF-SC} - \phi'_{sTAN,SC-PS} - \phi'_{sTAN,SC-BUF} - \phi'_{sTAN,SC,sludge} - \phi'_{sTAN,SC,disch} - \phi'_{sTAN,SC,set} + \phi'_{setTAN,SC,resusp} + \phi'_{sN_{org},SC,ammon} - \phi'_{sTAN,SC,diss} - \phi'_{sTAN,SC,nit} \quad [mg_N\ h^{-1}] \quad (2.47)$$

$$Dm_{sNO_3,SC} = \phi'_{sNO_3,MF-SC} - \phi'_{sNO_3,SC-PS} - \phi'_{sNO_3,SC-BUF} - \phi'_{sNO_3,SC,sludge} - \phi'_{sNO_3,SC,disch} + \phi'_{sTAN,SC,nit} - \phi'_{sNO_3,SC,set} + \phi'_{setNO_3,SC,resusp} - \phi'_{sNO_3,SC,diss} \quad [mg_N\ h^{-1}] \quad (2.48)$$

$$Dm_{setN_{org},SC} = \phi'_{sN_{org},SC,set} - \phi'_{setN_{org},SC,resusp} - \phi'_{setN_{org},SC,ammon} - \phi'_{setN_{org},SC,sludge} \quad [mg_N\ h^{-1}] \quad (2.49)$$

$$Dm_{setTAN,SC} = \phi'_{sTAN,SC,set} - \phi'_{setTAN,SC,resusp} + \phi'_{setN_{org},SC,ammon} - \phi'_{setTAN,SC,diss} - \phi'_{setTAN,SC,nit} - \phi'_{setTAN,SC,sludge} \quad [mg_N\ h^{-1}] \quad (2.50)$$

$$Dm_{setNO_3,SC} = \phi'_{sNO_3,SC,set} - \phi'_{setNO_3,SC,resusp} + \phi'_{setTAN,SC,nit} - \phi'_{setNO_3,SC,diss} - \phi'_{setNO_3,SC,sludge} \quad [mg_N\ h^{-1}] \quad (2.51)$$

Nitrogen fluxes

Relevant nitrogen fluxes are described in *Appendices 2.8.3 Nitrogen flows*, *2.8.4 Volatilisation of ammonia*, *2.8.5 Ammonification*, *2.8.6 Nitrification*, *2.8.7 Dissolving of solids, 2.8.8* Settling of solids, *2.8.9 Resuspension of settled solids* and *2.8.10 Sludge removal.*

2.6 Biological filter

Ammonia is toxic to tilapia in low concentrations, but tilapia can cope with relatively high levels of nitrate. The RAS therefore contains a biological (nitrifying) filter, in which ammonium is converted into nitrate (NO_3^-). Nitrification is modelled with one of two options:

1. A set percentage of 60% of incoming TAN is nitrified and leaves the filter as NO_3;
2. The nitrification rate is surface area and TAN concentration dependent (Greiner & Timmons 1998), with a maximum nitrification percentage of 60%.

Water balance

Water accumulation DV_{BF} in the biological filter is assumed zero; the water volume is considered constant. The outflow to the fish tanks $\phi'_{H_2O,BF-FT}$ is then equal to the inflow from the pump sump $\phi'_{H_2O,PS-BF}$ minus evaporation $\phi'_{H_2O,BF,evap}$:

$$DV_{BF} = \phi'_{H_2O,PS-BF} - \phi'_{H_2O,BF-FT} - \phi'_{H_2O,BF,evap} = 0 \qquad [l\ h^{-1}] \qquad (2.52)$$

Water fluxes

Water fluxes are described in *Appendices 2.8.1 Water flows* and *2.8.2 Evaporation from tanks*.

Nitrogen balances

Inside the biological filter, nitrification of TAN takes place. Furthermore, volatilisation of ammonia, ammonification, and nitrification in solids are modelled:

$$Dm_{NO_3,BF} = \phi'_{NO_3,PS-BF} - \phi'_{NO_3,BF-FT} + \phi'_{TAN,BF,nit} \qquad [mg_N\ h^{-1}] \qquad (2.53)$$

$$Dm_{TAN,BF} = \phi'_{TAN,PS-BF} - \phi'_{TAN,BF-FT} - \phi'_{TAN,BF,nit} - \phi'_{TAN,BF,volat} \qquad [mg_N\ h^{-1}] \qquad (2.54)$$

$$Dm_{sN_{org},BF} = \phi'_{sN_{org},PS-BF} - \phi'_{sN_{org},BF-FT} - \phi'_{sN_{org},BF,ammon} \qquad [mg_N\ h^{-1}] \qquad (2.55)$$

$$Dm_{sTAN,BF} = \phi'_{sTAN,PS-BF} - \phi'_{sTAN,BF-FT} + \phi'_{sN_{org},BF,ammon} - \phi'_{sTAN,BF,nit} \qquad [mg_N\ h^{-1}] \qquad (2.56)$$

$$Dm_{sNO_3,BF} = \phi'_{sNO_3,PS-BF} - \phi'_{sNO_3,BF-FT} + \phi'_{sTAN,BF,nit} \qquad [mg_N\ h^{-1}] \qquad (2.57)$$

Nitrogen fluxes

Relevant nitrogen fluxes are described in *Appendices 2.8.3 Nitrogen flows*, *2.8.4 Volatilisation of ammonia*, *2.8.5 Ammonification* and *2.8.6 Nitrification*.

2.7 Pump sump

The pump sump contains pumps for the recirculation flow. The flow rate of these pumps $\phi'_{H_2O,PS-BF}$ is considered constant. It is assumed that the pump sump volume is so small relatively to the amount of water pumped every time step, that no nitrogen processes take place. No nitrogen accumulation is modelled and outflow is equalled to inflow. The water volume inside the sump is also considered to be constant.

Water balance

$$DV_{PS} = \phi'_{H_2O,MF-PS} + \phi'_{H_2O,SC-PS} + \phi'_{H_2O,STOR-PS} - \phi'_{H_2O,PS-BF} = 0 \qquad [l\ h^{-1}] \qquad (2.58)$$

Water fluxes

Excel® solver can be used to find the minimum RAS pump flow $\phi'_{H_2O,PS-BF}$ required to keep the fish tank TAN concentration below an arbitrary value.

When outflow to the biological filter is greater than inflow from the drum filter and settling tank, water from the water storage tank is added:

$$\phi'_{H_2O,STOR-PS} = \phi'_{H_2O,PS-BF} - \phi'_{H_2O,MF-PS} - \phi'_{H_2O,SC-PS} \qquad [l\ h^{-1}] \qquad (2.59)$$

Other water fluxes are described in *Appendix 2.8.1 Water flows*.

Nitrogen balances

No nitrogen processes or accumulation in the pump sump are modelled. The outflow of nitrogen to the biological filter is then equal to the sum of inflows:

$$Dm_{NO_3,PS} = \phi'_{NO_3,MF-PS} + \phi'_{NO_3,SC-PS} - \phi'_{NO_3,PS-BF} = 0 \qquad [mg_N\ h^{-1}] \qquad (2.60)$$

$$Dm_{TAN,PS} = \phi'_{TAN,MF-PS} + \phi'_{TAN,SC-PS} - \phi'_{TAN_3,PS-BF} = 0 \qquad [mg_N\ h^{-1}] \qquad (2.61)$$

$$Dm_{sN_{org},PS} = \phi'_{sN_{org},MF-PS} + \phi'_{sN_{org},SC-PS} - \phi'_{sN_{org},PS-BF} = 0 \qquad [mg_N\ h^{-1}] \qquad (2.62)$$

$$Dm_{sTAN,PS} = \phi'_{sTAN,MF-PS} + \phi'_{sTAN,SC-PS} - \phi'_{sTAN,PS-BF} = 0 \qquad [mg_N\ h^{-1}] \qquad (2.63)$$

$$Dm_{sNO_3,PS} = \phi'_{sNO_3,MF-PS} + \phi'_{sNO_3,SC-PS} - \phi'_{sNO_3,PS-BF} = 0 \qquad [mg_N\ h^{-1}] \qquad (2.64)$$

Nitrogen fluxes

Relevant nitrogen fluxes are described in *Appendix 2.8.3 Nitrogen flows.*

2.8 Appendix

2.8.1 Water flows

Water flows in the RAS system are defined by a constant recirculation flow $\phi'_{H_2O,PS-BF}$ from the pump sump; other flows are calculated as the remainder of this flow after evaporation and outgoing flows are subtracted.

$$\phi'_{H_2O,PS-BF} = 45000 \quad [l\ h^{-1}] \quad (2.65)$$

$$\phi'_{H_2O,BF-FT} = \phi'_{H_2O,PS-BF} - \phi'_{H_2O,BF,evap} \quad [l\ h^{-1}] \quad (2.66)$$

$$\phi'_{H_2O,FT-MF} = \phi'_{H_2O,BF-FT} - \phi'_{H_2O,FT,evap} \quad [l\ h^{-1}] \quad (2.67)$$

$$\phi'_{H_2O,MF-PS} = \phi'_{H_2O,FT-MF} - \phi'_{H_2O,MF-SC} \quad [l\ h^{-1}] \quad (2.68)$$

2.8.2 Evaporation from tanks

Tank evaporation is modelled as an (arbitrary) constant flow, with a constant condensation rate of 90%:

$$\phi'_{H_2O,BF,evap} = 5 \cdot (1 - \eta_{cond}) \quad [l\ h^{-1}] \quad (2.69)$$

$$\phi'_{H_2O,FT,evap} = 10 \cdot (1 - \eta_{cond}) \quad [l\ h^{-1}] \quad (2.70)$$

$$\phi'_{H_2O,SC,evap} = 5 \cdot (1 - \eta_{cond}) \quad [l\ h^{-1}] \quad (2.71)$$

2.8.3 Nitrogen flows

Outgoing nitrogen flows (between tanks) are calculated as the product of the water flow leaving the tank and the nitrogen compound concentration inside the tank. In the case of the pump sump, outgoing nitrogen flow is equalled to the incoming nitrogen flow. Outgoing nitrogen flows of the drum filter are described in Chapter 2.4.

$$\phi'_{x,BF-FT} = \phi'_{H_2O,BF-FT} \cdot c_{x,BF} \quad [mg_N\ h^{-1}] \quad (2.72)$$

$$\phi'_{x,FT-MF} = \phi'_{H_2O,FT-MF} \cdot c_{x,FT} \quad [mg_N\ h^{-1}] \quad (2.73)$$

$$\phi'_{x,SC-PS} = \phi'_{H_2O,SC-PS} \cdot c_{x,SC} \quad [mg_N\ h^{-1}] \quad (2.74)$$

$$\phi'_{x,SC-BUF} = \phi'_{H_2O,SC-BUF} \cdot c_{x,SC} \quad [mg_N\ h^{-1}] \quad (2.75)$$

$$\phi'_{x,SC,disch} = \phi'_{H_2O,SC,disch} \cdot c_{x,SC} \quad [mg_N\ h^{-1}] \quad (2.76)$$

$$\phi'_{x,SC,sludge} = \phi'_{H_2O,SC,sludge} \cdot c_{x,SC} \quad [mg_N\ h^{-1}] \quad (2.77)$$

$$\phi'_{x,PS-BF} = \phi'_{x,MF-PS} + \phi'_{x,SC-PS} \quad [mg_N\ h^{-1}] \quad (2.78)$$

$$\phi'_{x,STOR-PS} = 0 \quad [mg_N\ h^{-1}] \quad (2.79)$$

Where $x = TAN, NO_3, sN_{org}, sTAN, sNO_3$.

2.8.4 Volatilisation of ammonia

Ammonium is in equilibrium with the dissolved gas ammonia (NH3), so volatilisation will take place. This is modelled as a fixed percentage ($\eta_{volat} = 15.9\%$) of ammonia per hour for each tank except the pump sump (Jiménez-Montealegre et al. 2002).

$$\phi'_{TAN,x,volat} = \eta_{volat} \cdot m_{NH_3,x} \quad [mg_N\ h^{-1}] \quad (2.80)$$

where:

$$m_{NH_3,x} = \frac{m_{TAN,x}}{\left(1 + \frac{10^{-pH_x}}{10^{-9.16}}\right)} \quad [mg_N\ h^{-1}] \quad (2.81)$$

and where pH=7 is assumed in every tank $x = FT, SC, MF, BF$.

2.8.5 Ammonification

Ammonification of the available organic nitrogen in solids takes place at a fixed rate of 15% per hour in all tanks except the pump sump. In the settling tank, ammonification also takes place in the settled solids at the same rate.

$$\phi'_{sN_{org},x,ammon} = \eta_{ammon} \cdot m_{sN_{org},x} \quad [mg_N\ h^{-1}] \quad (2.82)$$

$$\phi'_{setN_{org},SC,ammon} = \eta_{ammon} \cdot m_{setN_{org},SC} \quad [mg_N\ h^{-1}] \quad (2.83)$$

where

$$m_{sN_{org},x} = c_{sN_{org},x} \cdot V_x \quad [mg_N\ h^{-1}] \quad (2.84)$$

$$m_{setN_{org},SC} = c_{setN_{org},SC} \cdot V_{SC} \quad [mg_N\ h^{-1}] \quad (2.85)$$

and $x = FT, SC, MF, BF$.

2.8.6 Nitrification

Nitrification of dissolved ammonia takes place in the biological filter, and to a lesser extent in the drum filter. Nitrification in other tanks is neglected. Two nitrification options are modelled; either a fixed percentage of the incoming TAN is nitrified ($\phi'_{TAN,x,nit1}$), or an area-based formula (Greiner & Timmons 1998) is used ($\phi'_{TAN,x,nit2}$).

$$\phi'_{TAN,MF,nit} = \phi'_{TAN,MF,nit1} + \phi'_{TAN,MF,nit2} \quad [mg_N\ h^{-1}] \quad (2.86)$$

$$\phi'_{TAN,BF,nit} = \phi'_{TAN,BF,nit1} + \phi'_{TAN,BF,nit2} \quad [mg_N\ h^{-1}] \quad (2.87)$$

$$\phi'_{TAN,MF,nit1} = \eta_{nit,MF} \cdot \left(\phi'_{TAN,FT-MF} - \phi'_{TAN,MF,volat}\right) \quad [mg_N\ h^{-1}] \quad (2.88)$$

$$\phi'_{TAN,BF,nit1} = \eta_{nit,BF} \cdot \left(\phi'_{TAN,PS-BF} - \phi'_{TAN,BF,volat}\right) \quad [mg_N\ h^{-1}] \quad (2.89)$$

$$\phi'_{TAN,MF,nit2} = min\left(\phi'_{TAN,MF,nit1},\ c_{TAN,MF} \cdot (C_{nit} \cdot A_{MF})\right) \quad [mg_N\ h^{-1}] \quad (2.90)$$

$$\phi'_{TAN,BF,nit2} = min\left(\phi'_{TAN,BF,nit1},\ c_{TAN,BF} \cdot (C_{nit} \cdot A_{BF})\right) \quad [mg_N\ h^{-1}] \quad (2.91)$$

Nitrification in suspended solids is assumed to take place at a constant rate of $\eta_{nit,sld} = 10\ \%\ h^{-1}$ in all tanks except the pump sump, and at the same rate in the settled solids in the settling tank:

$$\phi'_{sTAN,x,nit} = \eta_{nit,sld} \cdot c_{sTAN,x} \cdot V_x \quad [mg_N\ h^{-1}] \quad (2.92)$$

$$\phi'_{setTAN,SC,nit} = \eta_{nit,sld} \cdot m_{setTAN,SC} \cdot V_{SC} \quad [mg_N\ h^{-1}] \quad (2.93)$$

where $x = FT, SC, MF, BF$.

2.8.7 Dissolving of solids

Dissolving of ammonia and nitrate in solids is modelled at a constant rate of $\eta_{dis} = 10\ \%\ h^{-1}$ in suspended solids (FT, SC), and $\eta_{dis,set} = 1\ \%\ h^{-1}$ in settled solids (SC):

$$\phi'_{sNO_3,FT,diss} = \eta_{dis} \cdot m_{sNO_3,FT} \quad [mg_N\ h^{-1}] \quad (2.94)$$

$$\phi'_{sTAN,FT,diss} = \eta_{dis} \cdot m_{sTAN,FT} \quad [mg_N\ h^{-1}] \quad (2.95)$$

$$\phi'_{sNO_3,SC,diss} = \eta_{dis} \cdot m_{sNO_3,SC} \quad [mg_N\ h^{-1}] \quad (2.96)$$

$$\phi'_{setNO_3,SC,diss} = \eta_{dis} \cdot m_{sNTAN,SC} \quad [mg_N\ h^{-1}] \quad (2.97)$$

$$\phi'_{sTAN,SC,diss} = \eta_{dis,set} \cdot m_{setNO_3,SC} \quad [mg_N\ h^{-1}] \quad (2.98)$$

$$\phi'_{setTAN,SC,diss} = \eta_{dis,set} \cdot m_{setTAN,SC} \quad [mg_N\ h^{-1}] \quad (2.99)$$

where

$$m_{x,y} = c_{x,y} \cdot V_y \quad [mg_N\ h^{-1}] \quad (2.100)$$

2.8.8 Settling of solids

Settling of solids in the settling tank is modelled using a constant rate of $\eta_{set} = 60\%$ of the inflow.

$$\phi'_{sN_{org},SC,set} = \eta_{set} \cdot \left(\phi'_{sN_{org},\mathrm{MF}-SC} + \phi'_{setN_{org},SC,resusp}\right) \quad [mg_N\ h^{-1}] \quad (2.101)$$

$$\phi'_{sTAN,SC,set} = \eta_{set} \cdot \left(\phi'_{sTAN,\mathrm{MF}-SC} + \phi'_{setTAN,SC,resusp}\right) \quad [mg_N\ h^{-1}] \quad (2.102)$$

$$\phi'_{sNO_3,SC,set} = \eta_{set} \cdot \left(\phi'_{sNO_3,\mathrm{MF}-SC} + \phi'_{setNO_3,SC,resusp}\right) \quad [mg_N\ h^{-1}] \quad (2.103)$$

2.8.9 Resuspension of settled solids

Resuspension of solids in the settling tank is modelled using a constant rate of $\eta_{resusp} = 5\ \%\ h^{-1}$ of the total settled amount.

$$\phi'_{setN_{org},SC,resusp} = m_{setN_{org},SC} \cdot \eta_{resusp} \quad [mg_N\ h^{-1}] \quad (2.104)$$

$$\phi'_{setTAN,SC,resusp} = m_{setTAN,SC} \cdot \eta_{resusp} \quad [mg_N\ h^{-1}] \quad (2.105)$$

$$\phi'_{setNO_3,SC,resusp} = m_{setNO_3,SC} \cdot \eta_{resusp} \quad [mg_N\ h^{-1}] \quad (2.106)$$

Where

$$m_{x,SC} = c_{x,SC} \cdot V_{SC} \quad [mg_N\ h^{-1}] \quad (2.107)$$

2.8.10 Sludge removal

Sludge removal is modelled to completely remove all settled solids in the settling tank, at set times. The amount of nitrogen sludge in the tank is calculated every time step:

$$m_{N,sludge}(t) = m_{N,sludge}(t-1) + \frac{\sum Dm_{x,SC}(t-1) \cdot \Delta t}{1000} \quad [g_N] \quad (2.108)$$

where x is $setN_{org}$, setTAN and $setNO_3$. From this, the total volume of sludge is calculated using a constant nitrogen percentage and sludge thickness. This is the amount of sludge removed when removal takes place (once every 24 hours). At the same time, all settled solids are removed:

$$V_{sludge} = \frac{m_{N,sludge}}{C_{N,sludge} \cdot C_{solids,sludge}} \quad [l] \quad (2.109)$$

$$\phi'_{H_2O,SC,sludge} = \begin{cases} V_{sludge}\ if\ removal \\ 0 \qquad else \end{cases} \quad [l\ h^{-1}] \quad (2.110)$$

$$\phi'_{x,SC,sludge} = \begin{cases} m_{x,SC}\ if\ removal \\ 0 \qquad else \end{cases} \quad [l\ h^{-1}] \quad (2.111)$$

where x is $setN_{org}$, setTAN and $setNO_3$.

2.8.11 List of parameters

Note: nitrogen compound masses, concentrations and fluxes are not included in this list but are described in Chapters 2.8.3 through 2.8.10.

Symbol	Value	Unit	Description	Excel® name	Sheet and cell
$C_{N,sludge}$	*4.4%*	%	Nitrogen weight percentage in solids	p_c_sludge_N	Tanks C61
$C_{SC,disch}$	*(2.41)*	–	Parameter for settling tank waste water discharge	-	-
$C_{SC,full}$	*(2.43)*	–	Parameter for settling tank overflow	-	-
$C_{feed,protein}$	*40%*	%	Fish feed protein content	p_feed_protein	Tanks C77
C_{feed}	*(2.3)*	%	Daily feeding weight per fish weight	Feed rate	Fish C
$C_{solids,sludge}$	*1.8*	$g\ l^{-1}$	Concentration of solids in sludge	p_c_sludge_perc	Tanks C60
V_{BF}	*500*	l	Biological filter volume	u_BF_volume	Tanks C22
V_{FT}	*40000*	l	Fish tanks total volume	x_FT_volume	Main O
V_{MF}	*500*	l	Mechanical filter volume	u_MF_volume	Tanks C21
V_{SC}	*(2.1)*	l	Secondary clarifier volume	x_SC_volume	Main P
V_{sludge}	*(2.110)*	l	Volume of sludge in secondary clarifier	SC total sludge volume	Main FP
d_{cycle}	*[1-241]*	day	Fish production cycle day number	Day	Fish A
$m_{N,sludge}$	*(2.108)*	g_N	Total nitrogen in sludge	SC total settled N	Main FO
$m_{fish,x}$	*(2.8)*	kg	Total fish stock in tank x	Stock	Fish E
$u_{F,SC,BUF}$	*See Chapter 2.4*	$l\ h^{-1}$	Minimum RAS-NFT coupling flow	u_flow_coupling	Tanks C4
η_{MF}	*70%*	%	Percentage of drum filter solids inflow that is removed	p_c_MF_sld_eff	Tanks C43
η_{ammon}	*15%*	$\%\ h^{-1}$	Ammonification rate of organic nitrogen in solids	p_c_ammon_sld	Tanks C50

η_{backw}	*1%*	%	Percentage of drum filter inflow used for backwashing flow	u_backwash	Tanks C45
η_{cond}	*90%*	%	Condensation rate of evaporated water in RAS system	u_evap_rtn	Tanks C66
$\eta_{dis,set}$	*1%*	$\% \, h^{-1}$	Dissolving rate of settled solids	p_c_diss_sldg	Tanks C56
η_{dis}	*10%*	$\% \, h^{-1}$	Dissolving rate of solids	p_c_diss	Tanks C49
η_{feed}	*95%*	%	Percentage of feed used by fish (rest is uneaten)	-	-
$\eta_{nit,BF}$	*60%*	%	(Maximum) percentage of biological filter inflow TAN that is nitrified	u_BF_nitr	Tanks C28
$\eta_{nit,MF}$	*0.2%*	%	(Maximum) percentage of drum filter inflow TAN that is nitrified	u_MF_nitr	Tanks C44
$\eta_{nit,sld}$	*10%*	$\% \, h^{-1}$	Nitrification rate in solids	p_c_nitr_sld	Tanks C51
η_{resusp}	*5%*	$\% \, h^{-1}$	Resuspension rate of settled solids	p_c_resusp	Tanks C55
η_{set}	*60%*	%	Percentage of inflowing solids in settling tank that settles	p_c_SC_sld_eff	Tanks C54
η_{volat}	*15.9%*	$\% \, h^{-1}$	Volatilisation rate of ammonia	p_c_nh3_volat	Tanks C119
$\phi'_{H_2O,BF,evap}$	*5*	$l \, h^{-1}$	Evaporation flow from biological filter	f_BF_evap	Main AL
$\phi'_{H_2O,BF-FT}$	*(2.66)*	$l \, h^{-1}$	Water flow from biological filter to fish tanks	f_BF_out	Main AK
$\phi'_{H_2O,FT,evap}$	*10*	$l \, h^{-1}$	Evaporation flow from fish tanks	f_FT_evap	Main Z
$\phi'_{H_2O,FT-MF}$	*(2.67)*	$l \, h^{-1}$	Water flow from fish tanks to mechanical filter	f_FT_out	Main Y
$\phi'_{H_2O,MF-PS}$	*(2.68)*	$l \, h^{-1}$	Water flow from mechanical filter to pump sump	f_MF_out	Main AA
$\phi'_{H_2O,MF-SC}$	*(2.22)*	$l \, h^{-1}$	Water flow from mechanical filter to secondary clarifier (backwash flow)	f_MF_bckw	Main AB
$\phi'_{H_2O,PS-BF}$	*45000*	$l \, h^{-1}$	Water flow from pump sump to biological filter	f_PS_out	Main AJ
$\phi'_{H_2O,SC,disch}$	*(2.40)*	$l \, h^{-1}$	Water flow from secondary clarifier to sewage system (discharging)	f_SC_disch	Main AF
$\phi'_{H_2O,SC,evap}$	*5*	$l \, h^{-1}$	Evaporation flow from secondary clarifier	f_SC_evap	Main AD
$\phi'_{H_2O,SC,sludge}$	*(2.110)*	$l \, h^{-1}$	Water flow from secondary clarifier due to sludge drainage	f_SC_sludge	Main AG

$\phi'_{H_2O,SC-BUF,const}$	*(2.35)*	$l\ h^{-1}$	Water flow from secondary clarifier to NFT buffer tank, constant	-	-
$\phi'_{H_2O,SC-BUF,fb}$	*(2.36)*	$l\ h^{-1}$	Water flow from secondary clarifier to NFT buffer tank, feed-based	-	-
$\phi'_{H_2O,SC-BUF,reg}$	*(2.37)*	$l\ h^{-1}$	Water flow from secondary clarifier to NFT buffer tank, regular flow	-	-
$\phi'_{H_2O,SC-BUF,x}$	*(2.38)*	$l\ h^{-1}$	Water flow from secondary clarifier to NFT buffer tank, flow modified to include increased water need when buffer is empty	-	-
$\phi'_{H_2O,SC-BUF}$	*(2.39)*	$l\ h^{-1}$	Water flow from secondary clarifier to NFT buffer tank	f_SC_out	Main AE
$\phi'_{H_2O,SC-PS}$	*(2.42)*	$l\ h^{-1}$	Water overflow from secondary clarifier to pump sump	f_SC_return	Main AC
$\phi'_{H_2O,STOR-PS}$	*(2.59)*	$l\ h^{-1}$	Water flow from water storage tank to pump sump	f_PS_H2O_in	Main AI
$\phi'_{N,feed,avg}$	*(2.11)*	$mg_N\ h^{-1}$	Hourly nitrogen influx in feed, averaged over one day	f_feed_evac	Main N
$\phi'_{N,feed,avgy}$	*See Ch. 2.5*	$mg_N\ h^{-1}$	Hourly nitrogen influx in feed, averaged over one year	p_feedbased	Tanks C154
$\phi'_{N,feed}$	*(2.10)*	$mg_N\ h^{-1}$	Hourly nitrogen influx in feed	f_feed_n_in	Main M
$\phi'_{TAN,FT,fish}$	*(2.12)*	$mg_N\ h^{-1}$	Fish gill excretion ending up as ammonia	f_FT_TAN_gills	Main AW
$\phi''_{feed,x}$	*(2.6)*	$kg\ day^{-1}$	Daily feeding rate in fish tank x	Feed3	Fish G
ϕ''_{feed}	*(2.9)*	$kg\ day^{-1}$	Daily total fish feeding rate	Feed13	Fish AK
$\phi'_{sNorg,FT,fish}$	*(2.13)*	$mg_N\ h^{-1}$	Fish organic nitrogen excretion in solid form	f_FT_sld_norg_prod	Main BD
$\phi'_{sNorg,FT,uneat}$	*(2.20)*	$mg_N\ h^{-1}$	Organic nitrogen excretion in solid form from uneaten feed	f_FT_sld_norg_uneaten	Main BC
Δt	*1*	h	Time step	-	-
$harvest_x$	*See Ch. 2.2.2*	$kg\ day^{-1}$	Fish harvest rate in tank x	Harvest	Fish K
DV_{BF}	*(2.52)*	$l\ h^{-1}$	Change in biological filter tank volume	-	-
DV_{FT}	*(2.14)*	$l\ h^{-1}$	Change in fish tank volume	-	-
DV_{MF}	*(2.21)*	$l\ h^{-1}$	Change in drum filter tank volume	-	-
DV_{PS}	*(2.58)*	$l\ h^{-1}$	Change in pump sump tank volume	-	-

DV_{SC}	*(2.34)*	$l\ h^{-1}$	Change in settling tank tank volume	-	-
$Dm_{fish,x}$	*(2.7)*	$kg\ day^{-1}$	Change in total fish stock per day in tank x	-	-
DMR	*(2.5)*	$\%\ day^{-1}$	Daily mortality rate (percentage of total stock per day)	Mortality	Fish D
FCR	*(2.4)*	$kg\ kg^{-1}$	Feed conversion ratio	FCR	Fish B

3. Greenhouse model

3.1 Introduction

The main goals of the greenhouse model are to calculate plant growth, plant nutrient uptake, plant water uptake and water condensation.

For accurate calculation of evaporation and condensation in the greenhouse, it was found necessary to build a complete greenhouse climate model. This greenhouse climate model assumes a closed greenhouse where no ventilation with the outside air takes place other than a small amount of leakage through the greenhouse cover. This model takes as input hourly climate data obtained from the Royal Dutch Meteorological Institute (KNMI) measured between January 2008 and December 2013 in de Bilt, the Netherlands (KNMI 2000; KNMI 2015). Climate values used are wind speed, global radiation, outside temperature, air pressure, cloud cover and relative humidity.

Where applicable, the subchapters in this chapter start with an energy, water and/or nutrient balance, followed by an explanation of or reference to the relevant fluxes. Energy balances are written in re-arranged form to express the unknown factor to be calculated. All fluxes are directly expressed in the units used in the Excel® model. Some equations therefore include modification factors, for instance from second to hour or from joule to Mega joule.

Initial conditions are not described, since it is assumed that their effect will die out within the first modelled year. The time step of the greenhouse climate model Δt is one hour, whereas the time step of parts of the plant growth model Δt_{plant} is one day. Again, the following differential operator is used: $D = {}^{d}/_{dt}$.

3.2 Plant growth

For plant growth, a simple LUE model is used, based on TOMSIM (Heuvelink 1999; Heuvelink 1996). The growth of a plant is dependent on various factors like irradiation, availability of nutrients and water availability. For the purpose of this sub-model, plant growth is assumed to be limited only by irradiation. The amount of radiation intercepted; $Q_{PAR,plant}$ *(3.91)*; is calculated from the incoming radiation, the plant leaf area index (LAI) and the plant extinction coefficient. Nutrients and water are assumed to be always available in non-limiting amounts, and light use efficiency (LUE) and light extinction coefficient (k_{PAR}) are assumed constant. The total plant dry matter production can then be described as follows:

$$DW_{tot} = Q_{PAR,plant} \cdot LUE \qquad [g\ m^{-2}\ h^{-1}] \qquad (3.1)$$

Plant dry matter partitioning is also assumed constant during generative and vegetative growth phases; the distinction between generative and vegetative being made depending on the LAI value. When the tomato crop is not fully developed and $LAI < 2.5$, 50% of the daily dry matter production is partitioned to the leaves and 0% to fruits, whereas a crop with $LAI \geq 2.5$ is modelled to partition 10% to the leaves and 80% to the fruits.

$$DW_{leaf} = \begin{cases} DW_{tot} \cdot 0.5 & if\ LAI < 2.5 \\ DW_{tot} \cdot 0.1 & if\ LAI \geq 2.5 \end{cases} \qquad [g\ m^{-2}\ h^{-1}] \qquad (3.2)$$

$$DW_{fruit} = \begin{cases} 0 & if\ LAI < 2.5 \\ DW_{tot} \cdot 0.8 & if\ LAI \geq 2.5 \end{cases} \qquad [g\ m^{-2}\ h^{-1}] \qquad (3.3)$$

Using the partitioned leaf dry matter production, the LAI value is updated daily. LAI is modelled to have a maximum value of 3.0, because it is assumed that when the crop is fully grown, old leaves are removed to keep the LAI constant.

$$DLAI(t) = SLA \cdot \sum_{i=t-\Delta t_{plant}}^{t} DW_{leaf}\,(i) \qquad [m^2\ m^{-2}\ day^{-1}] \qquad (3.4)$$

$$LAI(t) = min\big(\ LAI(t-1) + DLAI(t-1) \cdot \Delta t_{plant},\quad 3.0\big) \qquad [m^2\ m^{-2}] \qquad (3.5)$$

The uptake of nitrogen by the plant; $\phi_{N,NFT-plants}$; is modelled as dependent only on the plant dry matter production, using a formula by (Gallardo et al. 2009). The uptake of water; $\phi'_{H_2O,NFT-plants}$; is calculated as the sum of plant evaporation, the water partition of fruit growth and the water partition of plant growth. Water converted into dry matter by photosynthesis is assumed negligible.

$$\phi_{N,NFT-plants} = 0{,}05569 \cdot \mathrm{DW_{tot}}^{0{,}9019} \qquad [g_N\ h^{-1}] \qquad (3.6)$$

$$\phi'_{H_2O,NFT-plants} = \phi'_{H_2O,evap} + \frac{\mathrm{DW_{fruit}}}{DMC_{fruit}} + \frac{\mathrm{DW_{tot}} - \mathrm{DW_{fruit}}}{DMC_{plant}} \qquad [kg\ h^{-1}] \qquad (3.7)$$

3.3 Plant evaporation

Plant evaporation is calculated using the Stanghellini model (Stanghellini 1987; Prenger et al. 2002; Bontsema et al. 2011), described in the following equations:

$$\phi''_{H_2O,evap} = \frac{2 \cdot LAI}{(1+\epsilon) \cdot r_b + r_s} \cdot \left(VD_{air} + \frac{\epsilon \cdot r_b}{2 \cdot LAI} \cdot \frac{Q_{\mathrm{R_n}}}{2450}\right) \qquad [g\ m^{-2}\ s^{-1}] \qquad (3.8)$$

$$\text{where: } \mathrm{r_s} = 82 \cdot \frac{\frac{\mathrm{Q_{R_n}}}{2*\mathrm{LAI}} + 4.30}{\frac{\mathrm{Q_{R_n}}}{2*\mathrm{LAI}} + 0.54} \cdot (1 + 0.0023(\mathrm{T_{air}} - 24.5)^2) \qquad [s\ m^{-1}] \qquad (3.9)$$

LAI, ϵ, VD_{air}, $Q_{\mathrm{R_n}}$ and $\mathrm{T_{air}}$ are described in equations (3.5), (3.143), (3.69), (3.89) and (3.40) respectively. $r_b = 200\ s\ m^{-1}$. Modifying eq. (3.8) to kg h^{-1}:

$$\phi'_{H_2O,evap} = \phi''_{H_2O,evap} \cdot \mathrm{A_{soil}} \cdot \frac{3600}{1000} \qquad [kg\ h^{-1}] \qquad (3.10)$$

The energy needed for evaporation is calculated as the product of the evaporation flow and the latent heat of vaporisation L_{evap} (3.147):

$$Q'_{evap}(t) = \phi'_{H_2O,evap} \cdot L_{evap} \cdot \frac{1}{1000} \qquad [MJ\ h^{-1}] \qquad (3.11)$$

3.4 NFT buffer tank

The NFT system is modelled as recirculating, where a constant flow of water with nutrients is pumped to the NFT gutters and the excess water and nutrients flow back to the buffer tank.

The effect of solids dissolving, settling, resuspension, ammonification and nitrification is modelled as the settling tank in the RAS model, described in Chapter 2.5 *Settling tank*.

Since the plants in the NFT gutters use water and nutrients, these have to be constantly replaced. This is done by way of a coupling flow between the RAS system and the greenhouse; there is a flow from the secondary clarifier into the NFT buffer tank. This coupling flow $\phi_{W,SC-BUF}$ is already described in Chapter 2.5 *Settling tank*. Whenever this flow is not large enough to maintain at least 10% of the buffer capacity, clean water from the water storage tank is added ($\phi'_{H_2O,STOR-BUF}$).

The heat and humidity interactions between the NFT buffer tank and the rest of the greenhouse are not taken into account.

Water balance

$$DV_{BUF} = (\phi'_{H_2O,SC-BUF} + \phi'_{H_2O,STOR-BUF} + \phi'_{H_2O,NFT-BUF} - \phi'_{H_2O,BUF-NFT})/\rho_{H_2O} \qquad [l\ h^{-1}] \qquad (3.12)$$

Water fluxes

$$\phi'_{H_2O,STOR-BUF} = max(0, 0.1 \cdot V_{BUF} - V_{BUF} + \phi'_{H_2O,SC-BUF} + \phi'_{H_2O,NFT-BUF} - \phi'_{H_2O,BUF-NFT}) \qquad [kg\ h^{-1}] \qquad (3.13)$$

$\phi'_{H_2O,NFT-BUF}$ is assumed constant at 3000 kg h^{-1}. The return flow $\phi'_{H_2O,NFT-BUF}$ is described in *eq. (3.20)*.

Nitrogen balances

$$Dm_{N,BUF} = \phi'_{N,SC-BUF} + \phi'_{N,NFT-BUF} - \phi'_{N,BUF-NFT} + \phi'_{N,BUF,prod} \quad [mg\ h^{-1}] \quad (3.14)$$

$$Dm_{x,BUF} = \phi'_{x,SC-BUF} + \phi'_{x,BUF,prod} \quad [mg\ h^{-1}] \quad (3.15)$$

where the subscript x can be organic N in solids, TAN in solids or NO_3 in solids.

Nitrogen fluxes

The net production terms $\phi'_{N,BUF,prod}$ and $\phi'_{x,BUF,prod}$ include both production and consumption, and are modelled the same way as the settling tank; see Chapter 2.5 *Settling tank*. The incoming flows $\phi'_{x,SC-BUF}$ and $\phi'_{N,SC-BUF}$ are also described in that chapter. The nitrogen return flow $\phi'_{N,NFT-BUF}$ is described in *eq. (3.21)*. The nitrogen outflow is described as the water flow multiplied by the nitrogen concentration:

$$\phi'_{N,BUF-NFT} = \frac{\phi'_{H_2O,NFT-BUF}}{\rho_{H_2O}} * \frac{m_{N,BUF}}{V_{BUF}} \quad [mg\ h^{-1}] \quad (3.16)$$

Solution

$$V_{BUF}(t) = V_{BUF}(t-1) + DV_{BUF}(t-1) \cdot \Delta t \quad [l] \quad (3.17)$$

$$m_{N,BUF}(t) = m_{N,BUF}(t-1) + Dm_{N,BUF}(t-1) \cdot \Delta t \quad [mg] \quad (3.18)$$

$$m_{x,BUF}(t) = m_{x,BUF}(t-1) + Dm_{x,BUF}(t-1) \cdot \Delta t \quad [mg] \quad (3.19)$$

3.5 NFT gutters

It is assumed that the volume of the NFT gutters is small compared to the flow; gutter volume and nutrient accumulation is therefore not modelled. The water and nitrogen balances can then be simplified, as outflows equal inflows. The total concentration of dissolved nitrogen compounds is used (comprising of both TAN and NO_3), because it is assumed that the plants can take up both ammonia-N and nitrate-N. To keep the plant root N concentration from becoming too low, a nitrogen fertiliser controller is added to the water inflow to the NFT gutters. The controller adds fertiliser to keep the NFT gutter return flow at a minimum total N concentration set point of 5 mM N/l.

The heat and humidity interactions between the NFT gutters and the rest of the greenhouse are not taken into account.

Water balance

$$\phi'_{H_2O,NFT-BUF} = \phi'_{H_2O,BUF-NFT} - \phi'_{H_2O,NFT-plants} \qquad [kg\ h^{-1}] \qquad (3.20)$$

Water fluxes

Incoming flow $\phi'_{H_2O,BUF-NFT}$ is assumed *constant at 3000 kg h^{-1}* and plant water uptake $\phi'_{H_2O,NFT-plants}$ is described in *eq. (3.7)*.

Nitrogen balance

$$\phi'_{N,NFT-BUF} = \phi'_{N,BUF-NFT} + \phi'_{N,FERT} - \phi'_{N,NFT-plants} \qquad [mg_N\ h^{-1}] \qquad (3.21)$$

Nitrogen fluxes

Incoming flow $\phi'_{N,BUF-NFT}$ is described in *eq. (3.16)* and plant nitrogen uptake $\phi'_{N,NFT-plants}$ is described in *eq. (3.6)*. The fertiliser controller function is described as follows:

$$\begin{aligned}\phi'_{N,FERT} = \max\big(0,\\ 5 \cdot 14.0067 \cdot (\phi'_{H_2O,BUF-NFT} - \phi'_{H_2O,NFT-plants})\\ - \phi'_{N,BUF-NFT} + \phi'_{N,NFT-plants}\big)\end{aligned} \qquad [mg_N\ h^{-1}] \qquad (3.22)$$

3.6 Water storage tank

A water storage tank is included, to collect the condensated water and distribute it when needed.

Water balance

$$DV_{STOR} = \frac{\phi'_{H_2O,in-STOR} + \phi'_{H_2O,cond} - \phi'_{H_2O,STOR-BUF} - \phi'_{H_2O,STOR-PS}}{\rho_{H_2O}} \qquad [l\ h^{-1}] \qquad (3.23)$$

Fluxes

Enough clean water is added every time step to ensure the volume does not become negative:

$$\begin{aligned}\phi'_{H_2O,in-STOR} = \max\big(0,\ V_{STOR} + \phi'_{H_2O,cond} - \phi'_{H_2O,STOR-BUF}\\ - \phi'_{H_2O,STOR-PS}\big)\end{aligned} \qquad [kg\ h^{-1}] \qquad (3.24)$$

The fluxes $\phi'_{H_2O,cond}$, $\phi'_{H_2O,STOR-BUF}$ and $\phi'_{H_2O,STOR-PS}$ are described in *eq. (3.70)*, *(3.13)* and *(2.59)* respectively. Relevant nitrogen fluxes are described in Appendices *2.8.3 Nitrogen flows*, *2.8.4 Volatilisation of ammonia*, *2.8.5 Ammonification* and *2.8.6 Nitrification*.

Pump sump

Solution

$$V_{STOR}(t) = V_{STOR}(t-1) + DV_{STOR}(t-1) \cdot \Delta t \qquad [l] \qquad (3.25)$$

3.7 Greenhouse climate

Introduction

It is assumed that the smallest time constant for the greenhouse climate processes is smaller than the one hour time step used in this model. A numerical solution would thus not be accurate, so an analytical solution was needed. A set of differential equations describing radiation and convection exchange on the greenhouse soil surface, the plant canopy, the lower and upper surface of the screen (when closed) and the lower and upper surface of the greenhouse cover was made. In these equations, both the screen and the cover are assumed to be in quasi-steady-state where the total energy input equals the total energy output. An analytical solution was found, describing the cover and screen temperatures as a function of known climate parameters. From these temperatures and parameters, all energy fluxes are calculated. These fluxes are based on research by R. van Ooteghem (Van Ooteghem 2007).

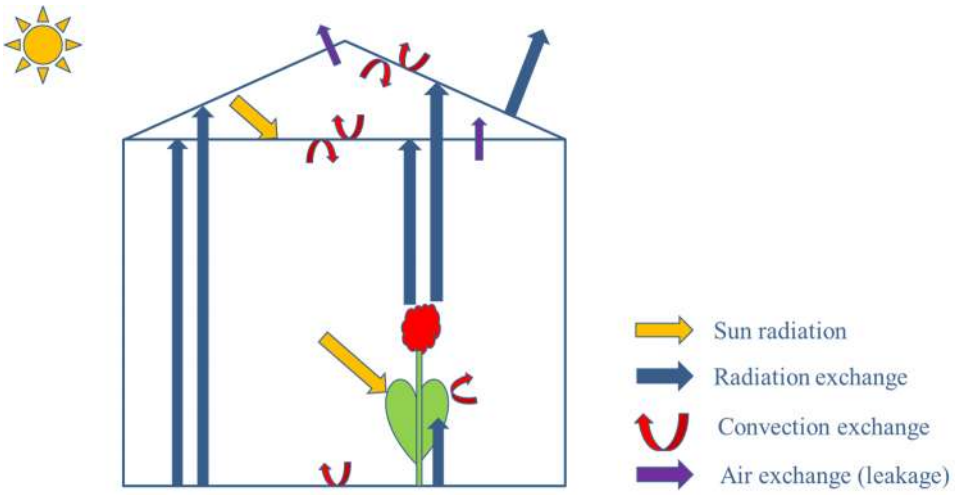

Figure 4 Heat fluxes in a greenhouse. Only vertical radiative exchange is modelled.

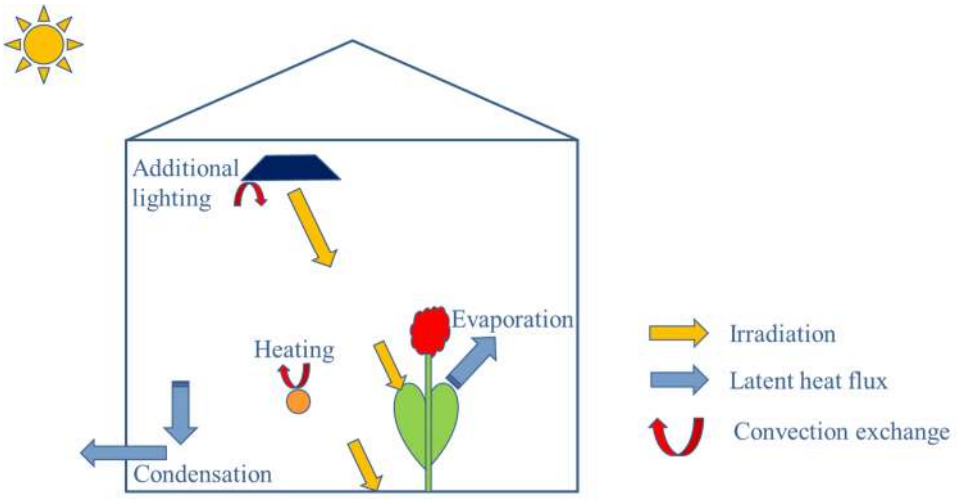

Figure 5 Additional heating and lighting heat fluxes, and latent heat fluxes in a greenhouse

Radiative exchange

In order to ease calculations, radiative heat exchange between surfaces (using the Stefan-Boltzmann law) is linearized (Van Ooteghem 2007):

$$Q_{a-b} = A_{a-b} \cdot F_{a-b} \cdot \varepsilon_a \cdot \varepsilon_b \cdot \sigma'_{lin} \cdot (T_a - T_b) \qquad [W] \qquad (3.26)$$

$$\text{where: } \sigma'_{lin} = 4 \cdot \sigma \cdot T_{lin}^3 \qquad [Wm^{-2}K^{-1}] \qquad (3.27)$$

A linearization temperature $T_{lin} = 17.5°C$ is used. The linearized Stefan-Boltzmann constant σ'_{lin} is grouped together with the view factor and emissivities to form a single heat transfer coefficient α_{a-b}. Converting the heat flow to a one hour time step, the following general formula is found and used for all radiative heat transfers:

$$Q'_{a-b} = A_{a-b} \cdot \alpha_{a-b} \cdot (T_a - T_b) \cdot \frac{3.6}{1000} \qquad [MJ\ h^{-1}] \qquad (3.28)$$

$$\text{where: } \alpha_{a-b} = F_{a-b} \cdot \varepsilon_a \cdot \varepsilon_b \cdot \sigma'_{lin} \qquad [Wm^{-2}K^{-1}] \qquad (3.29)$$

The following view factors are used:

$$F'_{screen} = (1 - Cl_{screen}) + \tau_{screen} \cdot Cl_{screen} - 10^{-6} \qquad [\%] \qquad (3.30)$$

$$F_{plant} = 1 - e^{-k_{plant} \cdot LAI} \qquad [\%] \qquad (3.31)$$

$$F_{cover} = (1 - \tau_{cover} - R_{cover}) \qquad [\%] \qquad (3.32)$$

The 10^{-6} modification is to make sure the formulas describing interaction between screen and cover keep working when the screen is open.

Convective exchange

For convective heat fluxes, the following formula is used:

$$Q_{a-b} = A_{a-b} \cdot \alpha_{a-b} \cdot (T_a - T_b) \qquad [W] \qquad (3.33)$$

This equation is modified for use with a one hour time step:

$$Q'_{a-b} = A_{a-b} \cdot \alpha_{a-b} \cdot (T_a - T_b) \cdot \frac{3.6}{1000} \qquad [MJ\ h^{-1}] \qquad (3.34)$$

Air exchange, condensation, heating and cooling

Air leakage through the cover and through the screen (when closed) are calculated separately. Different psychometric values are also calculated for the greenhouse air below and above the screen and for the outside air, to find the total vapour balance and calculate the amount of vapour that needs to be condensated to keep the greenhouse vapour deficit at set values. From the vapour balance, the loss of water through leakage ventilation is also calculated. From the total energy balance, the required amounts of heating and cooling are calculated.

3.7.1 Soil

The greenhouse soil is modelled as a single layer with a constant specific heat capacity $C_{th,soil}$. Soil interactions outside the greenhouse are neglected.

Energy balance

Energy storage in the soil is calculated as the remainder in the soil energy balance:

$$DQ'_{soil} = Q'_{rad,soil} - Q'_{soil-air} - Q'_{soil-plant} - Q'_{soil-screen} - Q'_{soil-cover} \qquad [MJ\ h^{-1}] \qquad (3.35)$$

Fluxes

The fluxes $Q'_{rad,soil}$, $Q'_{soil-air}$, $Q'_{soil-plant}$, $Q'_{soil-screen}$ and $Q'_{soil-cover}$ are described in *eq. (3.93)*, *(3.78)*, *(3.96)*, *(3.97)* and *(3.98)* respectively.

Solution

From the energy storage, the total heat energy of the soil and the soil temperature can be calculated at every time step:

$$T_{soil} = \frac{E_{soil}}{A_{soil} \cdot C_{th,soil}} \quad [°C] \quad (3.36)$$

where: $E_{soil}(t) = E_{soil}(t-1) + DQ'_{soil}(t-1) \cdot \Delta t \quad [MJ] \quad (3.37)$

The initial soil temperature may still have an effect on the heat balances after one modelled year. Therefore, after modelling the system with an arbitrary initial soil temperature, the initial soil temperature is changed to the final soil temperature on the same date after three modelled years and the model is run again.

3.7.2 Plant

The energy balance of the plant does not take into account storage. Energy inflow is equalled to energy outflow, and the convective exchange between the plant and the greenhouse air is calculated as the remainder in the energy balance, as it is the only unknown term.

The plant temperature used in calculating the plant energy flows is modelled using the following formula (Donatelli et al. 2006; Stanghellini 1987):

$$T_{plant} = \begin{cases} T_{air} + 1.67 \cdot Q'_{rad,in} - 0.25 \cdot \frac{VPD_{air}}{\gamma_{\text{air}}} & if\ Q'_{rad,in} > 0 \\ T_{air} - 0.1 \cdot \frac{VPD_{air}}{\gamma_{\text{air}}} & if\ Q'_{rad,in} = 0 \end{cases} \quad [°C] \quad (3.38)$$

Energy balance

$$Q'_{air-plant} = Q'_{evap} + Q'_{plant-screen} + Q'_{plant-cover} - Q'_{rad-plant} - Q'_{soil-plant} \quad [MJ\ h^{-1}] \quad (3.39)$$

Fluxes

The fluxes Q'_{evap}, $Q'_{plant-screen}$, $Q'_{plant-cover}$, $Q'_{rad-plant}$ and $Q'_{soil-plant}$ are described in eq. *(3.11)*, *(3.99)*, *(3.100)*, (3.90) and *(3.96)* respectively.

3.7.3 Greenhouse air

The greenhouse air temperature below the screen is modelled as an input to the rest of the climate model. A set point temperature is assumed to be always reached (de Gelder et al. 2010):

$$T_{air} = 17.5 + 1.5 \cdot Q'_{rad,in} \quad [°C] \quad (3.40)$$

Energy balance

The greenhouse air energy balance takes all energy flows into and out of the air into account, as well as heating, cooling and air storage. The heating or cooling demand $Q'_{cool,heat}$ is calculated as the remaining term:

$$\begin{aligned} Q'_{cool,heat} = {} & Q'_{out-air} + Q'_{soil-air} + Q'_{evap} + Q'_{cond,release} + Q'_{light-air} \\ & + Q'_{fan-air} - Q'_{air-out} - Q'_{air-plant} - Cl_{screen} \\ & \cdot \left(Q'_{air-screen} + Q'_{air-top}\right) - (1 - Cl_{screen}) \\ & \cdot \left(Q'_{top-cover} + Q'_{top-out}\right) \; - DQ'_{air} \end{aligned} \qquad [MJ\ h^{-1}] \qquad (3.41)$$

Fluxes

The fluxes $Q'_{out-air}$, $Q'_{soil-air}$, Q'_{evap}, $Q'_{cond,release}$, $Q'_{light-air}$, $Q'_{fan-air}$, $Q'_{air-out}$, $Q'_{air-plant}$, $Q'_{air-screen}$, $Q'_{air-top}$, $Q'_{top-cover}$ and $Q'_{top-out}$ are described in *eq. (3.120), (3.78), (3.11), (3.77), (3.65), (3.68), (3.119), (3.39), (3.79), (3.121), (3.81)* and *(3.118)* respectively.

The energy storage in the greenhouse air is calculated as the difference in total air energy between the previous and current time step:

$$DQ'_{air}(t) = \frac{\left(E_{air}(t) - E_{air}(t-1)\right)}{\Delta t} \qquad [MJ\ h^{-1}] \qquad (3.42)$$

$$\text{where: } E_{air} = h_{air} \cdot \rho_{air} \cdot A_{soil} \cdot C_{height} \cdot \frac{1}{1000} \qquad [MJ] \qquad (3.43)$$

Heat removal and heating requirement are calculated from the total heating and cooling demand $Q'_{cool,heat}$. The energy removed from the air to condensate water from it is transferred to the cooling medium. In some cases, part of this energy can be regained using a heat exchanger. This is reflected in the regeneration efficiency η_{regen};

$$Q'_{cond,remove} = \min\left(Q'_{cond}, \max\left(Q'_{cool,heat}, \left(1 - \eta_{regen}\right) \cdot\ Q'_{cond}\right)\right) \qquad [MJ\ h^{-1}] \qquad (3.44)$$

$$Q'_{cool} = \min\left(0, Q'_{cool,heat} - Q'_{cond,remove}\right) \qquad [MJ\ h^{-1}] \qquad (3.45)$$

$$Q'_{heat} = \min\left(0, Q'_{cond,remove} - Q'_{cool,heat}\ \right) \qquad [MJ\ h^{-1}] \qquad (3.46)$$

3.7.4 Screen

The greenhouse climate model includes an energy screen that closes when there is no or very little incoming solar radiation. This screen insulates the greenhouse and minimises heat and vapour losses. The screen is modelled to open when hourly average solar radiation reaches 70 W/m² and to close when the hourly average radiation falls below 55 W/m².

$$Cl_{screen} = \begin{cases} 1 \; if \; screen \; closed \\ 0 \; if \; screen \; open \end{cases} \qquad [-] \qquad (3.47)$$

Energy balance

$$Q_{rad,screen} + Q_{soil-screen} + Q_{plant-screen} + Q_{air-screen} - Q_{screen-top} - Q_{screen-cover} = 0 \qquad [W\ m^{-2}] \qquad (3.48)$$

Expanding the energy flows into their heat transfer coefficients and temperatures:

$$Q_{rad,screen} + \alpha_{soil-screen} \cdot (T_{soil} - T_{screen}) + \alpha_{plant-screen} \cdot (T_{plant} - T_{screen}) + \alpha_{air-screen} \cdot (T_{air} - T_{screen}) - \alpha_{screen-top} \cdot (T_{screen} - T_{top}) - \alpha_{screen-cover} \cdot (T_{screen} - T_{cover}) = 0 \qquad [W\ m^{-2}] \qquad (3.49)$$

Fluxes

The energy fluxes and heat transfer coefficients in the above equations are described in *Appendix 3.8.1 Convective exchange*, *3.8.2 Shortwave radiative exchange* and *3.8.3 Longwave radiative exchange.*

Solution

Grouping the heat transfer coefficients together into a single variable:

$$\alpha_{screen} = \alpha_{air-screen} + \alpha_{plant-screen} + \alpha_{screen-top} + \alpha_{screen-cover} + \alpha_{soil-screen} \qquad [W\ m^{-2}\ K^{-1}] \qquad (3.50)$$

then *eq. (3.49)* can be simplified to:

$$\alpha_{screen} \cdot T_{screen} = Q_{rad,screen} + \alpha_{soil-screen} \cdot T_{soil} + \alpha_{plant-screen} \cdot T_{plant} + \alpha_{air-screen} \cdot T_{air} - \alpha_{screen-top} \cdot T_{top} - \alpha_{screen-cover} \cdot T_{cover} \qquad [W\ m^{-2}] \qquad (3.51)$$

When the screen is open, its temperature is assumed to be equal to the greenhouse air temperature. The screen temperature can then be expressed as:

$$T_{screen} = Cl_{screen} \cdot \frac{T_{air} \cdot \alpha_{air-screen} + T_{cover} \cdot \alpha_{screen-cover} + T_{plant} \cdot \alpha_{plant-screen} + T_{soil} \cdot \alpha_{soil-screen} + T_{top} \cdot \alpha_{screen-top} + Q_{rad,screen}}{\alpha_{screen}} + (1 - Cl\_screen) \cdot T_{air} \qquad [°C] \qquad (3.52)$$

3.7.5 Air above screen

The greenhouse temperature above the screen, when the screen is closed, is modelled as the weighted average between the lower greenhouse air temperature and the outside air temperature:

$$T_{top} = Cl_{screen} \cdot C_{top-out} \cdot T_{air} + \left(1 - C_{top-out}\right) \cdot T_{out} + (1 - Cl_{screen}) \cdot T_{air} \quad [°C] \quad (3.53)$$

The humidity factor of the air above the screen is modelled as the minimum of the greenhouse air humidity factor and the top air humidity factor at saturation:

$$x_{top} = \min(x_{air}, x_{s,top}) \quad [kg\ kg^{-1}] \quad (3.54)$$

When the screen is open, the temperature and humidity factor of the top air are equal to that of the lower greenhouse air.

Since no energy accumulation is assumed in the greenhouse air above the screen, the calculated energy accumulation DQ'_{top} is seen as an error value. This error value takes into account all energy flows regarding the top air, including the heat released by condensation. It is assumed that the water condensated above the screen is neither collected nor re-evaporated, and is therefore included in the $Q'_{top,out}$ energy flow *(3.118)*.

Energy balance

$$DQ'_{top} = Cl_{screen} \cdot \left(\left(Q'_{screen-top} + Q'_{air-top} + Q'_{cond,release,top}\right) - \left(Q'_{top-cover} + Q'_{top-out}\right)\right) \quad [MJ\ h^{-1}] \quad (3.55)$$

Fluxes

Because the air leaking upwards through the screen is often cooled to saturation, condensation can take place:

$$\phi'_{H_2O,cond,top} = \left(x_{air} - x_{s,top}\right) \cdot \rho_{air} \cdot \phi_{V,air-top} \cdot 3600 \quad [kg\ h^{-1}] \quad (3.56)$$

$$Q'_{cond,release,top} = \phi_{H_2O,cond,top} \cdot L_{cond,top} \cdot \frac{1}{1000} \quad [MJ\ h^{-1}] \quad (3.57)$$

The fluxes $Q'_{screen-top}$, $Q'_{air-top}$, $Q'_{top-cover}$ and $Q'_{top-out}$ are described in *eq. (3.93)*, *(3.121)*, *(3.81)* and *(3.118)* respectively.

Solution

The total sum of the DQ'_{top} error value over the entire modelled time period was minimised to 0 MJ by using the standard built-in linear solver in Excel® with the temperature weighting constant $C_{top-out}$ as input. A value of $C_{top-out} = 0.41$ was found and used.

3.7.6 Cover

The greenhouse includes a translucent cover. The cover temperature is calculated using an analytical solution to the energy balance that takes into account all convective and radiative heat transfers including the cover.

Energy balance

$$Q_{rad,cover} + Q_{soil-cover} + Q_{plant-cover} + Q_{screen-cover} + Q_{top-cover} - Q_{cover-sky} - Q_{cover-out} = 0 \qquad [W\ m^{-2}] \qquad (3.58)$$

Expanding the energy flows into their heat transfer coefficients and temperatures:

$$Q_{rad,cover} + \alpha_{soil-cover} \cdot (T_{soil} - T_{cover}) + \alpha_{plant-cover} \cdot (T_{plant} - T_{cover}) + \alpha_{screen-cover} \cdot (T_{screen} - T_{cover}) + \alpha_{top-cover} \cdot (T_{top} - T_{cover}) - \alpha_{cover-sky} \cdot (T_{cover} - T_{sky}) - \alpha_{cover-out} \cdot (T_{cover} - T_{out}) = 0 \qquad [W\ m^{-2}] \qquad (3.59)$$

Fluxes

The energy fluxes and heat transfer coefficients in the above equations are described in *Appendix 3.8.1 Convective exchange*, *3.8.2 Shortwave radiative exchange* and *3.8.3 Longwave radiative exchange.*

Solution

Grouping the heat transfer coefficients together into a single variable:

$$\alpha_{cover} = \alpha_{cover-sky} + \alpha_{cover-out} + \alpha_{plant-cover} + \alpha_{screen-cover} + \alpha_{soil-cover} + \alpha_{top-cover} \qquad [W\ m^{-2}\ K^{-1}] \qquad (3.60)$$

Then *equation (3.59)* can be rewritten as:

$$\alpha_{cover} \cdot T_{cover} = Q_{rad,cover} + \alpha_{soil-cover} \cdot T_{soil} + \alpha_{plant-cover} \cdot T_{plant} + \alpha_{screen-cover} \cdot T_{screen} + \alpha_{top-cover} \cdot T_{top} + \alpha_{cover-sky} \cdot T_{sky} + \alpha_{cover-out} \cdot T_{out} \quad [W\ m^{-2}] \quad (3.61)$$

Finally:

$$T_{cover} = \frac{Q_{rad,cover} + \alpha_{soil-cover} \cdot T_{soil} + \alpha_{plant-cover} \cdot T_{plant} + \alpha_{screen-cover} \cdot T_{screen} + \alpha_{top-cover} \cdot T_{top} + \alpha_{cover-sky} \cdot T_{sky} + \alpha_{cover-out} \cdot T_{out}}{\alpha_{cover}} \quad [°C] \quad (3.62)$$

Using Matlab® to combine the previously found expression for T_{screen} (*eq. (3.52)*) into the equation, T_{cover} can be expressed in only already known temperatures:

$$T_{cover} = \frac{\left(\begin{array}{l} \alpha_{screen} \cdot (T_{out} \cdot \alpha_{cover-out} \cdot + T_{sky} \cdot \alpha_{cover-sky}) \\ + T_{soil} \cdot (\alpha_{soil-screen} \cdot \alpha_{screen-cover} + \alpha_{soil-cover} \cdot \alpha_{screen}) \\ + T_{plant} \cdot (\alpha_{plant-screen} \cdot \alpha_{screen-cover} + \alpha_{plant-cover} \cdot \alpha_{screen}) \\ + T_{top} \cdot (\alpha_{screen-top} \cdot \alpha_{screen-cover} + \alpha_{top-cover} \cdot \alpha_{screen}) \\ + Q_{sun} \cdot (\tau_{cover} \cdot (1 - F'_{screen}) \cdot \alpha_{screen-cover} + F_{cover} \cdot \alpha_{screen}) \\ + T_{air} \cdot \alpha_{air-screen} \cdot \alpha_{screen-cover} \end{array}\right)}{(\alpha_{cover} \cdot \alpha_{screen} - (\alpha_{screen-cover})^2)} \quad [°C] \quad (3.63)$$

3.7.7 Supplemental lighting

It is assumed that the greenhouse includes supplemental plant lighting of 100 W/m². The modelled lighting schedule includes sixteen hours of additional lighting per day, from early in the morning until the sun goes down, from the first of October till the fifteenth of February. From the fifteenth of February till the fifteenth of March, the lighting schedule is the same but the lights are turned off when hourly average solar radiation exceeds 300 W/m². Finally, from the fifteenth of March till the fifteenth of April, lighting starts sixteen hours before sundown and ends at 10:00 in the morning. After the fifteenth of April, no additional lighting is used.

$$P_{light} = \begin{cases} 100\ if\ light\ on \\ 0\ if\ light\ off \end{cases} \quad [W\ m^{-2}] \quad (3.64)$$

$$Q'_{light-air} = (1 - \eta_{light}) \cdot P_{light} \cdot A_{soil} \cdot \frac{3.6}{1000} \quad [MJ\ h^{-1}] \quad (3.65)$$

3.7.8 Ventilation

Three different types of ventilation fans are modelled; a condensation airflow fan ($\phi'_{V,cond}$ (3.75)), a recirculation airflow fan ($\phi_{V,vent,in}$) and an outside air exchange fan ($\phi_{V,vent}$). The power used by these fans is assumed to be dissipated completely into the greenhouse air.

$$Q'_{fan,cond} = \frac{\phi'_{V,cond}}{\rho_{air} \cdot \eta_{fan,cond}} \qquad [MJ\ h^{-1}] \qquad (3.66)$$

$$Q'_{fan,vent} = \left(\phi_{V,vent} + \phi_{V,vent,in}\right) \cdot \frac{A_{soil}}{\eta_{fan,vent}} \cdot \frac{3.6}{1000} \qquad [MJ\ h^{-1}] \qquad (3.67)$$

$$Q'_{fan-air} = Q'_{fan,vent} + Q'_{fan,cond} \qquad [MJ\ h^{-1}] \qquad (3.68)$$

3.7.9 Dehumidification

The greenhouse is assumed to include a humidity controller that keeps the greenhouse vapour deficit; the amount of water (in grams) that can still evaporate into a cubic meter of air before it is saturated; at a set value. This VD is modelled as an input, using the following formula (linear fit based on (Stanghellini 2009)):

$$VD_{air} = 2.5 + 0.004 \cdot Q_{rad,in} \qquad [g\ m^{-3}] \qquad (3.69)$$

This set point vapour deficit is assumed to be always reached. The amount of water to be condensated from the air is the remainder in the vapour balance, which includes evaporation, vapour flows through the greenhouse cover and vapour storage.

Vapour balance

$$\phi'_{H_2O,cond} = \phi'_{H_2O,evap} + \phi'_{H_2O,in} - \phi'_{H_2O,out} - Dm_{H_2O,air} \qquad [kg\ h^{-1}] \qquad (3.70)$$

Vapour fluxes

The vapour flows into and out of the greenhouse air depend on flow, humidity factor and air density:

$$\phi'_{H_2O,in} = \phi_{V,out-air} \cdot x_{out} \cdot \rho_{out} \cdot 3600 \qquad [kg\ h^{-1}] \qquad (3.71)$$

$$\phi'_{H_2O,out} = \left(\phi_{V,air-out} + Cl_{screen} \cdot \phi_{V,air-top} + (1 - Cl_{screen}) \cdot \phi_{V,top-out}\right) \cdot x_{air} \cdot \rho_{air} \cdot 3600 \qquad [kg\ h^{-1}] \qquad (3.72)$$

The plant evaporation flux $\phi'_{H_2O,evap}$ is described in equation (3.10).

The total mass of water in the air is calculated from the humidity factor, air density and total greenhouse air volume:

$$m_{H_2O,air} = x_{air} \cdot \rho_{air} \cdot A_{soil} \cdot C_{height} \qquad [kg] \qquad (3.73)$$

$$Dm_{H_2O,air}(t) = \frac{m_{H_2O,air}(t) - m_{H_2O,air}(t-1)}{\Delta t} \qquad [kg\ h^{-1}] \qquad (3.74)$$

Energy fluxes

Water is condensated from the air by cooling it to below dew point. The amount of air that needs to be cooled to the condensation temperature to remove the desired amount of humidity is calculated using the humidity factors of both the un-cooled and cooled air, with the latter modified to express the humidity ratio as humidity per original air weight. To approximate the imperfect efficiency of heat exchange, an efficiency factor is added.

$$\phi'_{V,cond} = \frac{\phi'_{H_2O,cond}}{\eta_{exch} \cdot \left(x_{air} - x_{sat,cool} \cdot \frac{1 - x_{air}}{1 - x_{sat,cool}}\right)} \qquad [kg\ h^{-1}] \qquad (3.75)$$

Cooling removes energy from the air. This is calculated using the flow of air that is cooled and the difference in enthalpy of the un-cooled and cooled air. Again, the latter is modified with a factor that expresses the change in weight due to water removal.

$$Q'_{cond} = \phi'_{V,cond} \cdot \left(h_{air} - h_{air,cool} \cdot \frac{1 - x_{air}}{1 - x_{s,cond}}\right) \cdot \frac{1}{1000} \qquad [MJ\ h^{-1}] \qquad (3.76)$$

The cooling needed for condensation usually removes more energy than needed to keep the greenhouse at temperature set point (Bootsveld & van Wolferen 2004). It is possible to regain some of this energy using a heat exchanger. The removal of energy from the greenhouse air and the possibility to regain some of this energy is described in *eq. (3.44)*.

Condensation also releases energy, since it is an exothermic process. The amount of energy released into the air is calculated as the product of the amount of water condensated and the latent heat of condensation:

$$Q'_{cond,release} = \phi'_{H_2O,cond} \cdot L_{cond} \cdot \frac{1}{1000} \qquad [MJ\ h^{-1}] \qquad (3.77)$$

3.8 Appendix

3.8.1 Convective exchange

Energy flows

$$Q'_{soil-air} = A_{soil} \cdot \alpha_{soil-air} \cdot (T_{soil} - T_{air}) \cdot \frac{3.6}{1000} \quad [MJ\ h^{-1}] \quad (3.78)$$

$$Q'_{air-screen} = A_{soil} \cdot \alpha_{air-screen} \cdot (T_{air} - T_{screen}) \cdot \frac{3.6}{1000} \quad [MJ\ h^{-1}] \quad (3.79)$$

$$Q'_{air-plant} = Q'_{plant-evap} + Q'_{plant-screen} + Q'_{plant-cover} - Q'_{rad-plant} - Q'_{soil-plant} \quad [MJ\ h^{-1}] \quad (3.39)$$

$$Q'_{screen-top} = A_{soil} \cdot \alpha_{screen-top} \cdot (T_{screen} - T_{top}) \cdot \frac{3.6}{1000} \quad [MJ\ h^{-1}] \quad (3.80)$$

$$Q'_{top-cover} = A_{soil} \cdot \alpha_{top-cover} \cdot (T_{top} - T_{cover}) \cdot \frac{3.6}{1000} \quad [MJ\ h^{-1}] \quad (3.81)$$

$$Q'_{cover-out} = A_{soil} \cdot \alpha_{cover-out} \cdot (T_{cover} - T_{out}) \cdot \frac{3.6}{1000} \quad [MJ\ h^{-1}] \quad (3.82)$$

Heat transfer coefficients

$$\alpha_{soil-air} = \alpha'_{soil-air} \cdot |T_{soil} - T_{air}|^{0.33} \quad [Wm^{-2}K^{-1}] \quad (3.83)$$

$$\alpha_{air-screen} = \alpha'_{air-screen} \cdot Cl_{screen} \quad [Wm^{-2}K^{-1}] \quad (3.84)$$

$$\alpha_{screen-top} = \alpha'_{screen-top} \cdot Cl_{screen} \quad [Wm^{-2}K^{-1}] \quad (3.85)$$

$$\alpha_{cover-out} = \alpha'_{cover-out} \cdot {\phi_{V,wind}}^{0.8} \quad [Wm^{-2}K^{-1}] \quad (3.86)$$

Heat transfer coefficients are based on (De Zwart 1996; Van Ooteghem 2007). It is assumed that Tsoil>Tair.

3.8.2 Shortwave radiative exchange

$$Q_{rad,in} = P_{light} \cdot \eta_{light} + Q_{sun} \cdot \tau_{cover} \cdot F'_{screen} \quad [W\ m^{-2}] \quad (3.87)$$

$$Q'_{rad,in} = Q_{rad,in} \cdot \frac{3.6}{1000} \quad [MJ\ h^{-1}] \quad (3.88)$$

$$Q_{R_n} = 0.86 \cdot (1 - e^{-0.7 \cdot LAI}) \cdot Q_{rad,in} \quad [W\ m^{-2}] \quad (3.89)$$

$$Q'_{rad,plant} = A_{soil} \cdot Q_{rad,in} \cdot F_{plant} \cdot \frac{3.6}{1000} \quad [MJ\ h^{-1}] \quad (3.90)$$

$$Q_{PAR,plant} = Q_{PAR,in} \cdot \left(1 - e^{-k_{plant} \cdot LAI}\right) \quad [MJm^{-2}h^{-1}] \quad (3.91)$$

$$Q_{PAR,in} = \left(Q_{sun} \cdot \tau_{cover} \cdot F'_{screen} \cdot \eta_{PAR,sun} + Q_{light} \cdot \eta_{PAR,light}\right) \cdot \frac{3.6}{1000} \quad [MJm^{-2}h^{-1}] \quad (3.92)$$

$$Q'_{rad,soil} = A_{soil} \cdot Q_{rad,in} \cdot (1 - F_{plant}) \cdot \frac{3.6}{1000} \quad [MJ\ h^{-1}] \quad (3.93)$$

$$Q'_{rad,screen} = A_{soil} \cdot Q_{sun} \cdot \tau_{cover} \cdot (1 - F'_{screen}) \cdot \frac{3.6}{1000} \quad [MJ\ h^{-1}] \quad (3.94)$$

$$Q'_{rad,cover} = A_{soil} \cdot Q_{sun} \cdot F_{cover} \cdot \frac{3.6}{1000} \quad [MJ\ h^{-1}] \quad (3.95)$$

3.8.3 Longwave radiative exchange

Energy flows

$$Q'_{soil-plant} = A_{soil} \cdot \alpha_{soil-plant} \cdot \left(T_{soil} - T_{plant}\right) \cdot \frac{3.6}{1000} \quad [MJ\ h^{-1}] \quad (3.96)$$

$$Q'_{soil-screen} = A_{soil} \cdot \alpha_{soil-screen} \cdot (T_{soil} - T_{screen}) \cdot \frac{3.6}{1000} \quad [MJ\ h^{-1}] \quad (3.97)$$

$$Q'_{soil-cover} = A_{soil} \cdot \alpha_{soil-cover} \cdot (T_{soil} - T_{cover}) \cdot \frac{3.6}{1000} \quad [MJ\ h^{-1}] \quad (3.98)$$

$$Q'_{plant-screen} = A_{soil} \cdot \alpha_{plant-screen} \cdot \left(T_{plant} - T_{screen}\right) \cdot \frac{3.6}{1000} \quad [MJ\ h^{-1}] \quad (3.99)$$

$$Q'_{plant-cover} = A_{soil} \cdot \alpha_{plant-cover} \cdot \left(T_{plant} - T_{cover}\right) \cdot \frac{3.6}{1000} \quad [MJ\ h^{-1}] \quad (3.100)$$

$$Q'_{screen-cover} = A_{soil} \cdot \alpha_{screen-cover} \cdot (T_{screen} - T_{cover}) \cdot \frac{3.6}{1000} \quad [MJ\ h^{-1}] \quad (3.101)$$

$$Q'_{cover-sky} = A_{soil} \cdot \alpha_{cover-sky} \cdot \left(T_{cover} - T_{sky}\right) \cdot \frac{3.6}{1000} \quad [MJ\ h^{-1}] \quad (3.102)$$

Heat transfer coefficients

$$\alpha_{soil-plant} = F_{plant} \cdot \varepsilon_{soil} \cdot \varepsilon_{plant} \cdot \sigma'_{lin} \quad [Wm^{-2}K^{-1}] \quad (3.103)$$

$$\alpha_{soil-screen} = (1 - F_{plant}) \cdot (1 - F'_{screen}) \cdot \varepsilon_{soil} \cdot \varepsilon_{screen,down} \cdot \sigma'_{lin} \quad [Wm^{-2}K^{-1}] \quad (3.104)$$

$$\alpha_{soil-cover} = (1 - F_{plant}) \cdot F'_{screen} \cdot \varepsilon_{soil} \cdot \varepsilon_{cover,down} \cdot \sigma'_{lin} \quad [Wm^{-2}K^{-1}] \quad (3.105)$$

$$\alpha_{plant-screen} = F_{plant} \cdot (1 - F'_{screen}) \cdot \varepsilon_{plant} \cdot \varepsilon_{screen,down} \cdot \sigma'_{lin} \quad [Wm^{-2}K^{-1}] \quad (3.106)$$

$$\alpha_{plant-cover} = F_{plant} \cdot F'_{screen} \cdot \varepsilon_{plant} \cdot \varepsilon_{cover,down} \cdot \sigma'_{lin} \quad [Wm^{-2}K^{-1}] \quad (3.107)$$

$$\alpha_{screen-cover} = (1 - F'_{screen}) \cdot \varepsilon_{screen,up} \cdot \varepsilon_{cover,down} \cdot \sigma'_{lin} \quad [Wm^{-2}K^{-1}] \quad (3.108)$$

$$\alpha_{cover-sky} = \varepsilon_{cover,up} \cdot \varepsilon_{sky} \cdot \sigma'_{lin} \quad [Wm^{-2}K^{-1}] \quad (3.109)$$

Sky temperature

$$T_{sky} = \sqrt[4]{(1 - Cl_{cloud}) \cdot \varepsilon_{sky,clear} \cdot T_{out}^4 + Cl_{cloud} \cdot \left(T_{out}^4 - \frac{9}{\sigma}\right)} - 273.15 \qquad [°C] \qquad (3.110)$$

$$\varepsilon_{sky,clear} = 0.53 + 6 \cdot 10^{-3} \sqrt{P_{v,out}} \qquad [Wm^{-2}K^{-1}] \qquad (3.111)$$

(Van Ooteghem 2007)

3.8.4 Air exchange

Leakage flows

$$\phi_{V,top-out} = A_{soil} \cdot \left(8.3 \cdot 10^{-5} + (3.5 \cdot 10^{-5}) \cdot \phi_{V,wind}\right) \qquad [m^3\ s^{-1}] \qquad (3.112)$$

$$\phi_{V,air-top} = A_{soil} \cdot \frac{0.3}{3600} \cdot \left(T_{air} - T_{top}\right) \qquad [m^3\ s^{-1}] \qquad (3.113)$$

(Van Ooteghem 2007)

$$\phi_{V,top-air} = \phi_{V,air-top} - \phi_{V,top-out} \qquad [m^3\ s^{-1}] \qquad (3.114)$$

$$\phi_{V,air-air} = A_{soil} \cdot \frac{1}{3600} \cdot c_{vent,in} \qquad [m^3\ s^{-1}] \qquad (3.115)$$

$$\phi_{V,air-out} = A_{soil} \cdot \frac{1}{3600} \cdot c_{vent} \qquad [m^3\ s^{-1}] \qquad (3.116)$$

$$\phi_{V,out-air} = \phi_{V,air-out} + \phi_{V,top-out} \qquad [m^3\ s^{-1}] \qquad (3.117)$$

Energy exchange due to leakage and ventilation

$$Q'_{top-out} = \phi_{V,top-out} \cdot \rho_{top} \cdot h_{top} \cdot \frac{3600}{1000} + \phi_{H_2O,cond,top} \cdot c_{P,H_2O} \cdot (T_{top} + 273.15) \cdot \frac{1}{1000} \qquad [MJ\ h^{-1}] \qquad (3.118)$$

$$Q'_{air-out} = \phi_{V,air-out} \cdot \rho_{air} \cdot h_{air} \cdot \frac{3600}{1000} \qquad [MJ\ h^{-1}] \qquad (3.119)$$

$$Q'_{out-air} = \phi_{V,out-air} \cdot \rho_{out} \cdot h_{out} \cdot \frac{3600}{1000} \qquad [MJ\ h^{-1}] \qquad (3.120)$$

$$Q'_{air-top} = Cl_{screen} \cdot (Q_{air-top} - Q_{top-air}) \cdot \frac{3600}{1000} \qquad [MJ\ h^{-1}] \qquad (3.121)$$

$$Q_{air-top} = \phi_{V,air-top} \cdot h_{air} \cdot \rho_{air} \qquad [W] \qquad (3.122)$$

$$Q_{top-air} = \phi_{V,top-air} \cdot h_{top} \cdot \rho_{top} \qquad [W] \qquad (3.123)$$

3.8.5 Psychometrics

$$P_{vs,air} = 10^{2.7857+\frac{7.5 \cdot T_{air}}{237.3+T_{air}}} \quad [Pa] \quad (3.124)$$

$$P_{vs,cond} = 10^{2.7857+\frac{7.5 \cdot T_{cond}}{237.3+T_{cond}}} \quad [Pa] \quad (3.125)$$

$$P_{vs,out} = \begin{cases} 10^{2.7857+\frac{9.5 \cdot T_{out}}{265.5+T_{out}}} \; if \; T_{out}(t) < 0°C \\ 10^{2.7857+\frac{7.5 \cdot T_{out}}{237.3+T_{out}}} \; if \; T_{out}(t) > 0°C \end{cases} \quad [Pa] \quad (3.126)$$

$$P_{vs,top} = \begin{cases} 10^{2.7857+\frac{9.5 \cdot T_{top}}{265.5+T_{top}}} \; if \; T_{top}(t) < 0°C \\ 10^{2.7857+\frac{7.5 \cdot T_{top}}{237.3+T_{top}}} \; if \; T_{top}(t) > 0°C \end{cases} \quad [Pa] \quad (3.127)$$

$$P_{v,out} = P_{vs,out} \cdot RH_{out} \quad [Pa] \quad (3.128)$$

$$VPD_{air} = (1 - RH_{air}) \cdot P_{vs,out} \quad [Pa] \quad (3.129)$$

$$RH_{air} = x_{air}/x_{s,air} \quad [\%] \quad (3.130)$$

$$x_{air} = x_{s,air} - VD_{air} \cdot \rho_{air} \quad [kg\ kg^{-1}] \quad (3.131)$$

$$x_{top} = c_{top-out} \cdot x_{air} + \left(1 - c_{top-out}\right) \cdot x_{out} \quad [kg\ kg^{-1}] \quad (3.54)$$

$$x_{out} = x_{s,out} \cdot RH_{out} \quad [kg\ kg^{-1}] \quad (3.132)$$

$$x_{s,air} = 0.62198 \cdot \frac{P_{vs,air}}{P_{out} - P_{vs,air}} \quad [kg\ kg^{-1}] \quad (3.133)$$

$$x_{s,top} = 0.62198 \cdot \frac{P_{vs,top}}{P_{out} - P_{vs,top}} \quad [kg\ kg^{-1}] \quad (3.134)$$

$$x_{s,cond} = 0.62198 \cdot \frac{P_{vs,cond}}{P_{out} - P_{vs,cond}} \quad [kg\ kg^{-1}] \quad (3.135)$$

$$h_{air} = 1.005 \cdot T_{air} + x_{air} \cdot (1.805 \cdot T_{air} + 2501) \quad [kJ\ kg^{-1}] \quad (3.136)$$

$$h_{air,cool} = 1.005 \cdot T_{cond} + x_{s,cond} \cdot (1.805 \cdot T_{cond} + 2501) \quad [kJ\ kg^{-1}] \quad (3.137)$$

$$h_{top} = 1.005 \cdot T_{top} + x_{top} \cdot \left(1.805 \cdot T_{top} + 2501\right) \quad [kJ\ kg^{-1}] \quad (3.138)$$

$$h_{out} = 1.005 \cdot T_{out} + x_{out} \cdot (1.805 \cdot T_{out} + 2501) \quad [kJ\ kg^{-1}] \quad (3.139)$$

$$\rho_{air} = \frac{P_{out}}{R \cdot (T_{air} + 273.15)} \quad [kg\ m^{-3}] \quad (3.140)$$

$$\rho_{top} = \frac{P_{out}}{R \cdot \left(T_{top} + 273.15\right)} \quad [kg\ m^{-3}] \quad (3.141)$$

$$\rho_{out} = \frac{P_{out}}{R \cdot (T_{out} + 273.15)} \qquad [kg\ m^{-3}] \qquad (3.142)$$

$$\epsilon = 0.7584 e^{0.0518 \cdot T_{air}} \qquad [-] \qquad (3.143)$$

$$\gamma_{air} = \frac{0.001013 \cdot P_{out}}{0.62198 \cdot (2.501 - 0.002361 \cdot T_{air})} \qquad [Pa\ °C^{-1}] \qquad (3.144)$$

Latent heats of condensation and vaporisation are approximated using an empirical cube function (Rogers & Yau 1989):

$$L_{cond} = 2500.8 + 2.36 \cdot T_{cond} + 0.0016 \cdot T_{cond}^2 - 0.00006 \cdot T_{cond}^3 \qquad [kJ\ kg^{-1}] \qquad (3.145)$$

$$L_{cond,top} = 2500.8 + 2.36 \cdot T_{top} + 0.0016 \cdot T_{top}^2 - 0.00006 \cdot T_{top}^3 \qquad [kJ\ kg^{-1}] \qquad (3.146)$$

$$L_{evap} = 2500.8 + 2.36 \cdot T_{evap} + 0.0016 \cdot T_{evap}^2 - 0.00006 \cdot T_{evap}^3 \qquad [kJ\ kg^{-1}] \qquad (3.147)$$

3.8.6 List of parameters

Symbol	Value	Unit	Description	Excel® name	Sheet and cell
$h_{air,cool}$	*(3.137)*	$kJ\ kg^{-1}$	Greenhouse air energy content at condensation temperature	-	-
h_{air}	*(3.136)*	$kJ\ kg^{-1}$	Greenhouse air energy content	air h	Climate CU
h_{out}	*(3.139)*	$kJ\ kg^{-1}$	Outside air energy content	out h	Climate CN
h_{top}	*(3.138)*	$kJ\ kg^{-1}$	Top air energy content	top h	Climate CT
A_{soil}	1000 (input value)	m^2	Total NFT production area	u_plant_sqm	Coupling C2
C_{height}	3	m	Greenhouse height	u_GH_height	Greenhouse C29
Cl_{cloud}	$\frac{1}{9} \cdot Cl'_{cloud}$	[0,1]	Cloud closure	-	-
Cl'_{cloud}	input (KNMI 2015)	[0,9]	Cloud closure	Cloud	Climate G
Cl_{screen}	*(3.47)*	[0,1]	Thermal screen closure	GH screen	Climate N
$C_{th,soil}$	10	$MJ\ K^{-1}\ m^{-2}$	Soil specific thermal mass	u_GH_c_th	Greenhouse C32
$C_{top-out}$	38.7%	%	Constant for calculating temperature of top air	p_airtemp	Greenhouse C2
DQ'_{air}	*(3.42)*	$MJ\ h^{-1}$	Air energy storage	air d	Climate BX
DQ'_{soil}	*(3.35)*	$MJ\ h^{-1}$	Soil energy storage	soil d	Climate AZ
DQ'_{top}	*(3.55)*	$MJ\ h^{-1}$	Top air energy storage (error)	GH air up error	Climate AO
DW_{fruit}	*(3.3)*	$g_{DM}\ h^{-1}$	Dry matter production of fruits	(DMFR_daily: daily value)	(Plant J: daily value)
DW_{leaf}	*(3.2)*	$g_{DM}\ h^{-1}$	Dry matter production of leafs	-	-
DW_{tot}	*(3.1)*	$g_{DM}\ h^{-1}$	Total plant dry matter production	(DMprod_daily: daily value)	(Plant G: daily value)
E_{air}	*(3.43)*	MJ	Air energy content	GH air energy	Climate AM
E_{soil}	*(3.37)*	MJ	Soil energy content	GH soil energy	Climate AR

F_{cover}	*(3.32)*	%	Cover light interception cover	p_GH_a	Greenhouse C77
F_{plant}	*(3.31)*	%	Plant light interception fraction	plant light interception	Climate W
F'_{screen}	*(3.30)*	%	Screen light transmission factor	GH screen tansm	Climate O
$L_{cond,top}$	*(3.147)*	$kJ\ kg^{-1}$	Latent heat of condensation in top air	-	-
L_{cond}	*(3.145)*	$kJ\ kg^{-1}$	Latent heat of condensation in dehumidifier	cond_h	Greenhouse C68
P_{light}	*(3.65)*	$W\ m^{-2}$	Lighting power	GH lighting2	Climate R
P_{out}	$P'_{out} \cdot 10$	Pa	Outside air pressure	-	-
P'_{out}	input (KNMI 2015)	$0.1\ Pa$	Measured air pressure	P	Climate F
$P_{v,out}$	*(3.128)*	Pa	Outside vapour pressure	out pv	Climate CL
$P_{vs,air}$	*(3.124)*	Pa	Greenhouse air vapour pressure at saturation	Air pvsat	Climate CO
$P_{vs,cond}$	*(3.125)*	Pa	Dehumidifier air vapour pressure at saturation	-	-
$P_{vs,out}$	*(3.126)*	Pa	Outside vapour pressure at saturation	out pvsat	Climate CK
$P_{vs,top}$	*(3.127)*	Pa	Top air vapour pressure at saturation	top pvs	Climate CS
Q_{R_n}	*(3.89)*	$W\ m^{-2}$	Total PAR absorbed by plant leafs (Stanghellini)	Rn	Climate DB
Q'_{heat}	*(3.46)*	$MJ\ m^{-2}\ h^{-1}$	Heating energy needed to keep greenhouse temperature at set point	heating	Climate CA
$Q_{PAR,in}$	*(3.92)*	$MJ\ m^{-2}\ h^{-1}$	Total PAR after passing screen	PAR (PARinside: daily value)	Climate U (Plant D: daily value)
$Q_{PAR,plant}$	*(3.91)*	$MJ\ m^{-2}\ h^{-1}$	Total PAR absorbed by plant leafs	(PAR_intercepted: daily value)	(Plant F: daily value)
$Q'_{air-out}$	*(3.119)*	$MJ\ h^{-1}$	Energy exchange due to cover leakage from inside to outside air	vent out	Climate BQ
$Q'_{air-plant}$	*(3.39)*	$MJ\ h^{-1}$	Convective energy transfer between air and plant	plant convection	Climate BB
$Q'_{air-screen}$	*(3.79)*	$MJ\ h^{-1}$	Convective energy transfer between air and screen	screen conv down	Climate BG
$Q'_{air-top}$	*(3.121)*	$MJ\ h^{-1}$	Energy leakage from air to top air through screen	screen leak2	Climate BK

$Q'_{cond,release,top}$	*(3.57)*	$MJ\ h^{-1}$	Energy released by condensation of water (above screen)	top cond release	Climate BV
$Q'_{cond,release}$	*(3.77)*	$MJ\ h^{-1}$	Energy released by condensation of water	condens release	Climate CC
$Q'_{cond,remove}$	*(3.44)*	$MJ\ h^{-1}$	Energy removed from air to condense water (minus regained energy)	cond cooling	Climate CB
Q'_{cond}	*(3.76)*	$MJ\ h^{-1}$	Total energy removed from air to condense water	cond remove	Climate DJ
$Q'_{cool,heat}$	*(3.41)*	$MJ\ h^{-1}$	Cooling (positive) or heating energy (negative) needed to keep greenhouse temperature at set point	air d to cool	Climate BW
Q'_{cool}	*(3.45)*	$MJ\ h^{-1}$	Cooling energy needed to keep greenhouse temperature at set point	extra cooling	Climate BZ
$Q'_{cover-out}$	*(3.82)*	$MJ\ h^{-1}$	Convective energy transfer between cover and outside air	cover conv up	Climate BT
$Q'_{cover-sky}$	*(3.102)*	$MJ\ h^{-1}$	Radiative energy transfer between cover and sky	cover rad out	Climate BN
Q'_{evap}	*(3.11)*	$MJ\ h^{-1}$	Energy of plant evaporation	plant evap	Climate BC
$Q'_{fan-air}$	*(3.68)*	$MJ\ h^{-1}$	Energy of ventilation fans released to air	fan power	Climate BY
$Q'_{fan-cond}$	*(3.66)*	$MJ\ h^{-1}$	Energy use of dehumidifier fan	-	-
$Q'_{fan-vent}$	*(3.67)*	$MJ\ h^{-1}$	Energy use of ventilation fans	-	-
Q_{light}	See *Ch. 3.7.7 Supplemental lighting*	$MJ\ m^{-2}\ h^{-1}$	Lighting irradiation	GH lighting	Climate Q
$Q'_{light-air}$	*(3.65)*	$MJ\ h^{-1}$	Heat of additional lighting released to air	-	-
$Q'_{out-air}$	*(3.120)*	$MJ\ h^{-1}$	Energy exchange due to leakage from outside to inside air	cover leak in	Climate BR
$Q'_{plant-cover}$	*(3.100)*	$MJ\ h^{-1}$	Radiative energy transfer between plant and cover	plant rad cover	Climate BE
$Q'_{plant-screen}$	*(3.99)*	$MJ\ h^{-1}$	Radiative energy transfer between plant and screen	plant rad screen	Climate BD
$Q'_{rad,cover}$	*(3.95)*	$MJ\ h^{-1}$	Total cover irradiation energy (sun)	cover rad in	Climate BM
$Q_{rad,in}$	*(3.87)*	$W\ m^{-2}$	Total incoming irradiation after passing screen (sun & lighting)	Qtot	Climate T
$Q'_{rad,in}$	*(3.88)*	$MJ\ h^{-1}$	Total incoming irradiation after passing screen (sun & lighting)	-	-
$Q'_{rad,plant}$	*(3.90)*	$MJ\ h^{-1}$	Total plant irradiation energy (sun & lighting)	plant rad in	Climate BA
$Q'_{rad,screen}$	*(3.94)*	$MJ\ h^{-1}$	Total screen irradiation energy (sun)	screen rad in	Climate BF

$Q'_{rad,soil}$	*(3.93)*	$MJ\ h^{-1}$	Total soil irradiation energy (sun & lighting)	soil rad in	Climate AU
$Q'_{screen-cover}$	*(3.101)*	$MJ\ h^{-1}$	Radiative energy transfer between screen and cover	screen rad cover	Climate BI
$Q'_{screen-top}$	*(3.80)*	$MJ\ h^{-1}$	Convective energy transfer between screen and top air	screen conv up	Climate BH
$Q'_{soil-air}$	*(3.78)*	$MJ\ h^{-1}$	Convective energy transfer between soil and air	soil conv	Climate AV
$Q'_{soil-cover}$	*(3.98)*	$MJ\ h^{-1}$	Radiative energy transfer between soil and cover	soil rad cover	Climate AY
$Q'_{soil-plant}$	*(3.96)*	$MJ\ h^{-1}$	Radiative energy transfer between soil and plant	soil rad plant	Climate AW
$Q'_{soil-screen}$	*(3.97)*	$MJ\ h^{-1}$	Radiative energy transfer between soil and screen	soil rad screen	Climate AX
Q_{sun}	$Q'_{sun} \cdot \frac{10}{3.6}$	$W\ m^{-2}$	Solar irradiation	-	-
Q'_{sun}	input (KNMI 2015)	$J\ cm^{-2}\ h^{-1}$	Measured solar irradiation	Q	Climate E
$Q'_{top-cover}$	*(3.81)*	$MJ\ h^{-1}$	Convective energy transfer between top air and cover	cover conv down	Climate BS
$Q'_{top-out}$	*(3.118)*	$MJ\ h^{-1}$	Energy exchange due to air leakage through greenhouse cover	cover leak out	Climate BP
RH_{air}	*(3.130)*	%	Greenhouse air relative humidity	air RH	Climate CJ
RH_{out}	$RH'_{out}/100$	%	Outside relative humidity	-	-
RH'_{out}	input (KNMI 2015)	100%	Measured outside relative humidity	RH	Climate H
R_{cover}	7%	%	Greenhouse reflectivity	p_GH_refl	Greenhouse C33
T_{air}	*(3.40)*	$°C$	Greenhouse air temperature	GH air temp	Climate AL
T_{cover}	*(3.32)*	$°C$	Temperature of greenhouse cover	GH cover temp	Climate AP
T_{lin}	17.5	$°C$	Temperature around which radiative heat transfer linearization takes place	p_Tlin	Greenhouse C51
T_{out}	$T'_{out} \cdot 10$	$°C$	Outside air temperature	Temp outside	Climate AJ
T'_{out}	input (KNMI 2015)	$0.1\ °C$	Measured outside temperature	T	Climate D
T_{plant}	*(3.38)*	$°C$	Temperature of plants	GH plant temp	Climate AS
T_{screen}	*(3.52)*	$°C$	Temperature of greenhouse screen	GH screen temp	Climate AT
T_{sky}	*(3.110)*	$°C$	Sky temperature	Temp sky	Climate AK

T_{soil}	*(3.36)*	$°C$	Temperature of greenhouse soil	GH soil temp	Climate AQ
T_{top}	*(3.53)*	$°C$	Air temperature above screen	GH air up	Climate AN
k_{plant}	0.7	$-$	Overall plant extinction coefficient	p_plant_k	Greenhouse C10
$m_{H_2O,air}$	*(3.73)*	kg	Total mass of water as vapour in the greenhouse air	GH water vapour	Climate CD
r_b	200	$s\ m^{-1}$	Leaf boundary resistance	rb	Climate CZ
r_s	*(3.9)*	$s\ m^{-1}$	Leaf stomatal resistance	rs	Climate DA
x_{air}	*(3.131)*	$kg\ kg^{-1}$	Greenhouse air humidity factor	air x	Climate CQ
x_{out}	*(3.132)*	$kg\ kg^{-1}$	Outside air humidity factor	out x	Climate CM
$x_{s,air}$	*(3.133)*	$kg\ kg^{-1}$	Greenhouse air humidity factor at saturation	air xsat	Climate CR
$x_{s,cond}$	*(3.135)*	$kg\ kg^{-1}$	Condensation air humidity factor at saturation	cond xsat	Climate DL
$x_{s,top}$	*(3.134)*	$kg\ kg^{-1}$	Top air humidity factor at saturation	-	-
x_{top}	*(3.54)*	$kg\ kg^{-1}$	Top air humidity factor	top x	Climate DI
$\alpha_{air-screen}$	*(3.84)*	$W\ m^{-2}\ K^{-1}$	Heat transfer coefficient between air and screen	k_airscreen	Climate AE
$\alpha'_{air-screen}$	4.0	$W\ m^{-2}\ K^{-1}$	Coefficient for heat transfer between air and screen	p_a_screen_down	Greenhouse C45
α_{cover}	*(3.60)*	$W\ m^{-2}\ K^{-1}$	Intermediate heat transfer coefficient for cover	k_A	Climate AH
$\alpha_{cover-out}$	*(3.86)*	$W\ m^{-2}\ K^{-1}$	Heat transfer coefficient between cover and outside air	k_coverout	Climate AG
$\alpha'_{cover-out}$	2.8	$W\ m^{-2}\ K^{-1}$	Coefficient for heat transfer between cover and outside air	p_a_cover_up	Greenhouse C48
$\alpha_{cover-sky}$	*(3.109)*	$W\ m^{-2}\ K^{-1}$	Heat transfer coefficient between cover and sky	k_coversky	Greenhouse C78
$\alpha_{plant-cover}$	*(3.107)*	$W\ m^{-2}\ K^{-1}$	Coefficient for heat transfer between plant and cover	k_plantcover	Climate AC
$\alpha_{plant-screen}$	*(3.106)*	$W\ m^{-2}\ K^{-1}$	Coefficient for heat transfer between plant and screen	k_plantscreen	Climate AB
α_{screen}	*(3.50)*	$W\ m^{-2}\ K^{-1}$	Intermediate heat transfer coefficient for screen	k_B	Climate AI
$\alpha_{screen-cover}$	*(3.108)*	$W\ m^{-2}\ K^{-1}$	Heat transfer coefficient between screen and cover	k_screencover	Climate AF
$\alpha_{screen-top}$	*(3.85)*	$W\ m^{-2}\ K^{-1}$	Heat transfer coefficient between screen and top air	k_screentop	Climate AD

$\alpha'_{screen-top}$	4.0	$W\ m^{-2}\ K^{-1}$	Coefficient for heat transfer between screen and top air	p_a_screen_up	Greenhouse C46
$\alpha_{soil-air}$	*(3.83)*	$W\ m^{-2}\ K^{-1}$	Heat transfer coefficient between soil and air	-	-
$\alpha'_{soil-air}$	1.86	$W\ m^{-2}\ K^{-1}$	Coefficient for heat transfer between soil and air	p_a_soil	Greenhouse C44
$\alpha_{soil-cover}$	*(3.105)*	$W\ m^{-2}\ K^{-1}$	Heat transfer coefficient between soil and cover	k_soilcover	Climate Z
$\alpha_{soil-plant}$	*(3.103)*	$W\ m^{-2}\ K^{-1}$	Heat transfer coefficient between soil and plant	k_soilplant	Climate AA
$\alpha_{soil-screen}$	*(3.104)*	$W\ m^{-2}\ K^{-1}$	Heat transfer coefficient between soil and screen	k_soilscreen	Climate Y
$\alpha_{top-cover}$	4.0	$W\ m^{-2}\ K^{-1}$	Heat transfer coefficient between top air and cover	p_a_cover_down	Greenhouse C45
γ_{air}	*(3.144)*	$Pa\ °C^{-1}$	Air heat capacity ratio	air gamma	Climate CV
$\varepsilon_{cover,down}$	0.95	$W\ m^{-2}\ K^{-4}$	Cover downward emissivity	p_e_cover	Greenhouse C42
$\varepsilon_{cover,up}$	0.95	$W\ m^{-2}\ K^{-4}$	Cover upward emissivity	p_e_cover_up	Greenhouse C43
ε_{plant}	0.7	$W\ m^{-2}\ K^{-4}$	Plant emissivity	p_e_plant	Greenhouse C39
$\varepsilon_{screen,down}$	0.5	$W\ m^{-2}\ K^{-4}$	Screen downward emissivity	p_e_screen	Greenhouse C40
$\varepsilon_{screen,up}$	0.5	$W\ m^{-2}\ K^{-4}$	Screen upward emissivity	p_e_screen_up	Greenhouse C41
$\varepsilon_{sky,clear}$	*(3.111)*	$W\ m^{-2}\ K^{-4}$	Clear sky emissivity	-	-
ε_{sky}	1.0	$W\ m^{-2}\ K^{-4}$	Sky emissivity	p_sky	Greenhouse C37
ε_{soil}	0.7	$W\ m^{-2}\ K^{-4}$	Soil emissivity	p_e_soil	Greenhouse C38
$\eta_{PAR,light}$	100%	%	PAR component of additional lighting irradiation	PAR%light	Greenhouse C15
$\eta_{PAR,sun}$	47%	%	PAR component of sunlight irradiation	PAR%RAD	Greenhouse C14
η_{cond}	0%	%	Condensation heat regeneration efficiency	regen_eff	Greenhouse C69
η_{exch}	90%	%	Heat exchange efficiency	cool_eff	Greenhouse C53
$\eta_{fan,vent}$	20	$m^3\ h^{-1}\ W^{-1}$	Ventilation fan efficiency	vent_eff	Greenhouse C72
$\eta_{fan,cond}$	5	$m^3\ h^{-1}\ W^{-1}$	Dehumidifier fan efficiency	fan_eff	Greenhouse C71
η_{light}	32%	%	Lighting efficiency	light_eff	Greenhouse C55
ρ_{H_2O}	1	$kg\ l^{-1}$	Water density	-	-

ρ_{air}	*(3.140)*	$kg\ m^{-3}$	Greenhouse air density	air rho	Climate CY
ρ_{out}	*(3.142)*	$kg\ m^{-3}$	Outside air density	out rho	Climate CW
ρ_{top}	*(3.141)*	$kg\ m^{-3}$	Greenhouse top air density	top rho	Climate CX
σ'_{lin}	*(3.27)*	$W\ m^{-2}\ K^{-1}$	Stefan-Boltzmann constant modified for linearized radiative heat transfer	p_sigmlin	Greenhouse C80
τ_{cover}	70%	%	Greenhouse transmittivity	p_GH_transm	Greenhouse C34
τ_{screen}	25%	%	Screen transmittivity	p_screen_transm	Greenhouse C49
$\phi'_{H_2O,NFT-plants}$	*(3.7)*	$kg\ h^{-1}$	Plant water uptake	F_NFT_plant_h2o (total water: $mm\ day^{-1}$)	Main X (Plant O: $mm\ day^{-1}$)
$\phi'_{H_2O,cond,top}$	*(3.56)*	$kg\ h^{-1}$	Top air condensation water flow	top cond	Climate DM
$\phi'_{H_2O,cond}$	*(3.70)*	$kg\ h^{-1}$	Dehumidifier condensation water flow	GH condens	Climate CH
$\phi'_{H_2O,evap}$	*(3.10)*	$kg\ h^{-1}$	Plant evaporation water flow	GH evap model	Climate CG
$\phi'_{H_2O,in}$	*(3.71)*	$kg\ h^{-1}$	Greenhouse incoming water flow (humidity)	water in	Climate CE
$\phi'_{H_2O,out}$	*(3.72)*	$kg\ h^{-1}$	Greenhouse outgoing water flow (humidity)	water out	Climate CF
$\phi_{N,NFT-plants}$	*(3.6)*	$g_N\ h$	Plant NFT uptake	f_NFT_plant_N (N-uptake: $g\ m^{-2}\ day^{-1}$)	Main GV (Plant L: $g\ m^{-2}\ day^{-1}$)
$\phi_{V,air-air}$	*(3.115)*	$m^3\ s^{-1}$	Recirculating air flow	-	-
$\phi_{V,air-out}$	*(3.116)*	$m^3\ s^{-1}$	Air flow from greenhouse air to outside air	vent_flow	Greenhouse C80
$\phi_{V,air-top}$	*(3.113)*	$m^3\ s^{-1}$	Air flow from greenhouse air to top air	screen leak	Climate BJ
$\phi'_{V,cond}$	*(3.75)*	$kg\ h^{-1}$	Required airflow for condensation	cond airflow	Climate DK
$\phi_{V,out-air}$	*(3.117)*	$m^3\ s^{-1}$	Air flow from outside air to greenhouse air	-	-
$\phi_{V,top-air}$	*(3.114)*	$m^3\ s^{-1}$	Air flow from top air to greenhouse air	-	-
$\phi_{V,top-out}$	*(3.112)*	$m^3\ s^{-1}$	Air flow from top air to outside air	cover leak	Climate BO

$\phi_{V,wind}$	$\phi'_{V,wind} \cdot 10$	$m^3\ s^{-1}$	Measured wind speed	-	-
$\phi'_{V,wind}$	input (KNMI 2015)	$0.1\ m^3\ s^{-1}$	Measured wind speed	U	Climate C
Δt_{plant}	*24*	h	Time step	-	-
Δt	*1*	h	Time step	-	-
DMC_{fruit}	7.5%	%	Fruit dry matter content	DMCfruits	Greenhouse C12
DMC_{plant}	11%	%	Plant dry matter content	DMCplant	Greenhouse C13
LAI	*(3.5)*	$m^2\ m^{-2}$	Plant leaf area index	Plant LAI	Climate V
LUE	4	$m^2\ m^{-2}$	Plant light use efficiency	p_LUE	Greenhouse C17
SLA	250	$cm^2\ g_{DM}^{-1}$	Plant specific leaf area	SLA	Greenhouse C16
VD_{air}	*(3.69)*	$g\ m^{-3}$	Vapour deficit	GH vapour deficit	Climate CI
VPD_{air}	*(3.129)*	Pa	Vapour pressure deficit	air VPD	Climate CP
$dLAI$	*(3.4)*	$m^2 m^{-2}$	Change in plant LAI	-	-
σ	$5.67 \cdot 10^{-8}$	$W\ m^{-2}\ K^{-4}$	Stefan-Boltzmann constant	p_stefboltz	Greenhouse C50
ϵ	*(3.143)*	$-$	Ratio of latent and sensible heat of saturated air for a change of 1°C	e	Climate DC

4. Results and discussion

In this chapter, modelling results are discussed.

4.1 RAS

4.1.1 Fish production

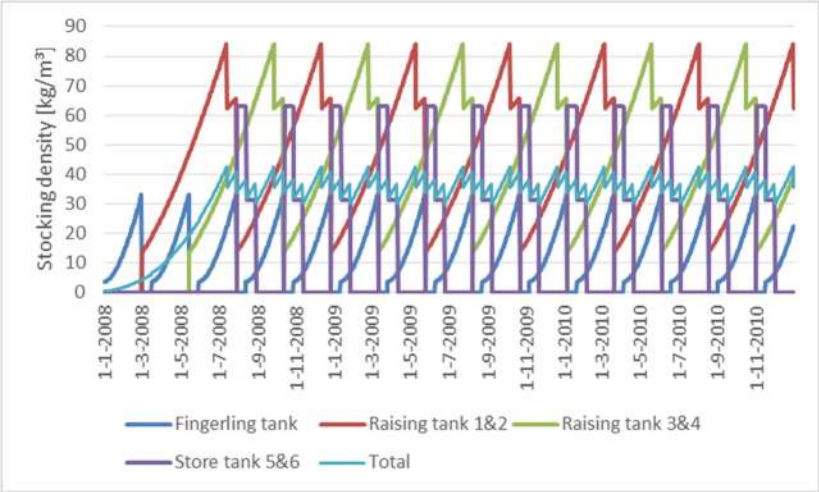

Figure 8 Fish stocking density through time, also shown divided over the different fish tanks

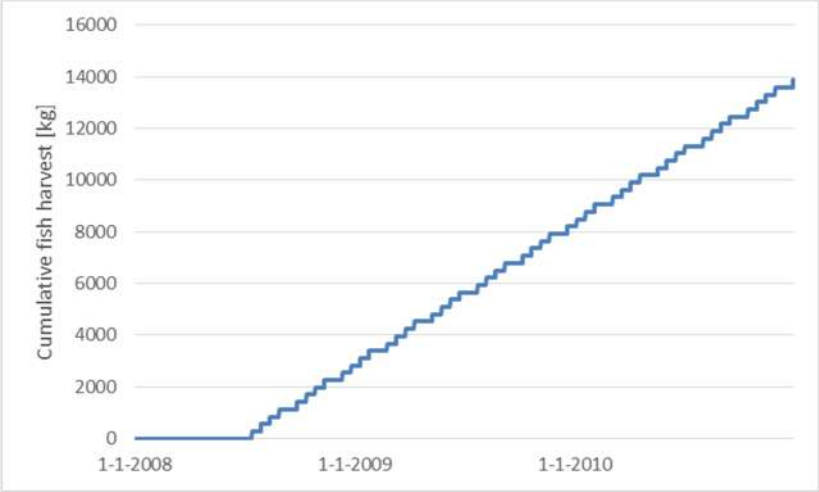

Figure 9 Cumulative fish harvest

Based on the given size of the fish tanks in the INAPRO system, the simulated fish standing stock is shown in Figure 8 using multiple tanks: one fingerling tank, four production tanks (grouped per two) and two store tanks (also grouped). It shows that the fingerling tank is almost continuously in use and supplies fish to the production tanks. From the production tanks, two batches of fish are harvested and after five months the fish are transferred to the store tanks from where the remainder is harvested again in two batches. This results in a repetitive total stocking pattern, with half a month between harvests for two months, followed by a whole month between harvests for one month. In

Figure 8, the total stocking density follows a saw tooth function around the total average stocking density, with a slight decrease in stocking density during the two months of bi-monthly harvest and a slight increase in density during the month of no harvest. The effect on the cumulative harvested fish weight is shown in Figure 9 .

4.1.2 Nitrogen compounds

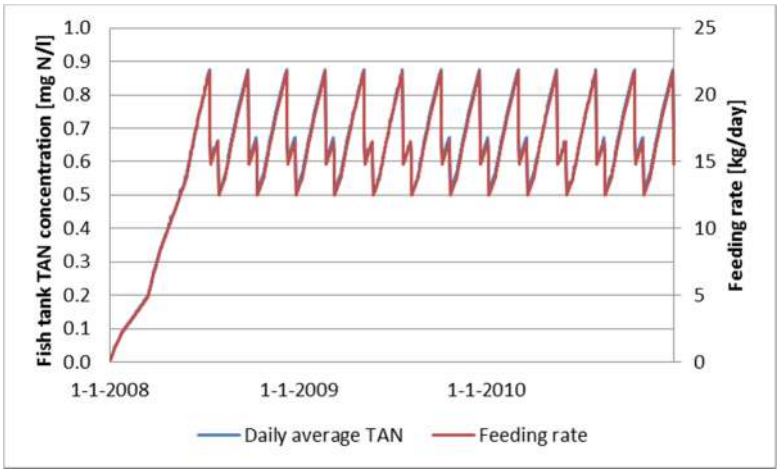

Figure 10 Fish tank TAN concentration and daily total feeding rate, evenly staggered production

As seen in Figure 10, the fish tank TAN concentration through time very closely follows the daily feeding rate. This is because of the nitrification taking place in the recirculating RAS system. TAN is nitrified at a concentration-dependent rate. The equilibrium concentration in the fish tanks is then dependent on the TAN excretion by the fish which in turn is dependent on the feeding rate.

Also, comparing Figure 10 to Figure 8, it can be seen that the feeding rate is mostly dependent on the stocking density in the raising tanks; the fish in the store tanks are not fed and the fish in the fingerling tank eat very little compared to the fish in the raising tanks.

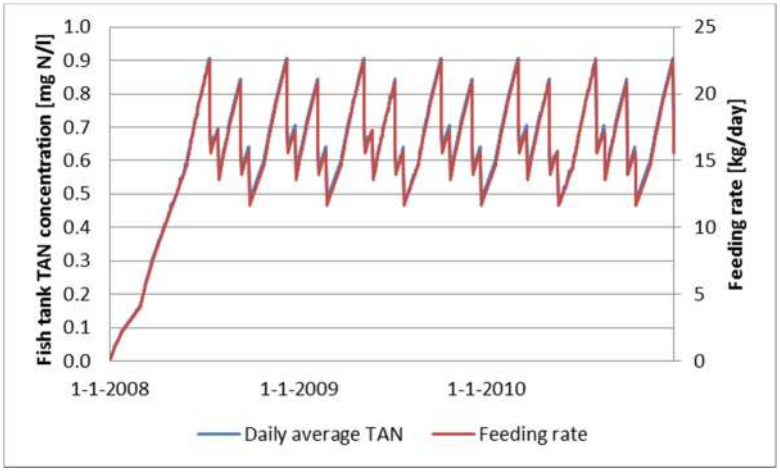

Figure 11 Fish tank TAN concentration and daily total feeding rate, unevenly staggered production

When comparing the unevenly staggered production in Figure 11 with Figure 10, it becomes apparent that the total feeding rate is most stable through time when the production cycle is staggered evenly (2.5 months between cycles; Figure 10) compared to an uneven staggering (alternating between 2 and 3 months between cycles; Figure 11). Furthermore, unevenly staggered production causes a slightly higher peak TAN concentration when compared to even staggering.

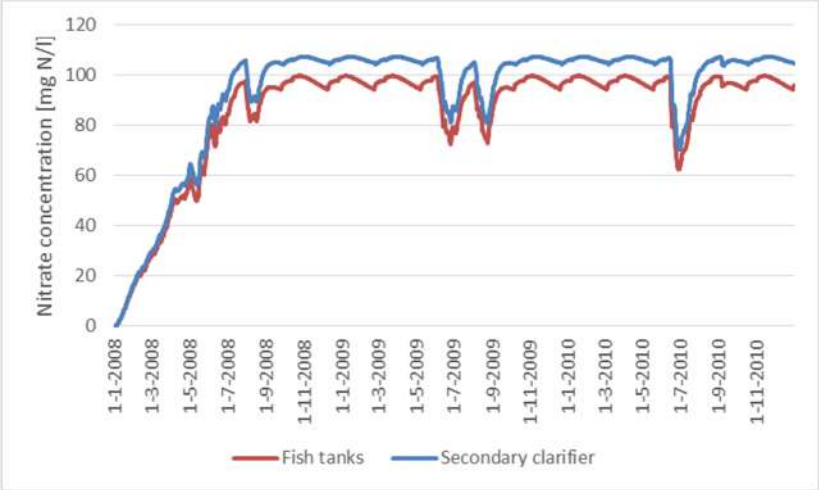

Figure 12 Nitrate concentration in secondary clarifier tank and average nitrate concentration in the fish tanks in case coupling flow is based on the feeding rate, with a minimum of 4800 l/day

In Figure 12, the effect of solids nitrification and dissolving of nitrate in solids in the secondary clarifier can be seen. These processes cause the nitrate concentration in the secondary clarifier to be higher than in the fish tanks. This is of use; an increased nitrate concentration will be closer to the plant nitrogen uptake concentration and hence less N fertiliser is needed for the same maximum nitrate concentration in the fish tanks.

The dips in nitrate concentration seen during the summer period are due to an increased coupling flow; in this period the demand from the NFT system is higher than the regular feed-based flow rate from the RAS system and additional water is pumped from RAS to NFT, causing a dip in the nitrogen concentration. This is also described in section 4.2.3.

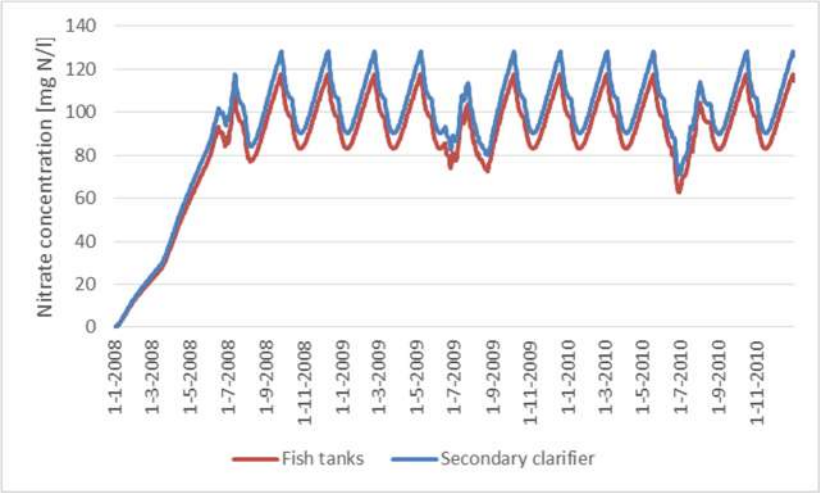

Figure 13 Nitrate concentration in secondary clarifier tank and average nitrate concentration in the fish tanks in case coupling flow is constant at 4800 l/day

Comparing a constant coupling flow rate of 4800 l/day in Figure 13 to Figure 12, it can be seen that the nitrate concentration in the fish tanks is more sensitive to the fish production cycle when the coupling flow between the RAS and NFT systems is constant (Figure 13) as opposed to feeding rate-dependent (Figure 12). The average concentrations stay the same, but the peak nitrate concentration has risen 18% from 100 mg N/l in case of feed-based flow to 118 mg N/l in case of constant flow. To prevent potentially toxic peaks in nitrate concentration, the coupling flow will need to be higher in case of a constant coupling flow rate. For the same peak nitrate concentration, the minimum flow rate needed to be increased from 4800 l/day to 5650 l/day.

4.2 NFT

4.2.1 Plant growth

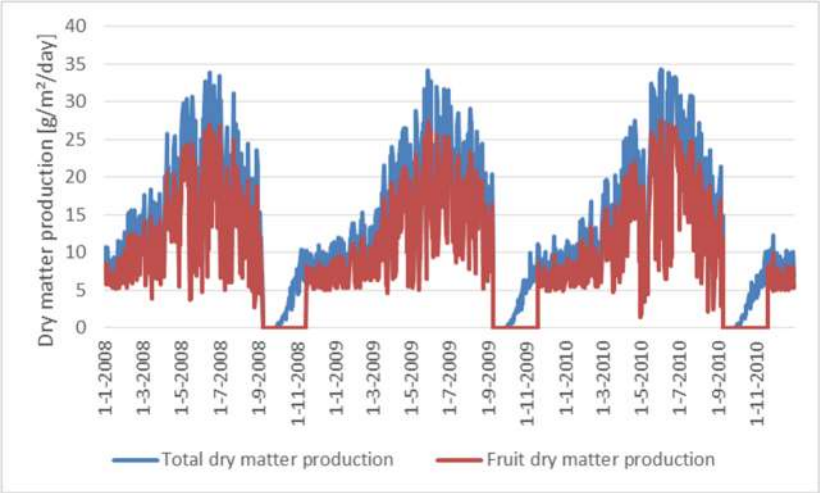

Figure 14 Plant growth expressed as dry matter production

Plant growth results, divided into total dry matter production and fruit dry matter production, are presented in Figure 14. The dry matter production shows a peak during summer, and relatively little growth in winter when there is little light available and the crop is not yet fully developed. It can also be seen that when the crop is fully developed, almost all of the dry matter production is partitioned to the fruits.

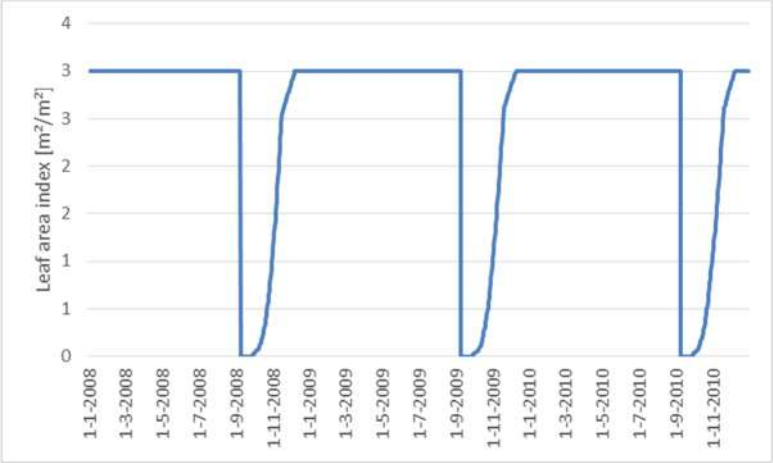

Figure 15 Plant leaf area index

In Figure 15, the development of the crop can be seen as an increase in LAI, which slows down when the plant starts partitioning dry matter production to the fruits and it is assumed that it stops increasing when an LAI of 3 is reached.

Table 2 Yearly tomato yield

	2008	**2009**	**2010**	**Average**
Yearly yield	50.4 kg/m²	49.6 kg/m²	48.8 kg/m²	49.6 kg/m²

The plant light use efficiency was modified to simulate a tomato cultivar with a yield of about 50 kg/m² under commercial conditions. The calculated yearly yield of the crop however, depicted in Table 2, is dependent on the weather input data. The slightly higher yield of the 2008 crop coincides with the slightly higher total amount of solar radiation in that growing period when comparing to the other crop years. This can also be seen by comparing the plant dry matter production in Figure 14 with the daily cumulative irradiation described in chapter 4.2.3 Greenhouse climate.

4.2.2 Nitrogen compounds

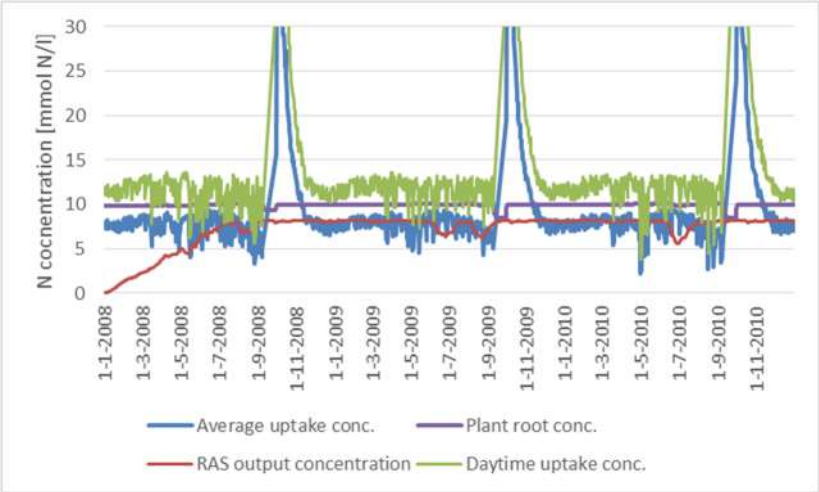

Figure 16 Plant nitrogen uptake concentration and root nitrogen concentration

In Figure 16, the effect of the plant growth stage on the nitrogen uptake concentration can be seen. The nitrogen uptake concentration is calculated by dividing the total plant nitrogen uptake, converted to mM, by the total water uptake of the plant:

$$C_{uptake,N} = \frac{\phi_{N,NFT-plants}}{\phi'_{H_2O,NFT-plants}/\rho_{H_2O} \cdot 14.0067} \qquad [mM] \qquad (4.1)$$

When the crop is not yet fully grown, the uptake concentration is high because plant evaporation (a main cause of plant water uptake) is still low compared to the dry matter production (and thus nitrogen uptake). The uptake concentration gradually declines until dry matter starts being partitioned to the fruit. After that time, the uptake concentration remains roughly constant.

The difference between average and daytime uptake concentration can be explained by low night-time growth of the plant while some evaporation still takes place; therefore the night-time uptake concentration will be low and the day-time uptake concentration is higher than the average.

In summer, plant production is highest and the coupling flow between RAS and NFT is increased. This causes a dip in the RAS output nitrogen concentration, as also seen in Chapter 4.1.2 and discussed in Chapter 4.2.3.

Also shown is the plant root nitrogen concentration, which has a minimum value determined by the fertiliser set point, here set to 10 mmol N/l. If the root nitrogen concentration is lower than the uptake concentration, active uptake is required, costing the plant energy and thereby decreasing yield. The effect of active uptake on plant yield is not modelled, because the plant growth model used is only light-limited. In the model, the plant root nitrogen concentration increases when the plant uptake concentration is lower than the incoming concentration. In practice, the plant will probably take up water at the nitrogen concentration provided and store any excess nitrogen.

In the simulation depicted in Figure 16, the root nitrogen concentration is roughly constant at the fertiliser set point. Every time the uptake concentration is higher than the root concentration, fertiliser is added to bridge the difference. In practice the plant will probably not show large peaks in uptake concentration, due to nitrogen and water storage in the plant which is not modelled in this thesis. This does not affect the average fertiliser need, because there is no loss of nutrients from the NFT system modelled.

4.2.3 Greenhouse climate

The main goal of the greenhouse climate sub-model is to calculate evapotranspiration and the amount of water that can be condensed from the greenhouse air. Evapotranspiration is the main cause of plant water uptake. Condensation is necessary to keep the humidity in the closed greenhouse at a set point value. The condensed water is re-used, as an input of clean water into the water buffer tank, from which water is fed to the RAS system.

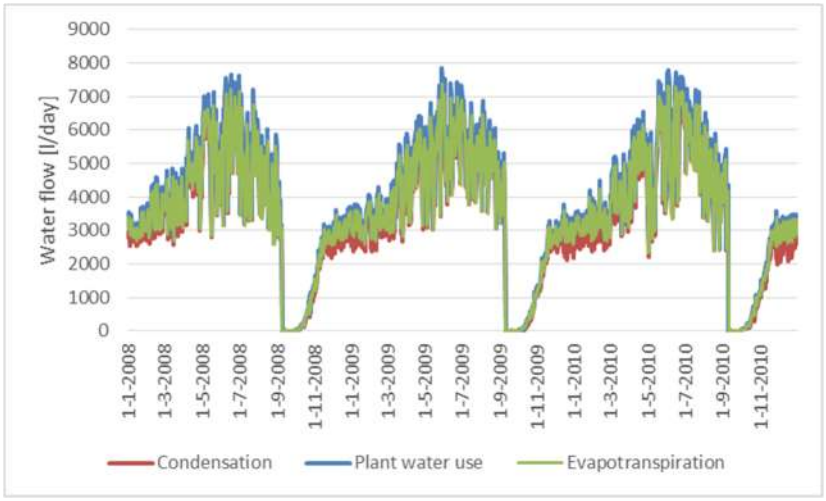

Figure 17 Greenhouse condensation flow, plant evapotranspiration and total water usage

As seen in Figure 17, the total plant water usage is mainly dependent on evapotranspiration. The condensation in the greenhouse very closely follows the total plant water usage through time. Comparing the figure with the dry matter production of the plant shown in Figure 14, it becomes apparent that plant evapotranspiration, total water uptake and greenhouse condensation are all dependent on the rate of plant growth.

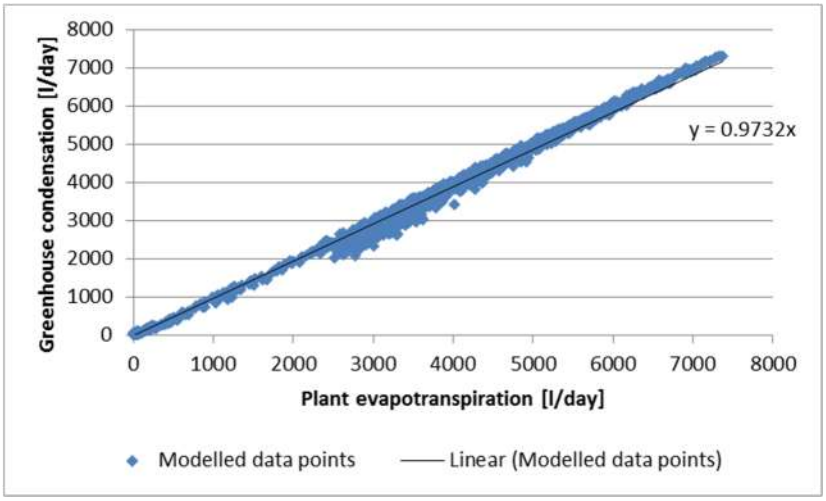

Figure 18 Greenhouse condensation versus evapotranspiration, described by a linear trend line

Plotting the condensation against plant water usage, shown in Figure 18, it follows that the rate of condensation can quite accurately be described by a linear relationship with plant evapotranspiration. This means that in this closed greenhouse model, 97.3% of the water evaporated by the plant can be recaptured through condensation. If the greenhouse is considered completely closed, with no leakage flows, then the condensation needed will be equal to the evapotranspiration.

Another goal of the greenhouse climate model is to investigate the amount of radiation that is supplied to the plant.

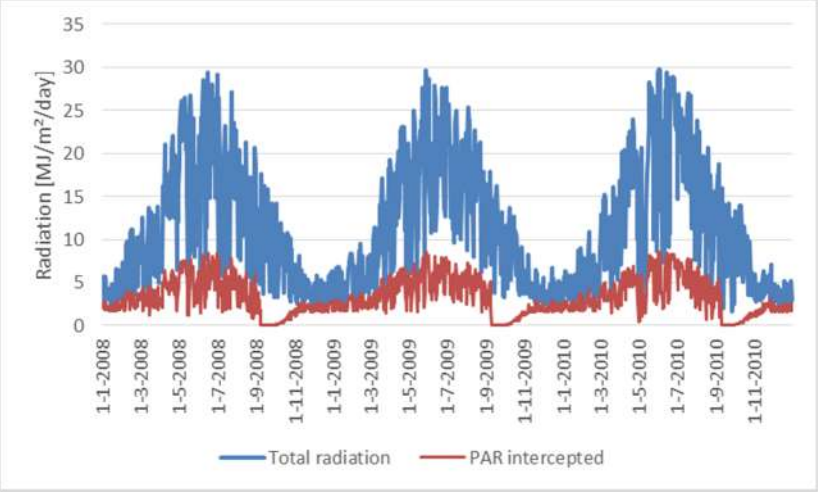

Figure 19 Total radiation (sum of solar radiation and lighting radiation) compared to photosynthetically active radiation (PAR) intercepted by plant

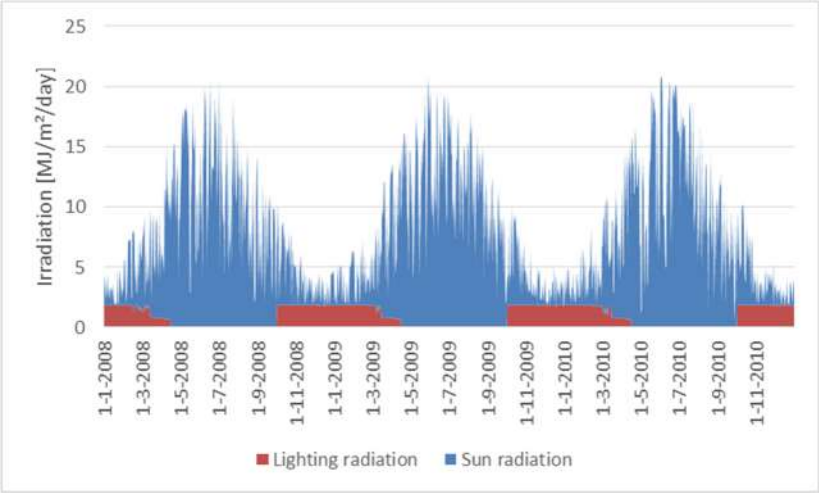

Figure 20 Daily cumulative irradiation inside the greenhouse

The amount of photosynthetically active radiation (PAR) intercepted by the plant is compared to the total amount of radiation available in Figure 19. At the beginning of the plant growth period, the intercepted radiation is very low because of the low leaf area of the plant. In spring, the intercepted PAR stays constant and a large portion of the total radiation is intercepted by the plant. This is because of the use of additional lighting, which does not have to pass the greenhouse cover. The daily cumulative irradiation inside the greenhouse is depicted in Figure 20. This shows the effect of additional lighting which is the main source of plant irradiation in the winter. Comparing the irradiation inside the greenhouse with the total irradiation in Figure 19, it is clear that a part of the radiation is lost. This loss is due to the imperfect transparency of the greenhouse cover, as well as the effect of the energy screen.

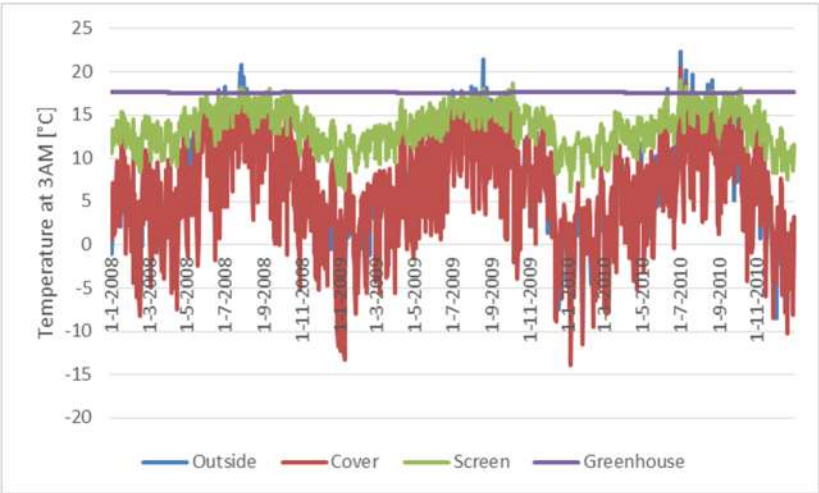

Figure 21 Nightly greenhouse temperatures at 3AM

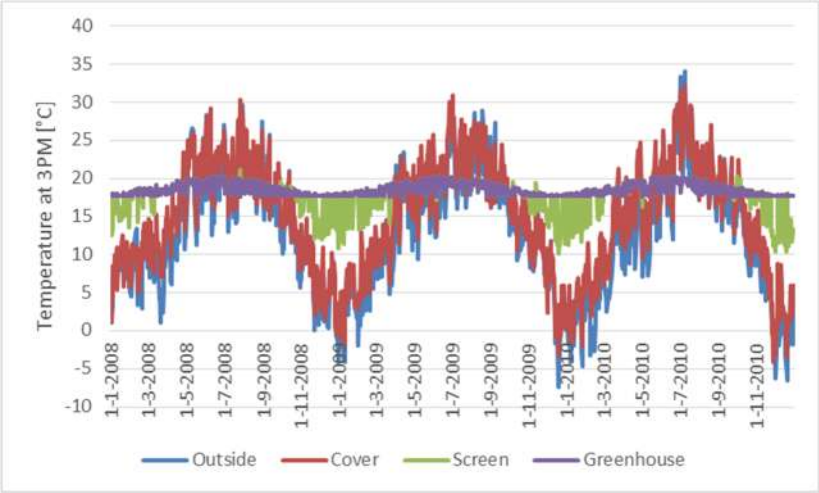

Figure 22 Daily greenhouse temperatures at 3PM

Other results calculated from the greenhouse model are the hourly temperatures in different parts of the greenhouse. Figure 21 and Figure 22 show the daily temperatures of the air in the greenhouse, the energy screen, the cover and the outside temperature at 3AM and 3PM respectively.

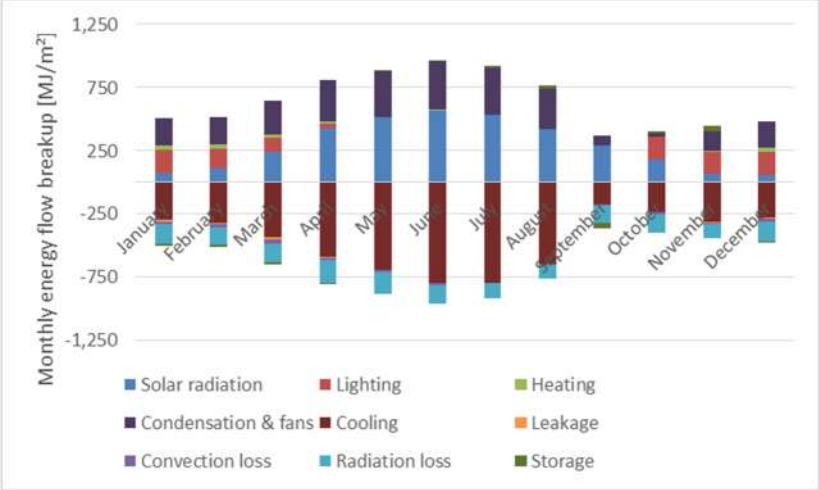

Figure 23 Monthly breakup of greenhouse energy flows

Table 3 Yearly greenhouse heating, cooling, condensation and lighting requirements

	2008	2009	2010	average	dimension
Heating	151	157	208	172	kWh/m²
Fans	65	66	66	66	kWh/m²
Heat removed	1535	1590	1534	1553	kWh/m²
Lighting	280	283	280	281	kWh/m²
Tomato yield	50.4	49.6	48.8	49.6	kg/m²
Water	1.03	1.06	1.04	1.04	m³/m²

The monthly breakup of greenhouse energy flows calculated in the model is depicted in Figure 23. Apart from solar radiation, most of the heat is supplied by the process of condensation. In summer, high condensation is required while in winter additional lighting takes up a significant part of the total energy flow. Only very little additional heating is required to keep the greenhouse at the set point temperature. This does however imply that a relatively large amount of heat needs to be removed from the greenhouse.

Table 3 shows the yearly breakup of required energy inputs. It is clear that the cooling demand is roughly nine times higher than the heating demand. The cooling heat could be stored in summer, for instance in an aquifer, and used in winter for efficient heating with a heat pump. However, this would only work if the heat production and demand are balanced; excess heat has to be removed into the air or used in an additional greenhouse or process for this to be feasible.

4.3 RAS-NFT coupling

4.3.1 Water

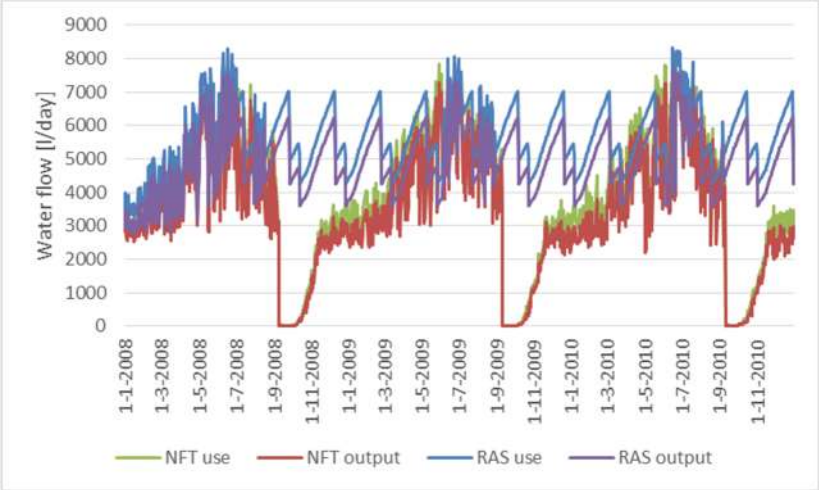

Figure 24 NFT water use and output (condensation), and RAS water use and output

The use and production of water in the NFT and RAS systems is depicted in Figure 24. The NFT water use, as also shown in chapter 4.2.1, follows the growth of the plant closely. The water output in the form of condensation is slightly lower but almost linearly dependent on the water use, as shown in chapter 4.2.3. The RAS water output mostly follows the staggered production cycle of the fish, as the coupling flow between RAS and NFT is set to be feeding rate-dependent. In summer, when the plant use is higher than the regular coupling flow rate, the flow rate is increased to match the NFT use as seen in the figure. The usage of water in the RAS system is slightly higher than the output, because of evaporation.

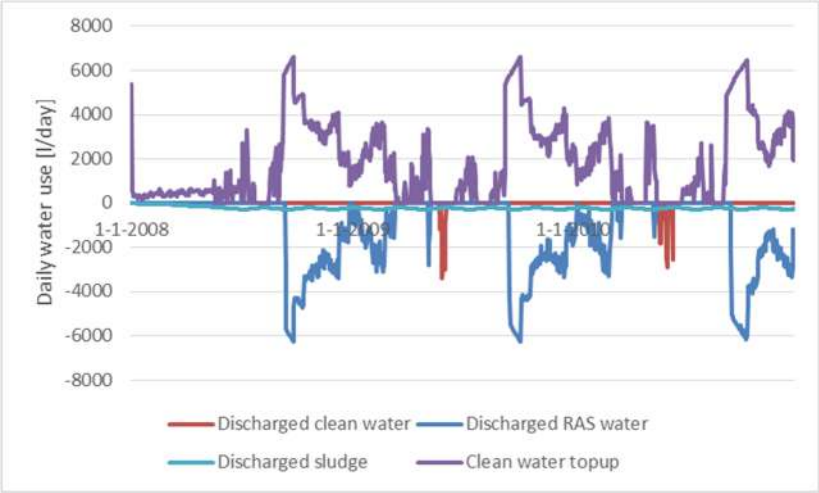

Figure 25 Total water input and output over time of the combined RAS-NFT system

The discharge of RAS water and clean water, as well as the need for additional clean water and the discharge of sludge through time is depicted in Figure 25. Whenever the needed outflow of water in the RAS system is higher than the amount of water needed in the NFT, the NFT buffer tank will fill up. When the buffer tank is full, the dirty RAS water has to be discharged. At the same time, the output of water from the NFT system (condensation) is lower than the usage of water in the RAS system. If there is not enough water in the clean water buffer, clean water has to be taken from elsewhere.

In summer, however, the amount of water produced in the NFT system can be higher than the usage in the RAS system, in which case the clean water buffer tank will fill up. If it reaches capacity, excess clean water will have to be discharged.

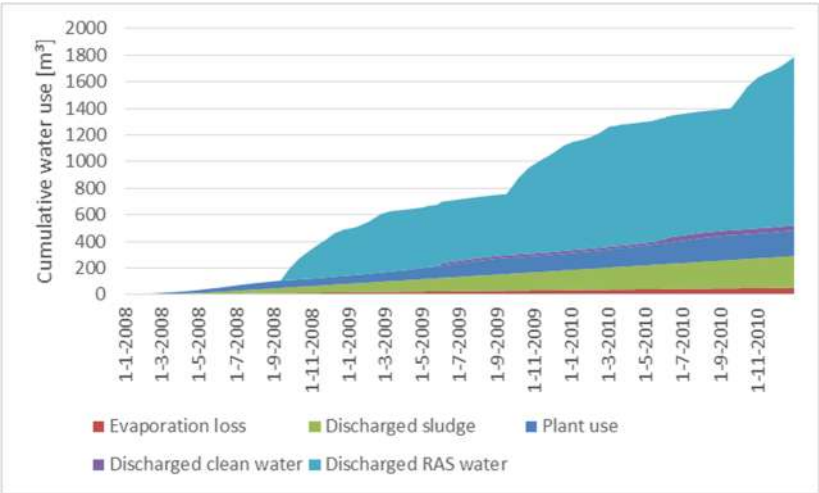

Figure 26 Breakup of water use over time

As seen in Figure 26, the discharge of RAS water has the largest effect on water usage, causing about two thirds of the total water use. The amount of water discharged with sludge removal is

relatively low, as is the water use for growth by the plant. Evaporation losses and discharging of excess clean water make up for a very small portion of the total water use.

4.3.2 Nitrogen

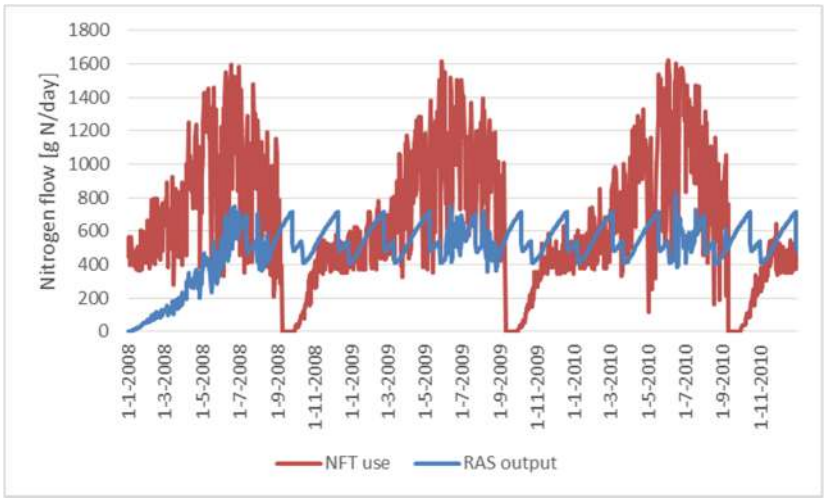

Figure 27 Plant N use and RAS N output

Figure 27 compares the nitrogen use by the plants in the NFT system, discussed in chapter 4.2.2, to the output of nitrogen from the RAS system, discussed in chapter 4.1.2. It is clear that in summer, plant nitrogen use exceeds the roughly constant output of nitrogen by the RAS system. Unless there is enough stored RAS water in the buffer tank, additional fertiliser is needed.

Another reason for the need for fertiliser is discussed in chapter 4.2.2, where it was shown that the plant nitrogen uptake concentration is higher than the nitrogen concentration supplied by the RAS system.

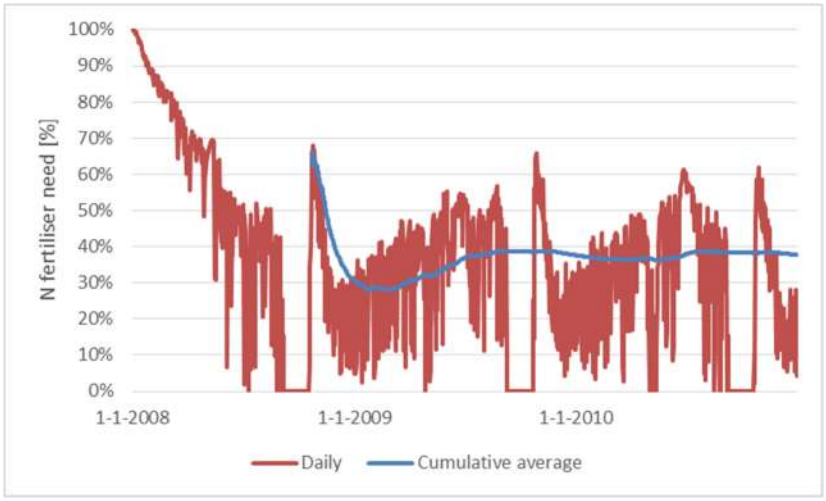

Figure 28 Plant N fertiliser need

Figure 28 shows the daily need for nitrogen fertiliser, and the cumulative average fertiliser need after the first growing season. In the first growing season, the RAS production is still starting up, so there is a higher than average need for fertiliser. The daily percentage fertiliser requirement fluctuates depending on the plant growth cycle and fish production cycles, with an average fertiliser need of 36.5%.

4.4 Design optimisation

Optimisation results of the aquaponic system model are highly dependent on the chosen input values, as well as the optimisation goal. For the purpose of this thesis, only the effect of changing the NFT production area with respect to a constant RAS production volume is investigated, as well as the type of coupling flow between the two systems and the size of the NFT buffer tank.

Other important model and input parameters, as well as the initial conditions of the state variables, can be changed in the Excel® implementation but their effect is not discussed in this thesis. Important input values that might influence coupling are tank volumes of the fish tanks, secondary clarifier, NFT buffer tank and water storage tank; pump flows for the RAS and NFT systems; coupling flow between the two systems; fish stocking density and feed ratio; and total plant area and plant light use efficiency.

Three optimisation goals are set:

- Minimal discharge of RAS water
- Minimal use of clean water
- Minimal use of additional N fertiliser

Firstly, the values of usage and discharge in different cases are discussed, and secondly, a cost function for optimisation is discussed.

4.4.1 Minimal discharge of RAS water

Discharge of untreated RAS water is sometimes necessary to keep ammonia and nitrate levels in the RAS system below maximum values. In the INAPRO aquaponics system modelled, this water is usually fed to the NFT buffer tank, however, when the tank is full RAS water has to be discharged to the sewage system instead. This is undesirable, because it is a loss of nutrients, and it poses a load on the municipal treatment facilities. Furthermore, waste discharge often gives rise to financial costs.

Water discharge results through time, for a single case, can be found in Chapter 4.3.1.

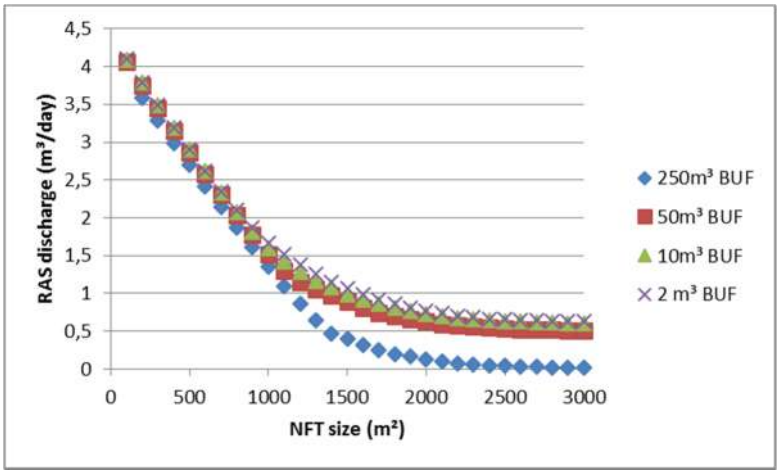

Figure 29 RAS waste discharge as a function of NFT production area, for three different NFT buffer tank sizes

As can be seen in Figure 29, the amount of RAS water that has to be discharged to the sewage system decreases with an increasing NFT production area. A larger buffer tank also causes a decrease in the amount of water that needs to be discharged. This amount however does not reach zero in either of the three cases with a small buffer tank size. The gap between RAS water production and NFT water use is only completely bridged in the case of the 250 m³ buffer tank with a very large NFT production area. In all other cases, some discharge of RAS water will occasionally be required.

4.4.2 Minimal use of clean water

One of the goals of the INAPRO system is to minimise water usage. Water usage breakup of the combined RAS and NFT systems through time, for a single case, is presented in Chapter 4.3.1.

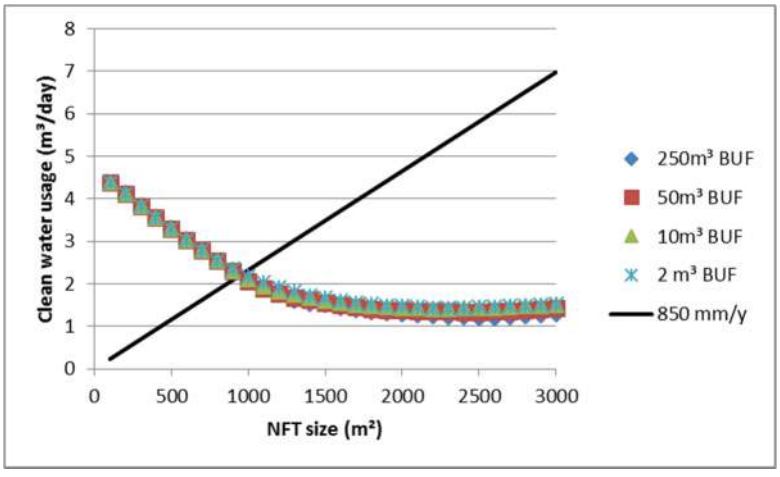

Figure 30 Clean water usage (expressed in m³/day) as a function of NFT production area, for three different NFT buffer tank sizes. Also included is the yearly average amount of rainwater that falls on the given NFT greenhouse area (also expressed in m³/day)

As can be seen in Figure 30, water usage as a function of NFT size has a minimum at an NFT area of about 2500 m². Below this area, the increased amount of discharged water means that more clean water has to be added to the system. Above this area, an increase in plant production also means an increase in water usage. At an NFT area of about 1000m², the yearly amount of rainfall on the greenhouse equals the yearly usage of water. In this case and with an adequately sized rainwater catchment tank, the water requirements of the combined system can be met by using only rain water.

4.4.3 Minimal use of nitrogen fertiliser

The amount of additional nitrogen fertiliser is to be minimised, because it poses an additional cost to the grower. Nitrogen usage and production through time, for a single case, are presented in Chapter 4.3.2.

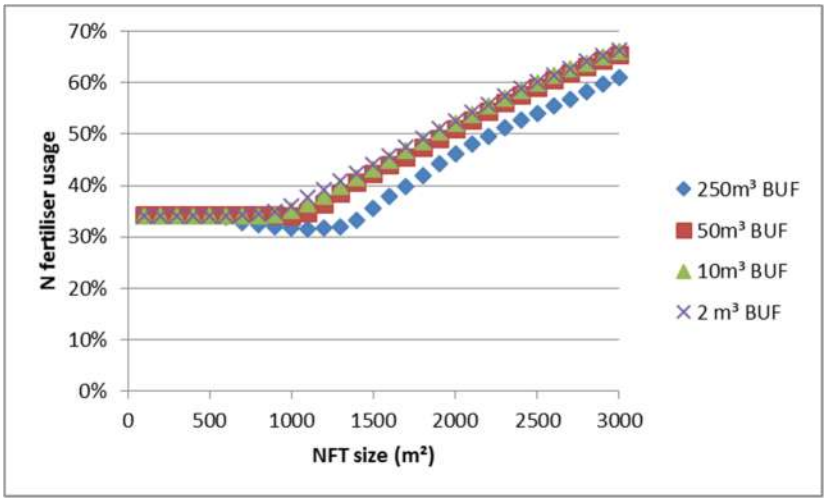

Figure 31 Additional nitrogen fertiliser usage as a function of NFT production area, for three different NFT buffer tank sizes

As can be seen in Figure 31, the percentage of additional fertiliser needed in the NFT system rises with an increasing NFT production area. This is due to the RAS system not being able to supply enough nitrogen for optimal plant growth in the NFT system. Nitrogen fertiliser usage stays roughly constant at about 34% at low NFT areas, because the average nitrogen uptake concentration of the plants is higher than the nitrogen concentration in the water provided by the RAS system no matter how much water is pumped to the NFT system. After about 1000m² of NFT production area, the fertiliser requirement increases quickly with an increasing NFT area. Interestingly, in case of the very large buffer tank of 250 m³, the fertiliser requirement first drops to 32% and then starts increasing as well but at a larger NFT production area when compared to the other buffer tank sizes. This is because the nutrient loss from discharge is lower or even non-existent when using such a large buffer tank.

4.4.4 Cost function

Comparing Figure 29, Figure 30 and Figure 31, it becomes clear that the three optimisation goals of minimising RAS discharge, clean water usage and N fertiliser usages are mutually exclusive. A relatively small NFT area would be optimal for water and fertiliser usage, but would mean a high rate of RAS water discharge. Therefore, to find an optimal solution, a cost function is used.

Each optimisation goal is given a penalty factor, and the optimisation is reduced to minimising the total penalty factor P. The NFT production area is used as an input variable for optimisation. The optimisation function can then be described as follows:

$$P_{tot} = L_{disch} \cdot \Phi_{\mathrm{H_2O,SC,disch}} + L_{H_2O} \cdot \phi_{H_2O,in-STOR} + L_N \cdot \frac{\phi_{N,FERT}}{\phi_{N,NFT-plants}} \qquad (4.2)$$

Table 4 Optimisation objectives

Objective	Description	Dimension	Cost factor
$\Phi_{\mathrm{H_2O,SC,disch}}$	Total discharged RAS water	$[\mathrm{m^3\ d^{-1}}]$	L_{disch}
$\phi_{H_2O,in-STOR}$	Total input of clean water	$[\mathrm{m^3\ d^{-1}}]$	L_{H_2O}
$\frac{\phi_{N,FERT}}{\phi_{N,NFT-plants}}$	Total N fertiliser need	$[\%]$	L_N

Unfortunately, the integrated model was found too complex for the built-in solver in Microsoft Excel®, as it was impossible to find a solution to the optimisation problem. Therefore, the problem is solved using iteratively computed data points. For each case described, a total of 25 data points were calculated for NFT production areas between 100 and 2500 m². The results are presented below.

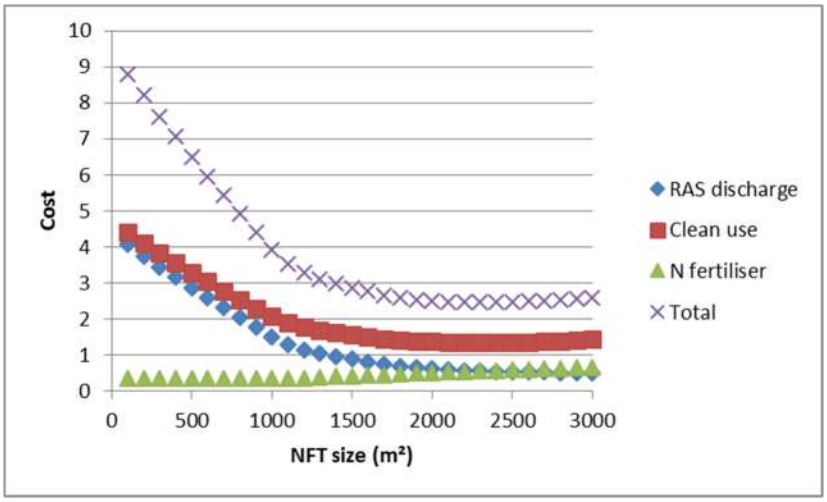

Figure 32 Visualisation of the optimisation problem $min\{P_{tot}\}$ with cost factors $L_{disch} = 1$, $L_{H_2O} = 1$ and $L_N = 1$. Shown are the total cost and the breakup of separate goal costs as a function of NFT size. A buffer tank size of 50 m³ is used

As depicted in the visualisation of the optimisation problem in Figure 33, equal cost factors for the three different objectives result in a relative low weight of the usage of fertiliser and a high weight of clean water usage. The total cost function shows minimal costs on the NFT size range from 2000 to 2500 m².

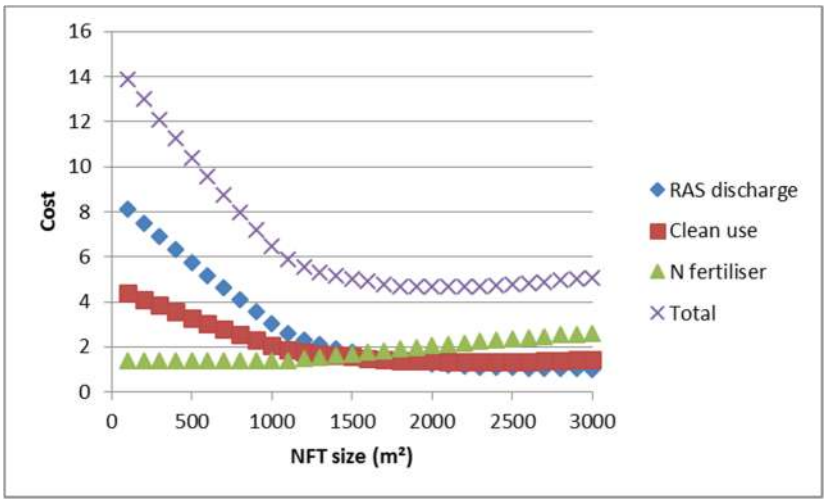

Figure 33 Visualisation of the optimisation problem $min\{P_{tot}\}$ with cost factors $L_{disch} = 2$, $L_{H_2O} = 1$ and $L_N = 4$. Shown are the total cost and the breakup of separate goal costs as a function of NFT size. A buffer tank size of 50 m³ is used

The different cost factors were changed to $L_{disch} = 2$, $L_{H_2O} = 1$ and $L_N = 4$ for more equal relative weighting of the three objectives around the optimal solution, as depicted in Figure 33. In this case, the optimal solution changes very little from the optimal solution calculated using equal cost factors. The absolute minimum is now found at 2100 m², but there is still a broad region around 1500 m² to 3000 m² where a change in NFT area only produces a small change in total cost.

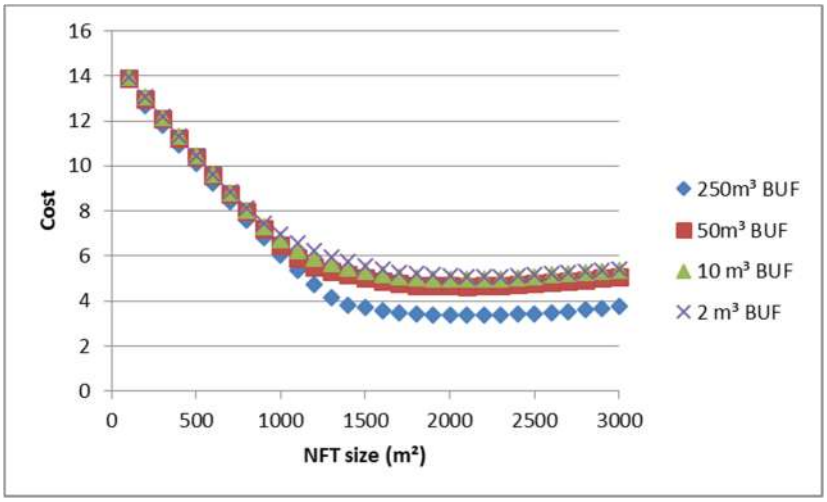

Figure 34 Visualisation of the optimisation problem $min\{P_{tot}\}$ with cost factors $L_{disch} = 2$, $L_{H_2O} = 1$ and $L_N = 4$. Shown is the total cost as a function of NFT size, for various buffer tank sizes

In Figure 34, the effect of the NFT buffer tank size on the total optimisation cost function can be seen. It is clear that a larger buffer tank allows for a lower total cost. However, the cost difference between the tank sizes is small considering each buffer tank size is a factor five larger than the previous one. The largest buffer tank size modelled (250 m³) reduces the total cost more significantly because it allows for a much lower discharge rate. A buffer tank of more than 10 m³ might be unpractically large, though, and could bring additional financial costs that are not considered in the optimisation cost function used.

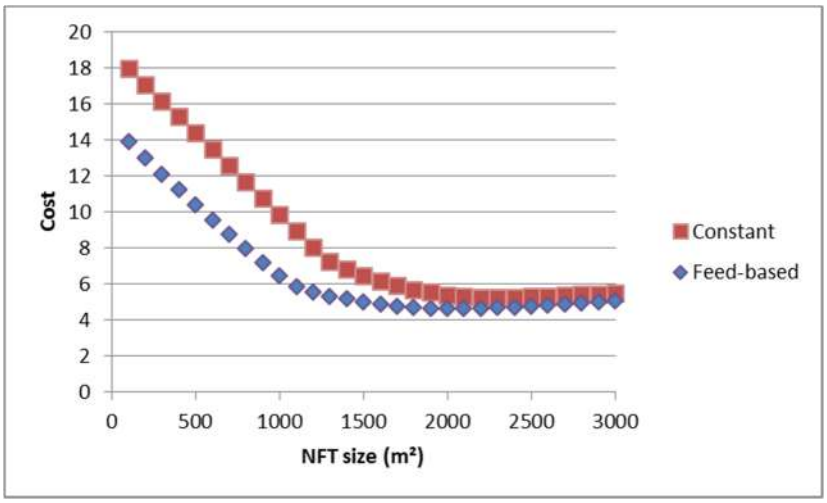

Figure 35 Visualisation of the optimisation problem $min\{P_{tot}\}$ with cost factors $L_{disch} = 2$, $L_{H_2O} = 1$ and $L_N = 4$. Shown is the total cost as a function of NFT size, for the case of a feed-based coupling flow and the case of a constant coupling flow between the RAS and NFT systems

In Figure 35, the effect of the type of coupling flow modelled can be seen. A feed-based coupling flow, where the flow of water $\phi'_{\mathrm{H_2O,SC-BUF}}$ pumped from the RAS settling tank to the NFT buffer tank depends on the amount of feed fed to the fish, has a positive effect on the total cost when the NFT production area is relatively low. At larger NFT sizes, the difference between the two flow schemes reduces. The large initial difference is caused by the different minimum coupling flow rate. As discussed in Chapter 4.1.2, the minimum flow rate had to be increased from 4800 l/day to 5650 l/day to keep the peak nitrogen concentration below 100 mg N/l in case of a constant coupling flow.

5. Conclusion and recommendations

A model of the INAPRO-system was developed using Microsoft Excel®. The model is based on nitrogen dynamics, using zero and first order dynamics of the production terms. The integrated RAS-NFT model presented gives qualitative insight into the relations between the flows and nitrogen processes in the RAS and NFT systems. For a full quantitative analysis, the model needs further calibration and validation.

RAS and NFT systems are optimised individually with respect to yield. However, the coupling flows between the two systems are found inadequate to realise this optimal yield at all times, due to fluctuations in production in both the RAS and NFT systems.

The production of nitrogen in the RAS system shows a repetitive curve that is highly dependent on the feeding rate, and therefore on the production schedule of the fish. To smooth out the production of nitrogen compounds, it is recommended that the fish are stocked as evenly as possible, with regular spacing between batches.

The usage of nitrogen in the NFT system was found to be mostly dependent on plant irradiation. Therefore, it is recommended to increase winter time production by the use of additional lighting. With the tomato crop chosen, there will still be a period of low nitrogen use in winter and about twice as high nitrogen use in summer. Additionally, between two cropping seasons there is a period where there are no plants in the greenhouse. For better matching of the RAS nitrogen production with the NFT use, crops with a more continuous production can be used. Alternatively, the RAS production schedule can be scaled to the plant production, for instance by having less fish batches in winter or planning a winter stop.

It was found that it is possible to absorb some of the fluctuations that cause discrepancies between RAS production and NFT use by way of a buffer tank. However, in this model it was found that such a buffer tank would have to be very large in order to absorb the seasonal difference completely. Near zero RAS water discharge was only achieved in the case of the largest buffer tank modelled (250 m^3) and the largest NFT production area modelled (3000 m^2).

It was also found that the plant nitrogen uptake concentration has an average daytime uptake concentration that fluctuates around 12 mmol N/l. Because of the maximum nitrate concentration in the fish system, the RAS output nitrogen concentration is limited to about 7 mmol N/l, or 7.5 mmol N/l if a slight increase in nitrogen concentration due to volatilisation in the settling tank is considered. It was found that therefore, additional nitrogen fertiliser is required. Even in cases with a small NFT production area and a large buffer tank, it was found that about one third of the plant nitrogen use has to be supplied in the form of additional fertiliser when RAS nitrate concentrations are limited to 100 mg N/l. With the RAS component sizing chosen in this study, the fertiliser usage percentage will increase when the NFT production area is larger than about 1000 m^2.

It was found that the amount of water that needs to be condensed in the greenhouse can accurately be approached by a linear dependency on evapotranspiration, when using Dutch climate data. If the greenhouse is considered completely closed with no air leakage, condensation can be set equal to evapotranspiration. In further research on integrating NFT and RAS models using a closed greenhouse, the greenhouse climate model can be left out and only evaporation and light interception need to be modelled.

The closed greenhouse succeeds in trapping evaporated water. The condensation that is needed to keep humidity low, however, is an exothermic process that adds a significant amount of heat to the greenhouse. Little additional heating is then needed, but the cooling demand throughout the year is quite large. In practice, a conventional non-closed greenhouse without condensation might be more economical, especially considering the relatively low cost of clean water in the Netherlands.

Optimisation results of the combined RAS-NFT system show that the objectives of minimal water usage and minimal fertiliser usage are mutually exclusive, when considering the size of the NFT with respect to the size of the RAS system as an optimisation input. The amount of water discharged and the amount of clean water needed can be minimised by increasing the NFT area, however, this will increase the amount of fertiliser needed. With arbitrarily chosen cost values for the three objectives, the total cost was lowest for an NFT area between 1500m² and 3000m², with an optimum solution found at an NFT area of 2100m².

It is recommended that further research into the effects of other nutrients and variables such as phosphorus, sodium, magnesium, dissolved oxygen and pH is done.

Finally, it is recommended to not use Microsoft Excel® for further integrated modelling. Although there are benefits to using the program, the model described had to be simplified on multiple occasions and even then operated on the edge of Excel®'s capabilities.

6. References

Bontsema, J. et al., 2011. *On-line monitoring van transpiratie en fotosynthese: de praktijk*, Wageningen UR.

Bootsveld, N.R. & van Wolferen, J., 2004. *Ontvochtiging van kassen met bestaande technieken uit de utiliteitsbouw Fase 1 . Kwalitatieve beoordeling Samenvatting*, TNO Apeldoorn.

Donatelli, M., Bellocchi, G. & Carlini, L., 2006. Sharing knowledge via software components: Models on reference evapotranspiration. *European Journal of Agronomy*, 24(2), pp.186–192.

Gallardo, M. et al., 2009. Simulation of transpiration, drainage, N uptake, nitrate leaching, and N uptake concentration in tomato grown in open substrate. *Agricultural Water Management*, 96(12), pp.1773–1784.

De Gelder, A., Warmenhoven, M. & Grootscholten, M., 2010. *Het Nieuwe Telen Tomaat 2010*, Wageningen UR.

Greiner, A.D. & Timmons, M.B., 1998. Evaluation of the nitrification rates of microbead and trickling filters in an intensive recirculating tilapia production facility. *Aquacultural Engineering*, 18, pp.189–200.

Heuvelink, E., 1996. Dry matter partitioning in tomato: Validation of a dynamic simulation model. *Annals of Botany*, 77(1), pp.71–80.

Heuvelink, E., 1999. TOMSIM - simulation of crop growth and development for tomato Literature : *Annals of Botany*, 83, pp.413–422.

IGB, 2014. INAPRO modelling calculation fish production. Internal INAPRO communication of fish production data.

Jiménez-Montealegre, R. et al., 2002. Conceptualization and validation of a dynamic model for the simulation of nitrogen transformations and fluxes in fish ponds. *Ecological Modelling*, 147(2), pp.123–152.

KNMI, 2015. Daggegevens van het weer in Nederland. Available at: http://projects.knmi.nl/klimatologie/daggegevens/ [Accessed October 7, 2015].

KNMI, 2000. *Handbook for the meteorological observation.*, Available at: http://projects.knmi.nl/hawa/pdf/Handbook_H01_H06.pdf.

Love, D.C. et al., 2015. Commercial aquaponics production and profitability: Findings from an international survey. *Aquaculture*, 435, pp.67–74.

Van Ooteghem, R.J.C., 2007. *Optimal control design for a solar greenhouse*. Wageningen UR.

Prenger, J.J., Fynn, R.P. & Hansen, R.C., 2002. A Comparison of four evapotranspiration models in a greenhouse environment. *Transactions of the ASAE*, 45(6), pp.1779–1788.

Rafiee, G. & Saad, C.R., 2005. Nutrient cycle and sludge production during different stages of red tilapia (Oreochromis sp.) growth in a recirculating aquaculture system. *Aquaculture*, 244(1-4), pp.109–118.

Rogers, R.R. & Yau, M.K., 1989. *A Short Course in Cloud Physics (3rd ed.)*, Pergamon Press.

Staaks, G., 2015. INAPRO. Available at: http://www.inapro-project.eu [Accessed October 7, 2015].

Stanghellini, C., 1987. *Transpiration of greenhouse crops: An aid to climate management*. Wageningen UR.

Stanghellini, C., 2009. *Vochtregulatie en verdamping*, Wageningen UR.

De Zwart, H.F., 1996. *Analyzing energy-saving options in greenhouse cultivation using a simulation model*,